

Aus dem Fachbereich Medizin
der Johann Wolfgang Goethe-Universität
Frankfurt am Main

betreut am
Georg-Speyer-Haus
Institut für Tumorbologie und Experimentelle Therapie
Direktor: Prof. Dr. Florian Greten

**Exploration of Nilotinib enhancing the anti-leukaemic Effects of
Gas6 Deletion in Ph⁺ B-ALL by inducing Immunogenic Cell Death**

Dissertation
zur Erlangung des Doktorgrades der Medizin
des Fachbereichs Medizin
der Johann Wolfgang Goethe-Universität
Frankfurt am Main

vorgelegt von
Carolin Wachtel

aus Heppenheim (Bergstraße)

Frankfurt am Main, 2020

Aus dem Fachbereich Medizin
der Johann Wolfgang Goethe-Universität
Frankfurt am Main

betreut am
Georg-Speyer-Haus
Institut für Tumorbologie und Experimentelle Therapie
Direktor: Prof. Dr. Florian Greten

**Exploration of Nilotinib enhancing the anti-leukaemic Effects of
Gas6 Deletion in Ph⁺ B-ALL by inducing Immunogenic Cell Death**

Dissertation
zur Erlangung des Doktorgrades der Medizin
des Fachbereichs Medizin
der Johann Wolfgang Goethe-Universität
Frankfurt am Main

vorgelegt von
Carolin Wachtel

aus Heppenheim (Bergstraße)

Frankfurt am Main, 2020

Dekan:

Referent:

Korreferent:

Tag der mündlichen Prüfung:

Prof. Dr. Stefan Zeuzem

Prof. Dr. Florian Greten

Prof. Dr. Hubert Serve

28.06.2021

In Dank und Liebe meinen Eltern,

Ute und Ralf Wachtel,

gewidmet

Table of Contents

1 Abstract	1
2 Zusammenfassung	3
3 Introduction	6
3.1 Philadelphia Chromosome-positive ALL (Ph+ ALL)	6
3.2 Immunotherapy and Tumour Microenvironment.....	8
3.3 Research Background.....	10
3.4 Immunogenic Cell Death (ICD)	13
3.5 Objective and Prospect	16
4 Material and Methods	18
4.1 Material	18
4.1.1 Consumable Material.....	18
4.1.2 Reagents and Chemicals	18
4.1.3 Antibodies.....	18
4.1.4 Chemotherapeutic Agents	20
4.1.5 Leukaemic Cell Lines (BCR-ABL B-ALL)	20
4.1.6 Mouse Stock.....	21
4.1.7 Devices and Software	21
4.2 Methods	22
4.2.1 Cell Culture.....	22
4.2.2 Growth Curve and Viability Count.....	22
4.2.3 Flow Cytometry	23
4.2.4 Western Blot	25
4.2.5 Cell Death Assay	27
4.2.6 Determination of ICD Markers	27
4.2.6.1 Calreticulin Exposure.....	27

4.2.6.2	Extracellular ATP Release.....	28
4.2.6.3	HMGB1 Release.....	28
4.2.7	Macrophages Co-Culture	30
4.2.8	Vaccination Assay	31
4.2.9	Haematoxylin-Eosin Stain and Immunohistochemistry	34
4.2.10	Statistical Analysis	34
5	Results	35
5.1	Effects of Nilotinib on Tumour Cell Growth and Viability	35
5.2	Characterisation of Nilotinib-induced Cell Death	38
5.3	Molecular Determinants of Immunogenic Cell Death	43
5.3.1	Calreticulin Exposure.....	43
5.3.2	Extracellular ATP Release.....	44
5.3.3	HMGB1 Release.....	46
5.4	Immunological Determinants of Immunogenic Cell Death.....	48
5.4.1	Macrophages Co-Culture	48
5.4.2	Vaccination Assay	50
6	Discussion	56
6.1	Results on Interpretation and Discussion.....	56
6.1.1	Growth Inhibition and Viability Assay	56
6.1.2	Cell Death Assay	56
6.1.3	ICD Marker Analysis	59
6.1.4	Macrophages Co-Culture.....	61
6.1.5	Vaccination Assay	63
6.1.6	Conclusion.....	65
6.2	Limitations and Options.....	66
6.3	Perspectives.....	68
7	References	70

8 Appendix	88
8.1 Supplementary Figure S1: The Role of Tumour-associated Macrophages in Tumour Progression	88
8.2 Table 1: Consumable Material	89
8.3 Table 2: Common Reagents and Chemicals.....	90
8.4 Table 3: Reagents and Chemicals for Cell Culture	91
8.5 Table 4: Reagents and Chemicals for Flow Cytometry	92
8.6 Table 5: Reagents and Chemicals for Western Blot.....	93
8.7 Table 6: Reagents and Chemicals for Haematoxylin-Eosin Stain and Immunohistochemistry	95
8.8 Table 7: Detection Kit for Extracellular ATP Release	96
8.9 Table 12: Devices and Software	96
8.10 Supplementary Figure S2: Gating Strategy of Flow Cytometry based Cell Death Assay	98
8.11 Supplementary Figure S3: Gating Strategy of Flow Cytometry Analysis of Calreticulin Exposure	99
8.12 Supplementary Figure S4: Gating Strategy of Flow Cytometry Analysis of Macrophages Co-Culture	100
8.13 Table 14: Shift in Macrophages Activation and Polarisation. Co-Culture Conditions with 10 nM Nilotinib	101
8.14 Table 15: Shift in Macrophages Activation and Polarisation. Co-Culture Conditions with 50 nM Nilotinib	102
8.15 Table 16: Shift in Macrophages Activation and Polarisation. Co-Culture Conditions with 1 μ M Mitoxantrone	103
8.16 Supplementary Figure S5: Gating Strategy of Flow Cytometry Analysis of Vaccination Assay. Quantifying Leukaemic Burden.....	104
9 Publication	105
9.1 Publication 2019.....	105
10 Curriculum Vitae	106

11 Acknowledgement.....	109
12 Schriftliche Erklärung	110

List of Abbreviations

ALL	Acute lymphoblastic leukaemia
ANXA1	Annexin A1
AnxV	Annexin V
ATP	Adenosine triphosphate
B-ALL	B-cell acute lymphoblastic leukaemia
BMDM	Bone marrow-derived macrophages
CAFs	Cancer-associated fibroblasts
CALR	Calreticulin
CD	Cluster of differentiation
CDKN2A	Cyclin-dependent kinase inhibitor 2A
CXCL	CXC motif chemokine ligand
DAMPs	Damage-associated molecular patterns
DMSO	Dimethyl sulfoxide
DPBS	Dulbecco's Phosphate Buffered Saline
ECM	Extracellular matrix
ELISA	Enzyme-linked immunosorbent assay
ER	Endoplasmic reticulum
FACS	Fluorescence-activated cell sorting
FBS	Foetal Bovine Serum
FS	Forward scatter
GFP	Green fluorescent protein
Gas6	Growth-arrest-specific gene-6
Gas6KO	Gas6 knockout
HD-TKI	High-dose TKI
HE	Haematoxylin-Eosin
HMGB1	High-mobility-group-protein B1
IC ₅₀	Half maximal inhibitory concentration
ICD	Immunogenic cell death
IHC	Immunohistochemistry

IL	Interleukin
INF	Interferon
IRES	Internal ribosomal entry site
LC3	Light chain 3
LPS	Lipopolysaccharide
M-CSF	Macrophage colony-stimulating factor
MDSCs	Myeloid-derived suppressor cells
MHC	Major histocompatibility complex
M-MDSCs	Monocyte-related myeloid-derived suppressor cells
MTX	Mitoxantrone
NCCD	Nomenclature Committee on Cell Death
NK	Natural killer
PAGE	Polyacrylamide gel electrophoresis
Pi	Propidium iodide
PRRs	Pattern recognition receptors
PVDF	Polyvinylidene difluoride
RIPK	Receptor-interacting protein kinases
rL/L-reagent	Recombinant Luciferin/Luciferase-reagent
RLU	Relative light units
rpm	Revolutions per minute
RTKs	Receptor tyrosine kinases
SD	Standard deviation
SDS	Sodium dodecyl sulphate
SDS-PAGE	Sodium dodecyl sulphate polyacrylamide gel electrophoresis
SS	Side scatter
TAM	Tyro3, Axl, Mer (collective term)
TAMs	Tumour-associated macrophages
TGF	Transforming growth factor
TIICs	Tumour-infiltrating immune cells
TIME	Tumour immune microenvironment
TKI	Tyrosine kinase inhibitor
TLR	Toll-like receptor
TME	Tumour microenvironment

TNF	Tumour necrosis factor
Tregs	Regulatory T cells
wt	Wild-type

List of Figures

Figure 1	Philadelphia Chromosome Formation.....	7
Figure 2	Investigational Strategies of Immunotherapy.....	9
Figure 3	Plasticity of the Tumour Microenvironment.....	10
Figure 4	The Role of Gas6/TAM in Cancer Cells and the Tumour Microenvironment.....	11
Figure 5	Macrophage Polarisation.....	12
Figure 6	Molecular Definition of Immunogenic Cell Death.....	15
Figure 7	Functional Definition of Immunogenic Cell Death.....	16
Figure 8	Light Scattering by the Cell.....	23
Figure 9	Determination of the Cell Population based on FS and SS in a flow cytometric Data Analysis.....	24
Figure 10	Set-up and functional Principle of Flow Cytometry and Data Analysis.....	24
Figure 11	The Technique of Western Blotting.....	28
Figure 12	Experimental Setup of Macrophages Co-Culture.....	31
Figure 13	Experimental Setup of Vaccination Assay.....	32
Figure 14	Effects of Nilotinib on Tumour Cell Growth.....	36
Figure 15	Effects of Mitoxantrone on Tumour Cell Growth.....	37
Figure 16	Effects of Nilotinib on Tumour Cell Viability.....	38
Figure 17	Flow Cytometry based Analysis of Nilotinib-induced Cell Death. Cell Line 1-1.....	40

Figure 18	Flow Cytometry based Analysis of Nilotinib-induced Cell Death. Cell Line 3.....	41
Figure 19	Cell Death Assay.....	42
Figure 20	ICD Marker Analysis of Calreticulin Exposure.....	44
Figure 21	Bioluminescence based ATP Assay for the Detection of Extracellular ATP. ATP Standard Curve and Luciferase Reaction Formula.....	45
Figure 22	ICD Marker Analysis of Extracellular ATP Release.....	46
Figure 23	ICD Marker Analysis of HMGB1 Release.....	47
Figure 24	Flow Cytometry based Analysis of Macrophages Co-Culture.....	49
Figure 25	Monitoring the Occurrence of Leukaemia after Vaccination..	50
Figure 26	Time of Manifestation of Leukaemia after Re-challenge.....	51
Figure 27	Final Analysis of Bone Marrow.....	53
Figure 28	Final Analysis of Peripheral Blood.....	53
Figure 29	Final Analysis of Spleen.....	54
Figure 30	Histological Examination of subcutaneous Tumours of the Nilotinib Cohort.....	55
Figure 31	Strategies for the Induction of ICD.....	69
Figure S1	The Role of Tumour-associated Macrophages in Tumour Progression.....	88
Figure S2	Gating Strategy of Flow Cytometry based Cell Death Assay.....	98
Figure S3	Gating Strategy of Flow Cytometry Analysis of Calreticulin Exposure.....	99

Figure S4	Gating Strategy of Flow Cytometry Analysis of Macrophages Co-Culture.....	100
Figure S5	Gating Strategy of Flow Cytometry Analysis of Vaccination Assay. Quantifying Leukaemic Burden.....	104

List of Tables

Table 1	Consumable Material.....	89
Table 2	Common Reagents and Chemicals.....	90
Table 3	Reagents and Chemicals for Cell Culture.....	91
Table 4	Reagents and Chemicals for Flow Cytometry.....	92
Table 5	Reagents and Chemicals for Western Blot.....	93
Table 6	Reagents and Chemicals for Haematoxylin-Eosin Stain and Immunohistochemistry.....	95
Table 7	Detection Kit for Extracellular ATP Release.....	96
Table 8	Antibodies for Flow Cytometry.....	18
Table 9	Antibodies for Western Blot.....	19
Table 10	Antibodies for Immunohistochemistry.....	20
Table 11	Chemotherapeutic Agents.....	20
Table 12	Devices and Software.....	96
Table 13	Extent and Procedure of the Final Analysis.....	33
Table 14	Shift in Macrophages Activation and Polarisation. Co-Culture Conditions with 10 nM Nilotinib.....	101
Table 15	Shift in Macrophages Activation and Polarisation. Co-Culture Conditions with 50 nM Nilotinib.....	102
Table 16	Shift in Macrophages Activation and Polarisation. Co-Culture Conditions with 1 μ M Mitoxantrone.....	103

1 Abstract

Cancer is the major cause of death besides cardiovascular disease. Leukaemia represents the most prevalent malignancy in children with a frequency of 30 % and is one of the ten leading types of cancer in adults. Philadelphia Chromosome-positive B-ALL (Ph⁺ B-ALL) is driven by the cytogenetic aberration of the reciprocal chromosomal translocation t(9;22)(q34;q11) leading to the formation of the Philadelphia chromosome with a BCR-ABL1 fusion gene. This fusion gene encodes a BCR-ABL1 oncoprotein which is characterized by a constitutively enhanced tyrosine kinase activity promoting amplified proliferation, differentiation arrest and resistance to cell death. Ph⁺ B-ALL is considered the most aggressive ALL subtype with a long-term survival rate in the range of only 30 % despite intensive standard of care including chemotherapy in combination with a tyrosine kinase inhibitor (TKI) followed by allogeneic stem cell transplantation after remission for clinically fit patients.

The efficacy of chemotherapy has long been mainly attributed to tumour cell toxicity while immune modulating effects have been overlooked, especially in light of known immunosuppressive properties. Accumulative evidence, however, emphasizes the ability of chemotherapeutic agents, including TKIs, to normalise or re-educate a dysfunctional tumour microenvironment (TME) resulting in enhanced anti-tumour immunity. One of the underlying mechanisms of immune modulation is the induction of immunogenic cell death (ICD). ICD is an anti-tumour agent-induced cell death modality determined by the capacity to convert cancer cells into anti-cancer vaccines. The induction of ICD relies on the release of damage-associated molecular patterns (DAMPs) from dying tumour cells succumbing to ICD. Translocation of CALR to the cell surface, extracellular secretion of ATP and release of HMGB1 from the nucleus are key hallmarks of ICD that mediate anti-tumour immunity upon binding to antigen presenting cells resulting in a tumour antigen-specific immune response. Besides these molecular determinants, ICD is functionally defined by the inhibition of tumour growth in a vaccination assay in which mice are injected with tumour cells exposed to the potential ICD inducer in-vitro and then re-challenged with live tumour cells of the same cancer type. Both molecular and functional criteria determine the gold

standard approach to assess ICD. By increasing the immunogenicity of cancer cells, ICD contributes to the restoration of immunosurveillance as an essential feature of tumour rejection, which is clinically reflected by improved therapeutic efficacy and disease outcome in patients. Therefore, identifying novel ICD inducers is an objective of interest in the context of cancer therapy.

In respect of these considerations, the aim addressed in the present work is the examination of the second-generation TKI Nilotinib for the ability to induce ICD. The thesis is set in the context of the group's research on the role of Gas6/TAM signalling within the TME regarding the pathogenesis of acute leukaemia. In in-vivo experiments of our research group it has been consistently observed that the use of Nilotinib enhances the anti-leukaemic immunity mediated by a deletion of Gas6. Against the background of increasing importance of chemotherapeutic agents as potent modulators of a dysregulated TME, it was hypothesized that Nilotinib may synergize with a Gas6-deficient environment by inducing ICD in Ph⁺ B-ALL cells.

In growth inhibition and Annexin V/Propidium iodide cell death assays Nilotinib was shown to induce cell death in concentration-dependent manner that occurs bimodally in terms of cell death modality ranging between apoptosis and necrosis. By ICD marker analysis, comprising flow-cytometric detection of CALR exposure, chemoluminescence-based ATP measurement and immunoblotting for HMGB1, it was found that Nilotinib-induced cell death is not accompanied by CALR exposure and ATP secretion, but is associated with the release of HMGB1. In macrophages co-culture experiments with Nilotinib-treated leukaemic cells, no relevant shift in terms of macrophages activation and polarisation was observed in either a juxtacrine or paracrine setup. In consistency with the results obtained in the in-vitro experiments, Nilotinib was not potent to elicit a protective immune response in mice within a vaccination assay.

Conclusively, Nilotinib was identified to not qualify as bona fide ICD inducer. The role of Nilotinib-induced cell death and HMGB1 release are proposed as objective for further investigation concerning the synergistic interplay between Nilotinib and a Gas6-deficient environment. Efforts addressing exploration and optimisation of the immunological potential of chemotherapeutic agents are a promising approach aimed at providing cancer patients with the best possible treatment in future.

2 Zusammenfassung

Krebs stellt neben Herz-Kreislauf-Erkrankungen eine der Haupttodesursachen da. Leukämie ist mit einer Häufigkeit von 30 % die häufigste bösartige Erkrankung bei Kindern und gehört zu den zehn führenden Krebsarten bei Erwachsenen. Die Philadelphia-Chromosom-positive B-ALL (Ph⁺ B-ALL) wird durch die zytogenetische Aberration der reziproken chromosomalen Translokation t(9;22)(q34;q11) hervorgerufen, die zur Bildung des Philadelphia-Chromosoms mit einem BCR-ABL1-Fusionsgen führt. Dieses Fusionsgen kodiert ein BCR-ABL1-Onkoprotein, das durch eine konstitutiv erhöhte Tyrosinkinase-Aktivität zu verstärkter Proliferation, Differenzierungsblock und Resistenz gegenüber Zelltod führt. Ph⁺ B-ALL gilt als die aggressivste Form der ALL mit einer Langzeitüberlebensrate von lediglich 30 % trotz intensiver Chemotherapie, die in Kombination mit einem Tyrosinkinase Inhibitor (TKI) eingesetzt wird und welcher sich bei klinisch geeigneten Patienten nach Remission eine allogene Stammzelltransplantation anschließt.

Die Wirksamkeit von Chemotherapien wurde lange Zeit hauptsächlich der Toxizität gegenüber Tumorzellen zugeschrieben, wohingegen immunmodulierende Effekte insbesondere angesichts der bekannten immunsuppressiven Eigenschaften weitgehend unberücksichtigt blieben. Zunehmend zeigt sich jedoch, dass Chemotherapeutika, einschließlich TKI, eine dysfunktionale Tumormikroumgebung (TME) normalisieren oder umstrukturieren und somit eine verstärkte Antitumorimmunität bewirken können. Einer der zugrunde liegenden Mechanismen der Immunmodulation stellt die Induktion von immunogenem Zelltod (ICD) da. ICD ist eine Form des Zelltods, die dadurch charakterisiert ist, dass innerhalb der Tumorthherapie abgetötete Krebszellen in Vakzinen gegen Krebs transformiert werden. Durch die Freisetzung von Damage Associated Molecular Patterns (DAMPs) aus sterbenden Tumorzellen wird ICD induziert, wobei die Translokation von CALR zur Zelloberfläche, die extrazelluläre Sekretion von ATP und die Freisetzung von HMGB1 aus dem Zellkern die zentralen Elemente des ICD darstellen und durch Bindung an antigen-präsentierende Zellen eine tumorantigenspezifische Immunantwort hervorrufen. Neben diesen molekularen Bestimmungsgrößen wird ICD funktionell über eine

Inhibition des Tumorwachstums im Rahmen eines Impftests definiert, in welchem Mäuse lebenden Tumorzellen ausgesetzt werden, nachdem sie zuvor mit den als Vakzine fungierenden Krebszellen geimpft wurden. Zusammen bilden molekulare und funktionelle Kriterien den Goldstandard zur Beurteilung von ICD. Durch die Erhöhung der Immunogenität von Krebszellen trägt ICD zur Wiederherstellung der Immunüberwachung bei, die ein wesentliches Merkmal der Tumorabwehr ist und sich klinisch in einem verbesserten Behandlungsergebnis äußert. Daher stellt die Identifizierung von neuen ICD-Induktoren ein Ziel von Interesse im Hinblick auf Behandlungsstrategien von Krebs dar.

Unter Berücksichtigung dieser Aspekte, ist die Untersuchung des TKI Nilotinib hinsichtlich seiner Fähigkeit, ICD zu induzieren, das Anliegen der vorliegenden Arbeit. Diese steht im Kontext der Forschungsarbeiten der Arbeitsgruppe zur Rolle der Gas6/TAM-Achse innerhalb des TME bei der Entstehung von akuten Leukämien. In den in-vivo-Experimenten unserer Forschungsgruppe wurde konsistent beobachtet, dass der Einsatz von Nilotinib die durch die Deletion von Gas6 vermittelte antileukämische Immunität verstärkt. Vor dem Hintergrund der zunehmenden Bedeutung von Chemotherapeutika als potente Modulatoren eines dysregulierten TME wurde daher die Hypothese aufgestellt, dass Nilotinib mit einer Gas6-defizienten Umgebung durch die Induktion von ICD in Ph⁺ B-ALL-Zellen synergistisch wirken könnte.

In Wachstumshemmungs- und Annexin V/Propidiumiodid-Zelltod-Assays konnte gezeigt werden, dass Nilotinib konzentrationsabhängig Zelltod induziert, welcher in Bezug auf die Zelltodmodalität bimodal apoptotisch und nekrotisch verläuft. Mittels ICD-Markeranalyse, die den durchflusszytometrischen Nachweis der Translokation von CALR, die Chemolumineszenz basierte ATP-Messung und das Immunoblotting für HMGB1 umfasst, wurde festgestellt, dass der durch Nilotinib induzierte Zelltod nicht mit einer CALR-Translokation oder ATP-Sekretion einhergeht, aber mit der Freisetzung von HMGB1 assoziiert ist. In Makrophagen-Co-Kultur-Experimenten mit Nilotinib behandelten leukämischen Zellen wurde weder in einem juxtakrinen noch in einem parakrinen Versuchsaufbau eine relevante Veränderung bezüglich der Makrophagenaktivierung und -polarisation beobachtet. In Übereinstimmung mit den Ergebnissen der in-vitro Experimente konnte Nilotinib im Rahmen des Impftests keine schützende Immunantwort in Mäusen hervorrufen.

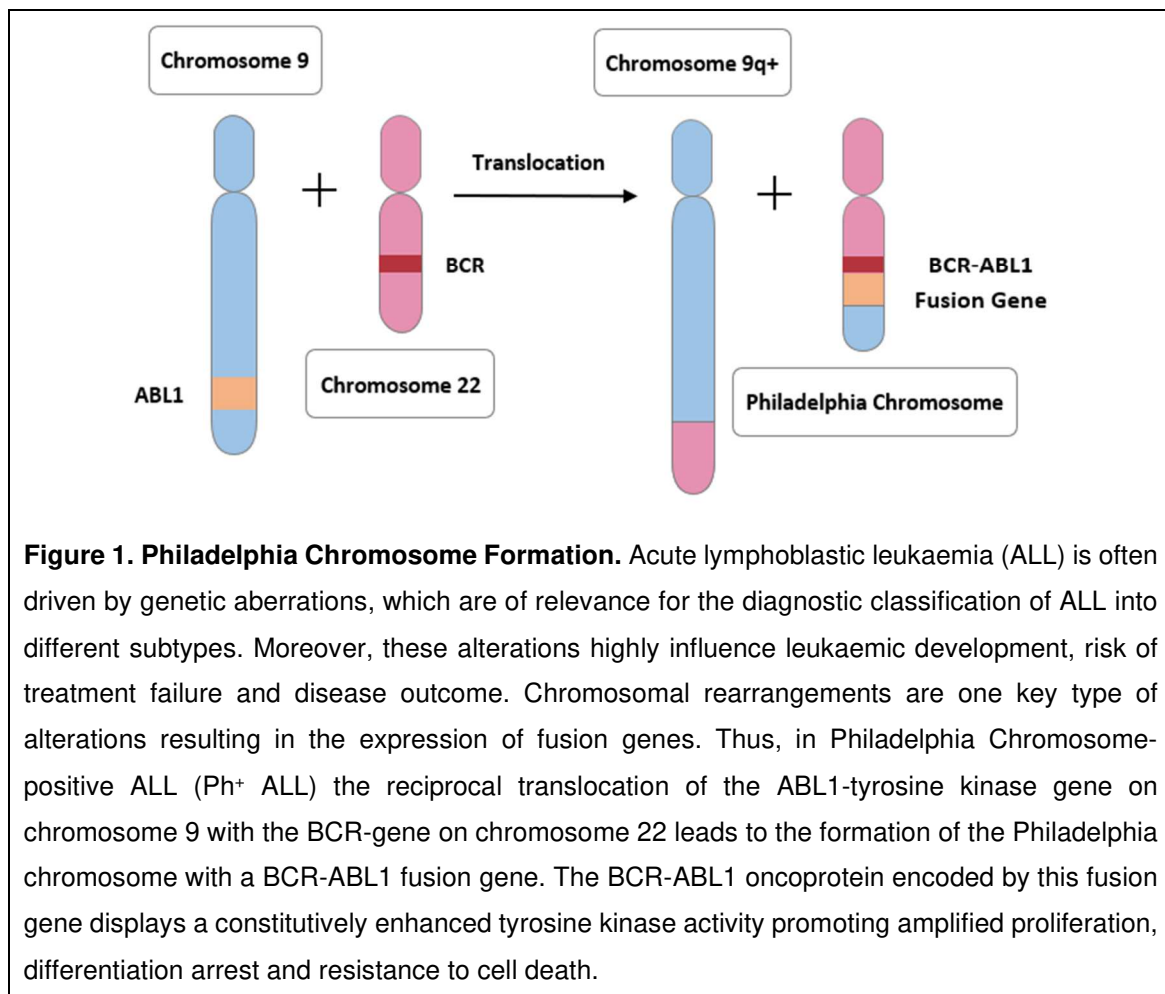
Zusammenfassend wurde herausgearbeitet, dass Nilotinib nicht als Induktor von ICD eingestuft werden kann. Aspekte des Nilotinib induzierten Zelltods und der HMGB1-Freisetzung werden als Gegenstand weiterer Untersuchungen bezüglich des synergistischen Zusammenspiels zwischen Nilotinib und einer Gas6-defizienten Umgebung vorgeschlagen. Bemühungen um die Erforschung und Optimierung des immunologischen Potenzials von Chemotherapeutika stellen einen vielversprechenden Ansatz dar, um Krebspatienten in Zukunft die bestmögliche Behandlung zukommen zu lassen.

3 Introduction

3.1 Philadelphia Chromosome-positive ALL (Ph⁺ ALL)

Cancer is the second leading cause of death after cardiovascular disease.¹ Regarding cancer type, leukaemia is the tenth most common cancer in adults with a frequency of 3.5 % and the most common one in children amounting 30 %.^{1,2} The classification of leukaemia is based on the course of the disease and the affected cell lineage so that a distinction is made between acute and chronic leukaemia on the one hand and between myeloid and lymphoblastic leukaemia on the other.³ Thereof, acute lymphoblastic leukaemia (ALL) is the most common subtype in children, representing up to 80 % of all cases and 20 % of leukaemia in adults.^{4,5} Pathogenetically, ALL is based on an uncontrolled clonal proliferation of aberrant lymphatic cells of haematopoiesis in the bone marrow with blocked cell maturation at a certain level of differentiation.^{6,5,6} The determination of this differentiation stage and the allocation to B- or T-cell lineage is determined according to the antigen expression pattern in immunophenotyping.⁷ Clinically, the increasing suppression of normal haematopoiesis results in progressive bone marrow insufficiency with symptoms typical of anaemia, susceptibility to infection due to leukocytopenia and tendency to bleed as a consequence of thrombocytopenia in addition to accompanying general symptoms such as fever, night sweats and fatigue.⁸ ALL is often characterised by various cytogenetic aberrations accounting for the heterogeneity in clinical disease course and prognosis, notably when comparing paediatric and adult ALL.^{9,10} One of those cytogenetic abnormalities is the chromosomal translocation t(9;22)(q34;q11) leading to the formation of the Philadelphia chromosome with a BCR-ABL1 fusion gene via the reciprocal fusion of the ABL1-tyrosine kinase gene on chromosome 9 with the BCR-gene on chromosome 22 (Figure 1).¹¹ This fusion gene encodes a BCR-ABL1 oncoprotein which is characterized by a constitutively enhanced tyrosine kinase activity resulting in amplified proliferation, differentiation arrest and resistance to cell death.^{12,13} Philadelphia chromosome-positive ALL (Ph⁺ ALL) presents 25 % of adult ALL, and about 4 % of paediatric ALL cases.^{14,15} The standard treatment

regimen includes intensive chemotherapy in combination with a tyrosine kinase inhibitor (TKI) followed by allogeneic stem cell transplantation after remission for clinically fit patients.¹⁶ The significant improvement in outcome compared to the very poor prognosis of Ph⁺ ALL prior to the introduction of TKI is due to both the fact that more patients are qualified to receive stem cell transplantation and to a reduced dependence on potentially highly toxic chemotherapy.^{16,17} Nevertheless, despite an initial remission rate of up to 95 %, the 5-year survival rate remains 33 % to 46 % because of emerging resistance to TKI and relapses.^{18,19} Various acquired and intrinsic mechanisms of resistance have been revealed, notably including mutations that prevent TKI binding, like T315I, or reduce TKI binding affinity by an altered protein confirmation, such as L248V.²⁰⁻²² This has led to the development of second (Nilotinib, Dasatinib, Bosutinib) and third (Ponatinib) generation TKIs overcoming the resistance observed in the first generation TKI Imatinib.²³



3.2 Immunotherapy and Tumour Microenvironment

However, despite great efforts and continuous improvement, the treatment of cancer with conventional therapy concepts such as tumour surgery, chemo- and radiotherapy remains suboptimal.²⁴ This gave rise to the investigation of alternative approaches such as immunotherapy, that has become an established part of cancer treatment improving prognosis and outcome in a broad field of malignant diseases.^{25,26} The functional principle of immunotherapy involves the enhancement of immune response in a general way and, in special, the promotion of the immune system in order to attack cancer cells.²⁷ More detailed, immunotherapy operates by (1) targeting immunosuppressive and tumour-promoting metabolism, (2) altering tumour microenvironment, (3) stimulating innate and adaptive anti-tumour immune response, (4) advancing detection of tumour cells that have escaped the immune system and (5) inhibiting oncogenic inflammation.²⁸ To address those objectives, several strategies are under investigation as illustrated in Figure 2, which are categorized in clinical use as antibody therapy, cellular immunotherapy, immune adjuvants therapy and combination immunotherapy.^{28,29} Although immunotherapy has proven to be a beneficial option for cancer treatment especially when used in synergistic combination with conventional tumour therapy, there is growing evidence that differences in the response to cancer immunotherapy are related to the heterogeneity of the tumour microenvironment (TME).³⁰⁻³² The tumour microenvironment is composed of tumour cells, tumour-infiltrating immune cells (TIICs), cancer-associated fibroblasts (CAFs), the tumour vasculature and the extracellular matrix (ECM).^{33,34} Strikingly, the tumour microenvironment is characterized by the contrary ability to provoke both beneficial and adverse conditions for tumorigenesis in dependency of the interactions within the TME underlining the important role in either suppressing or enhancing anti-tumour immune response (Figure 3).³⁵⁻³⁸ A tumour-promoting, immune-suppressive tumour microenvironment exhibits a variety of mechanisms such as (1) supporting neoplastic transformation and sustaining tumour growth, (2) inducing angiogenesis, (3) enabling immortality by resistance to cell death, (4) altering and escaping the immune system of the host, (5) activating invasion and metastasis, (6) providing niches for dormancy and (7) fostering therapeutic resistance.³⁹⁻⁴¹

As a consequence, targeting the complexity of the tumour microenvironment is a promising approach in the field of cancer therapy.^{42,43}

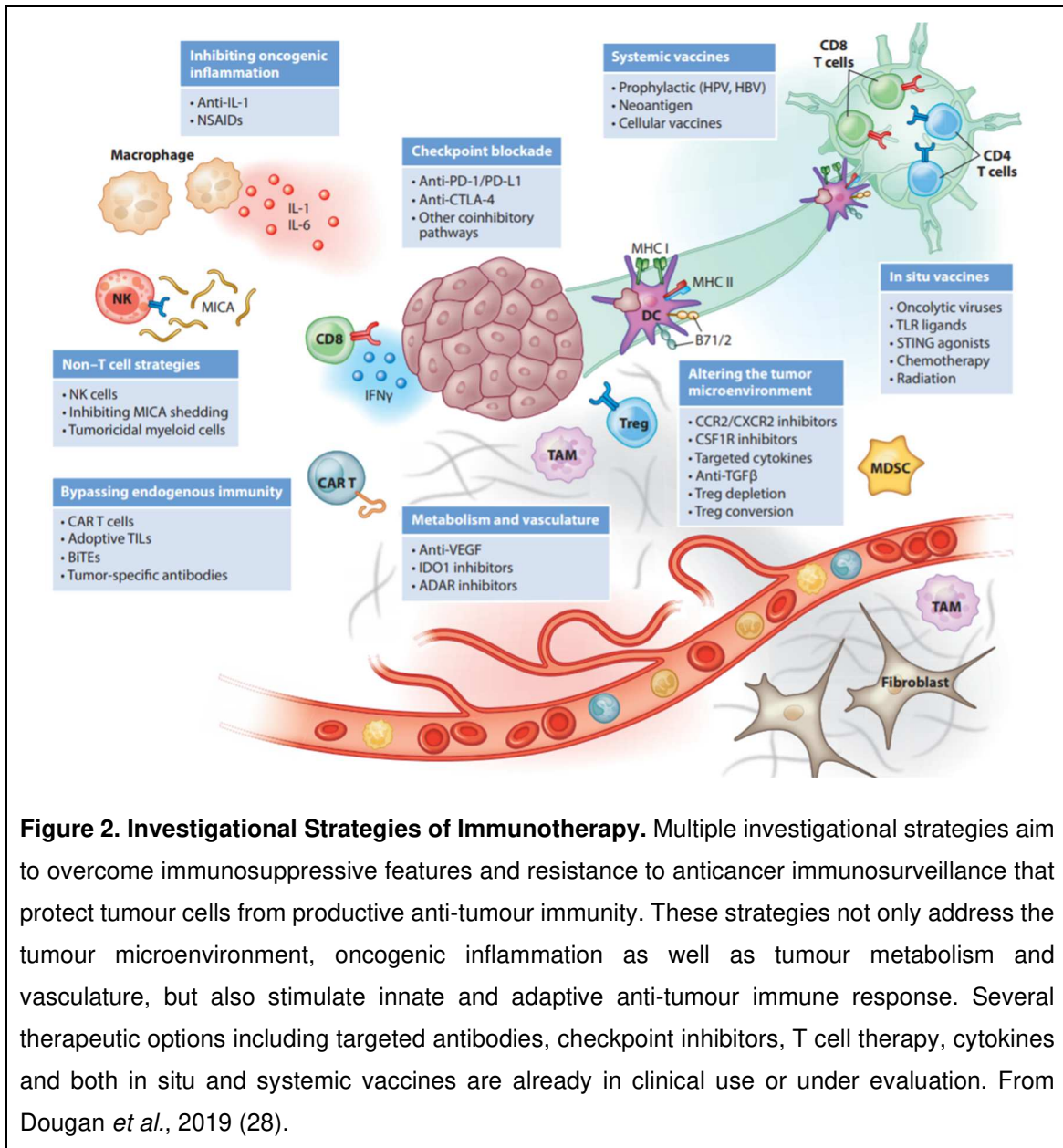
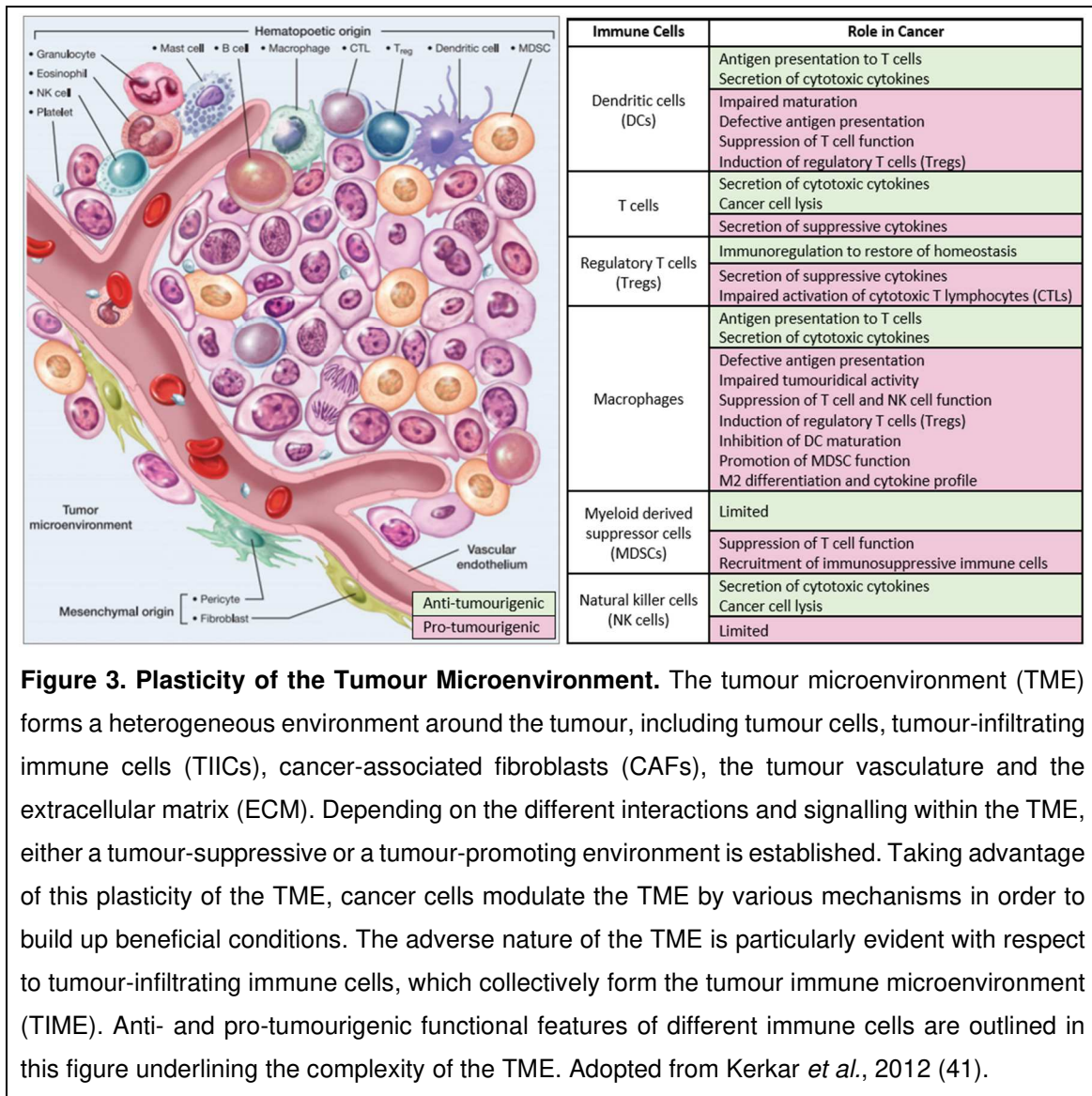


Figure 2. Investigational Strategies of Immunotherapy. Multiple investigational strategies aim to overcome immunosuppressive features and resistance to anticancer immunosurveillance that protect tumour cells from productive anti-tumour immunity. These strategies not only address the tumour microenvironment, oncogenic inflammation as well as tumour metabolism and vasculature, but also stimulate innate and adaptive anti-tumour immune response. Several therapeutic options including targeted antibodies, checkpoint inhibitors, T cell therapy, cytokines and both in situ and systemic vaccines are already in clinical use or under evaluation. From Dougan *et al.*, 2019 (28).



3.3 Research Background

The research work of our group is aimed to address the tumour microenvironment in the context of the pathogenesis of malignant diseases in the haematopoietic system. The work is focused on the mechanisms contributing to the establishment of an immune-suppressive environment in acute leukaemia and, in particular, on the role of the Gas6/TAM axis in anti-leukaemic immunity.

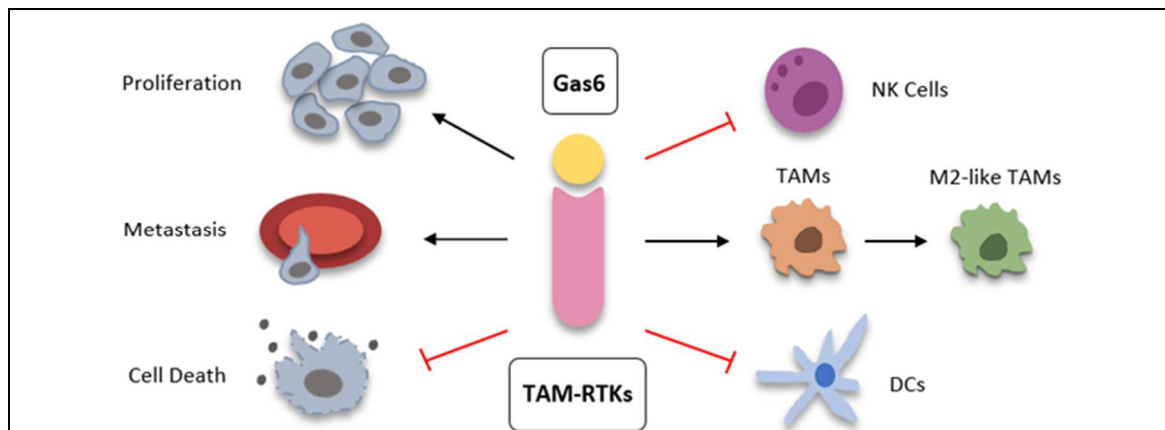


Figure 4. The Role of Gas6/TAM in Cancer Cells and the Tumour Microenvironment. Growth arrest-specific 6 (Gas6) displays its effects by binding to the receptor tyrosine kinases (RTKs) Axl, Tyro3 and Mer, that are collectively named TAM. In cancer cells Gas6/TAM signalling not only promotes cancer cell proliferation and metastasis but also inhibits cell death. Moreover, Gas6/TAM targets diverse immune cell functions resulting in the establishment of an immune-suppressive tumour microenvironment (TME). These transformations include both the inhibition of natural killer (NK) and dendritic cell function as well as the polarisation of tumour-associated macrophages (TAMs) towards a M2-like phenotype.

Gas6, also known as Growth arrest-specific 6, is a member of the vitamin K-dependent family of proteins binding with decreasing affinity to the receptor tyrosine kinases (RTKs) Axl, Tyro3 and Mer, that are collectively named TAM.⁴⁴ Next to diverse processes including proliferation, differentiation, apoptosis, leucocyte migration and platelet aggregation,^{45,46} Gas6 has been found to contribute to the development of several cancers,⁴⁷⁻⁵² including acute leukaemia,⁵³⁻⁵⁵ in which overexpression of Gas6/TAM is associated with an unfavourable prognosis.^{54,55} In the context of cancer development and progression, Gas6 has been described to promote cancer cell proliferation, sustain cancer cell survival by inhibiting apoptosis and induce cancer cell migration.⁵⁶⁻⁵⁸ Moreover, Gas6/TAM signalling has been found to modulate the tumour microenvironment resulting in an immune-suppressive, non-inflammatory, tissue-repair phenotype.^{59,60} The Gas6/TAM axis affects the tumour microenvironment by targeting diverse components and functions, including those of immune cells.⁶¹ The effects on the tumour immune microenvironment (TIME) result from the instruction of stromal cells and macrophages to secrete Gas6 into the TME altering cellular immune response by

binding to TAM receptors on immune cells.^{61,62} The changes in cellular immune response comprise (1) the inhibition of tumour eradicating activity of natural killer cells (NK cells), (2) the impairment of cytokine production and antigen presentation of dendritic cells (DCs) and (3) the polarisation of tumour-associated macrophages (TAMs) towards a M2-like phenotype (Figure 4).⁶³⁻⁶⁶ With regard to their immunogenic function, cytokine profile and surface marker expression, macrophages can be classified into classically activated (M1) and alternatively activated (M2) macrophages.⁶⁷ While M1 macrophages exhibit pro-inflammatory, tissue-damaging, immune-stimulating and tumour-suppressive attributes, M2 macrophages display anti-inflammatory, tissue-remodelling, immune-regulatory and tumour-promoting properties (Figure 5).⁶⁸⁻⁷⁰ However, typical M1 and M2 phenotypes represent extremes of the heterogeneity in macrophage functional stage, emphasising the dynamic plasticity in macrophage polarisation as a reaction to different microenvironmental stimuli.⁷⁰ Remarkably, tumour-associated macrophages cannot be explicitly assigned to a M1 or M2 phenotype, but they are often associated with a tumour-promoting M2-like phenotype (Supplementary Figure S1, page 88).⁷¹⁻⁷⁴

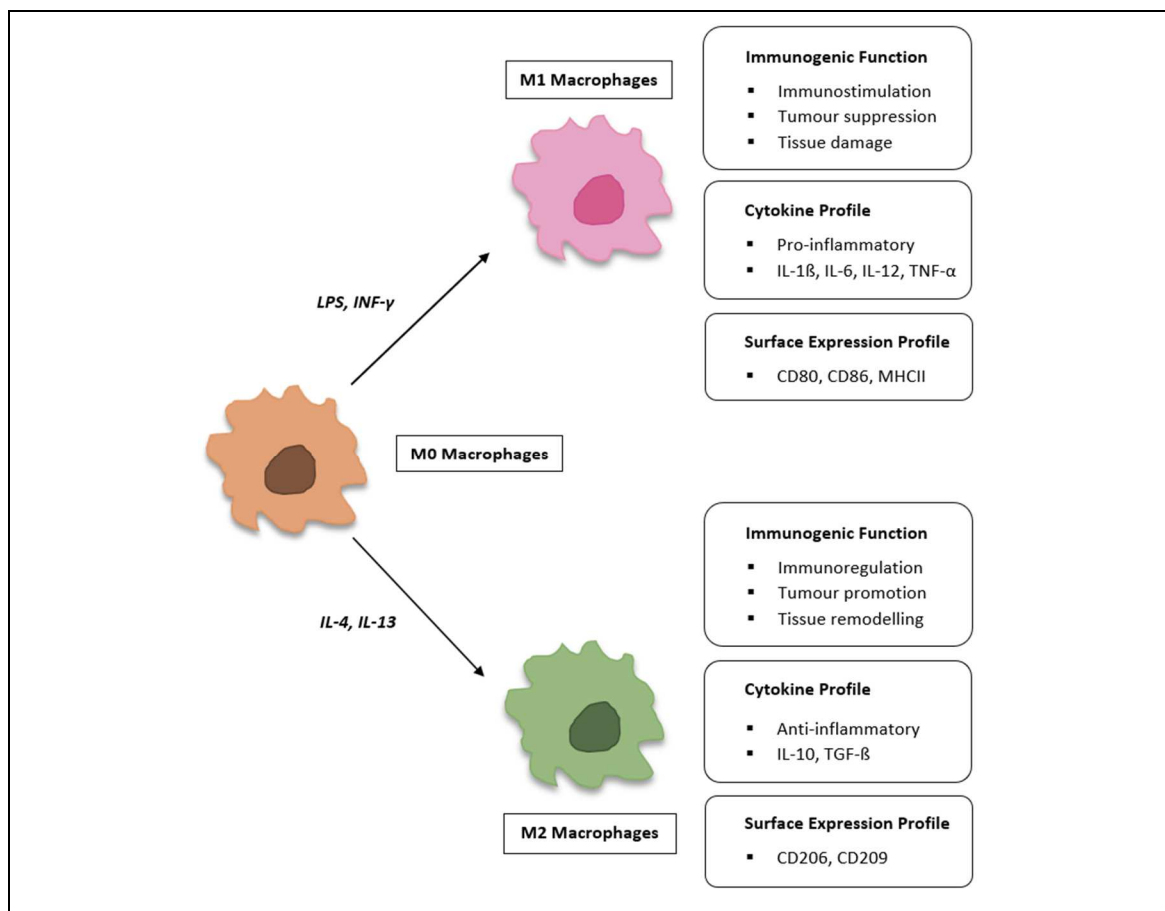


Figure 5. Macrophage Polarisation. Macrophage polarisation describes the process of macrophage differentiation to adopt a phenotype in response to different environmental stimuli. According to the binary polarisation concept, macrophages are classified into classically activated (M1) and alternatively activated (M2) macrophages regarding their immunogenic function, cytokine profile and surface marker expression. Thus, M1 macrophages exhibit immune-stimulating, tumour-suppressive, tissue-damaging and pro-inflammatory attributes, whereas M2 macrophages display immune-regulatory, tumour-promoting, tissue-remodelling and anti-inflammatory properties. However, typical M1 and M2 phenotypes represent extremes of heterogeneity in macrophage functional stage, emphasising the diverse spectrum of macrophage subtypes and the dynamic plasticity of polarisation.

3.4 Immunogenic Cell Death (ICD)

Targeting Gas6/Axl axis is a complex but promising approach in cancer treatment. The findings of our group demonstrate that addressing Gas6/Axl signalling, by ablation of Gas6 in the TME or Axl in macrophages, promotes both anti-leukaemic immune response and memory resulting in leukaemic clearance and prolonged survival in pre-clinical mouse models of acute leukaemia when combined with standard of treatment.

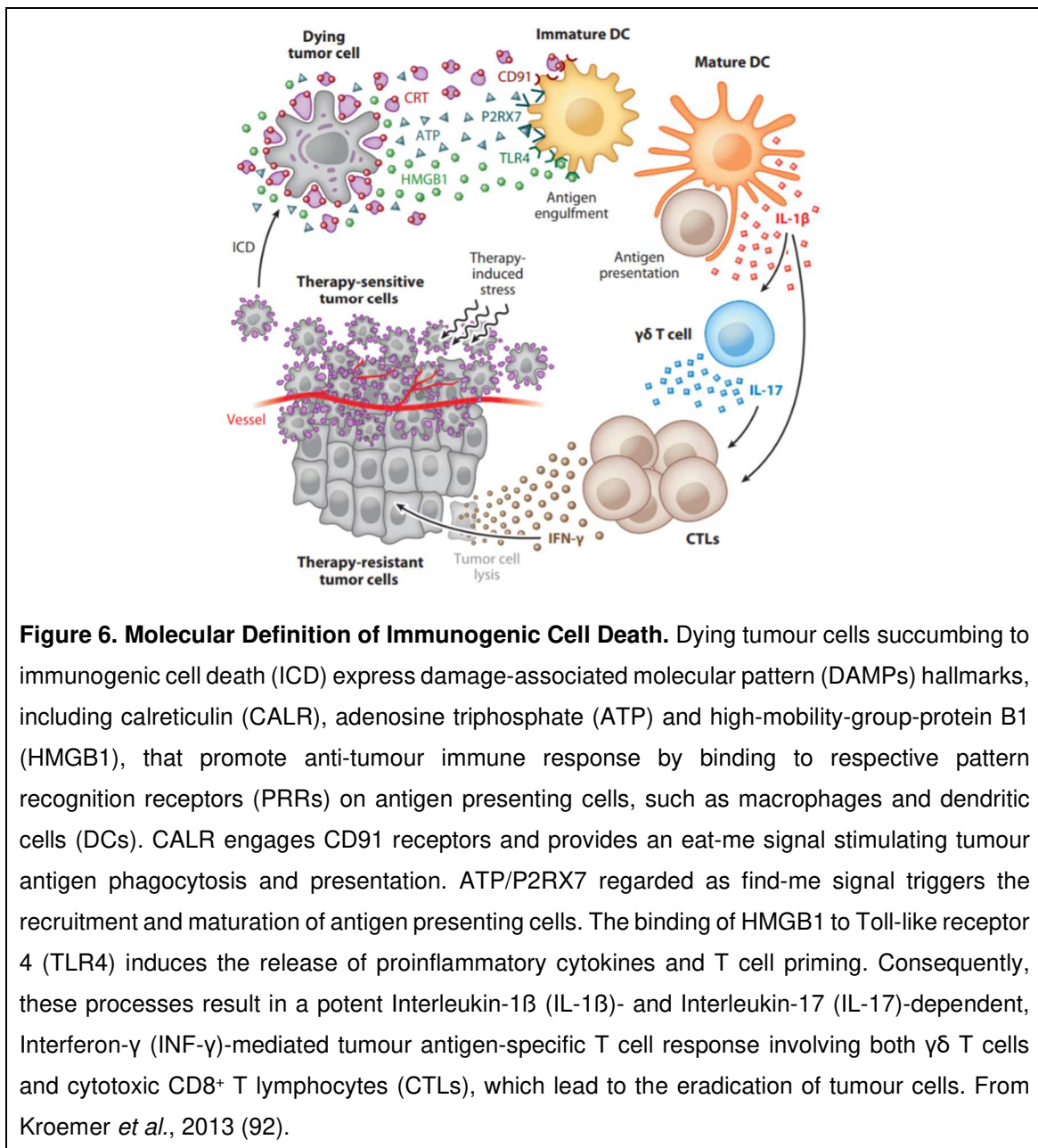
The combination of immunotherapy with conventional chemotherapy is a conducive strategy to improve cancer treatment, but little is known about the effects of chemotherapeutic agents on the tumour microenvironment.⁷⁵ Given the concerns about the various immunosuppressive effects, chemotherapy has not been considered an immunological modality.⁷⁶ However, in different studies certain chemotherapeutic agents have been shown to improve anti-tumour immune response and even reverse immune tolerance by modulating the TME.⁷⁶⁻⁷⁸ The underlying mechanisms of immune modulation include (1) the eradication of immune-suppressing regulatory T cells (Tregs) and myeloid-derived suppressor cells (MDSCs), (2) the activation and maturation of DCs, (3) the promotion of TAM accumulation and reprogramming towards an immune-stimulating activity, (4) the facilitation of tumour infiltration by NK cells and cytotoxic T lymphocytes (CTLs), (5) the upregulation of class I major histocompatibility complex (MHCI) molecules on cancer cells and (6) the induction of immunogenic cell death (ICD).^{77,79,80}

Immunosurveillance is an essential feature of cancer rejection.⁸¹ Resistance to host anticancer immunosurveillance and anti-tumour immunity is acquired through several mechanisms, involving exhibition of low immunogenicity, induction of immunotolerance or active immunosuppression and evasion of immune cell-mediated lysis.^{82,83} To reinforce immunosurveillance, immunogenicity of dying or dead cancer cells can be increased by immunogenic cell death.⁸⁴

ICD is a cell death modality determined by the capacity to convert dying or dead cancer cells into vaccines leading to an antigen-specific anti-cancer immune response.⁸⁵ So far, a variety of agents have been identified as potent inducers of ICD, including chemotherapeutics, radiotherapy, biological therapeutics and physio-chemical or mechanical stress-based therapies.⁸⁶ Molecularly, ICD is characterised by spatiotemporal release of damage-associated molecular patterns (DAMPs) via endoplasmic reticulum (ER) stress triggering immune-stimulating effects upon binding to pattern recognition receptors (PRRs) expressed by immune cells.⁸⁷ Thus, DAMPs act as danger signals mediating the immunogenicity and anti-cancer vaccine effect of ICD.^{88,89} With regard to the mechanism of ICD induction, ICD is classified in type I and type II ICD.⁹⁰ Type I ICD is induced through collateral ER stress effect, indirectly evoking ICD-associated danger signalling, whereas, in contrast, type II ICD induction selectively targets the ER, promoting focused ER stress effect.⁹⁰ Next to diverse DAMPs contributing to the immunogenicity of cell death in a limited amount, translocation of ER chaperon calreticulin (CALR) to the cell surface, extracellular secretion of adenosine triphosphate (ATP) and release of endogenous Toll-like receptor (TLR) agonist high-mobility-group-protein B1 (HMGB1) from the nucleus are attributed a key role.⁹¹⁻⁹⁴ CALR, ATP and HMGB1 released by dying tumour cells succumbing to ICD bind to CD91, P2RX7 and TLR4, respectively, on macrophages and dendritic cells to mediate anti-tumour immune effects.⁹⁵ These effects comprise (1) the engulfment and presentation of tumour antigens operated by CALR as eat-me signal, (2) the recruitment and maturation of antigen presenting cells facilitated by ATP as find-me signal and (3) the release of proinflammatory cytokines as well as T cell priming stimulated by HMGB1, finally resulting in (4) the eradication of tumour cells by tumour-specific cytotoxic CD8⁺ T lymphocytes (Figure 6).^{84,95,96} Accordingly, CALR exposure, ATP secretion and

HMGB1 release are considered as references for predicting the ICD-inducing capacity of anti-cancer agents.⁹⁷

However, besides these molecular determinants of immunogenic cell death, ICD is defined by tumour-rejecting immunity in a vaccination context.⁹⁶ In fact, gold-standard approach to assess bona fide ICD is based on in-vivo vaccination assays.⁹⁸ In this setting, cancer cells are exposed to a potential ICD inducer in-vitro and then injected into immunocompetent mice, followed by a re-challenge with live cancer cells of the same cancer type.⁹⁹ Hence, bona fide ICD is induced if resulting in inhibition of tumour growth, that is based on the activation of an effective anti-tumour immune response (Figure 7).⁸⁰



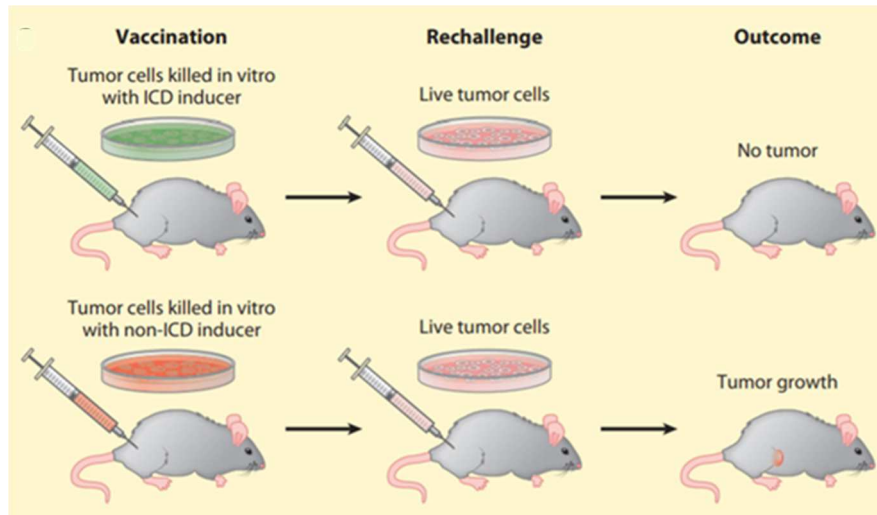


Figure 7. Functional Definition of Immunogenic Cell Death. From an operational point of view, immunogenic cell death (ICD) is defined by tumour-rejecting immunity in an in-vivo vaccination assay. Therefore, tumour cells are exposed to a potential ICD inducer in-vitro and then injected into immunocompetent mice, followed by a re-challenge with live tumour cells of the same cancer type. The operational definition of a bona fide ICD-inducer is fulfilled if a protective tumour-specific immune response is elicited resulting in the inhibition of tumour growth. From Kroemer *et al.*, 2013 (92).

3.5 Objective and Prospect

Addressing immunogenic cell death in the tumour microenvironment provides a strategy to simulate a dysfunctional anti-tumour immune system.⁹⁷ The induction of ICD contributes to the restoration of immunosurveillance and the establishment of immunological memory with long-lasting protective anti-tumour immunity, resulting in improved therapeutic efficacy and disease outcome in patients.^{100,101} Therefore, identifying novel ICD inducers is an objective of interest in the context of cancer immunotherapy.¹⁰¹

In respect of these considerations, the aim addressed in the present work is to examine the second-generation tyrosine kinase inhibitor Nilotinib for its ability to induce immunogenic cell death. The work is in the context of the group's research on the role of Gas6/TAM signalling within the tumour microenvironment regarding the pathogenesis of acute leukaemia. Hence, the question arises whether Nilotinib synergizes with a Gas6-deficient environment by inducing immunogenic cell death in Ph⁺ ALL to promote anti-tumour immunity.

In accordance with the criteria for assessing an anti-cancer agent for its capacity to induce immunogenic cell death, Nilotinib was investigated for the molecular and functional determinants of ICD in in-vitro and in-vivo experiments. The in-vitro experiments were performed on Ph⁺ ALL cell lines, whereby those were exposed to Nilotinib as a potential ICD inducer as well as to the commonly known ICD inducer Mitoxantrone^{85,80,85} in the sense of a positive control. In addition, untreated leukemic cells were used as negative control in the experiments. For in-vivo evaluation, a vaccination assay was performed on a Gas6 knockout (Gas6KO) mouse model on a C57BL/6 background.

The underlying methods as well as the obtained results and their evaluation are displayed hereinafter.

4 Material and Methods

4.1 Material

4.1.1 Consumable Material

The list of the consumable material is attached in the appendix (Table 1, page 89).

4.1.2 Reagents and Chemicals

Reagents and chemicals used in the experiments are listed in the appendix (Tables 2-7, page 90-96).

4.1.3 Antibodies

Table 8: Antibodies for Flow Cytometry

<i>Antigen (Catalogue Number)</i>	<i>Conjugate</i>	<i>Dilution</i>	<i>Manufacturer</i>
Annexin V (550474)	APC	1:20	BD Bioscience, Franklin Lakes, NJ, US
Calreticulin (MAB38981)	-	0.25 µg/10 ⁶ cells, 500 µg/mL	R&D Systems, Minneapolis, MN, US
CD11b (562317)	PE-CF594	1:1000	BD Bioscience, Franklin Lakes, NJ, US
CD16/CD32 Fc receptor block (553141)	-	1:1000	BD Bioscience, Franklin Lakes, NJ, US
CD45 (564225)	BV786	1:300	BD Bioscience, Franklin Lakes, NJ, US

CD45R/B220 (553092)	APC	1:1000	BD Bioscience, Franklin Lakes, NJ, US
CD45R/B220 (563894)	BV786	1:1000	BD Bioscience, Franklin Lakes, NJ, US
CD80 (560523)	V450	1:300	BD Bioscience, Franklin Lakes, NJ, US
CD86 (560582)	PE-Cy7	1:1000	BD Bioscience, Franklin Lakes, NJ, US
CD206 (565250)	APC	1:100	BD Bioscience, Franklin Lakes, NJ, US
F(ab') ₂ Fragment (715-586-150)	Alexa Fluor 594	1:500	Jackson ImmunoResearch, Bar Harbor, ME, US
F4/80 (565410)	PE	1:300	BD Bioscience, Franklin Lakes, NJ, US
MHCII (563415)	BV650	1:1000	BD Bioscience, Franklin Lakes, NJ, US
Propidium iodide (P1304MP)	PerCP	1:5000	Thermo Fisher Scientific, Waltham, MA, US

Table 9: Antibodies for Western Blot

<i>Antigen (Catalogue Number)</i>	<i>Conjugate</i>	<i>Dilution</i>	<i>Manufacturer</i>
HMGB1 (MAB16901)	-	1:5000	R&D Systems, Minneapolis, MN, US
IgG (NA935)	HRP	1:10000	Amersham Biosciences, Little Chalfont, UK
α -Tubulin (ab4074)	-	1:300	Abcam, Cambridge, UK
IgG (ab6721)	HRP	1:10000	Abcam, Cambridge, UK

Table 10: Antibodies for Immunohistochemistry

<i>Antigen (Catalogue Number)</i>	<i>Conjugate</i>	<i>Dilution</i>	<i>Manufacturer</i>
GFP (ab6673)	-	1:1000	Abcam, Cambridge, UK
Granzyme B (ab4059)	-	1:500	Abcam, Cambridge, UK

4.1.4 Chemotherapeutic Agents

Mitoxantrone was purchased from Sigma-Aldrich and supplied as crystalline solid of Mitoxantrone hydrochloride. A 2 mM stock solution was made by dissolving 10 mg Mitoxantrone hydrochloride in 9.7 mL ethanol while sonicating to be then aliquoted and stored at -20 °C.

Nilotinib was purchased from APEX BIO and supplied as lyophilized powder. To prepare a 10 mM stock solution 100 mg of Nilotinib was dissolved in 18.9 mL Dimethyl sulfoxide (DMSO). Aliquots were stored at -20 °C.

Table 11: Chemotherapeutic Agents

<i>Product Name (Catalogue Number)</i>	<i>Manufacturer</i>
Mitoxantrone dihydrochloride (M6545)	Sigma-Aldrich, St. Louis, MO, US
Nilotinib, AMN-107 (A8232)	APEX BIO, Houston, TX, US

4.1.5 Leukaemic Cell Lines (BCR-ABL B-ALL)

BCR-ABL B-ALL leukaemic cell lines were generated by Jacques Ghysdael, Research Director of Cellular Signaling and Oncogenesis at the Institut Curie in Paris. For this, whole bone marrow from Arf knockout (*Arf*^{-/-}) mice (CDKN2A) was transduced with BCR-ABL-IRES-GFP retrovirus and subsequently transplanted

intravenously into sub-lethally irradiated (9 Gy) recipient wild-type mice. BCR-ABL-induced B-ALL developed individually in mice as primary leukaemias. Then primary leukaemias were cell culture adapted to generate successively stable leukaemic cell lines, such as the leukaemic cell lines L1-1 and L3 that are used in the experiments.

4.1.6 Mouse Stock

C57BL/6 wild-type mice were obtained from Charles River Laboratories. Gas6 knockout mice on a C57BL/6 background were generated by UCDAVIS KOMP Repository at the University of California Davis and Children's Hospital Oakland Research Institute.

Keeping of animals was performed according to the guidelines of Regierungspräsidium Darmstadt, Dezernat V 54 für Veterinärwesen und Verbraucherschutz. All experiments involving mice procedures were approved by the IACUC.

4.1.7 Devices and Software

The list of the devices and software is attached in the appendix (Table 12, page 96).

4.2 Methods

4.2.1 Cell Culture

L1-1 and L3 leukaemic suspension cells were routinely cultured in tissue culture flasks in leukaemic cell line medium containing RPMI 1640 Medium supplemented with 15 % heat-inactivated Foetal Bovine Serum (FBS), 1 % L-Glutamine (200 mM) and 1 % Pen Strep (10000 U/mL Penicillin, 10000 µg/nL Streptomycin) at 37 °C in a 5 % CO₂ humidified incubator. In order to keep growth and colony conditions constant, leukaemic cells were passaged every second or third day according to their cell density. As suitable cell density 0.2 x 10⁶ to 0.5 x 10⁶ leukaemic cells per 1 mL medium were considered. Leukaemic cells were cultured no more than 12 passages before used in in-vitro or in-vivo experiments.

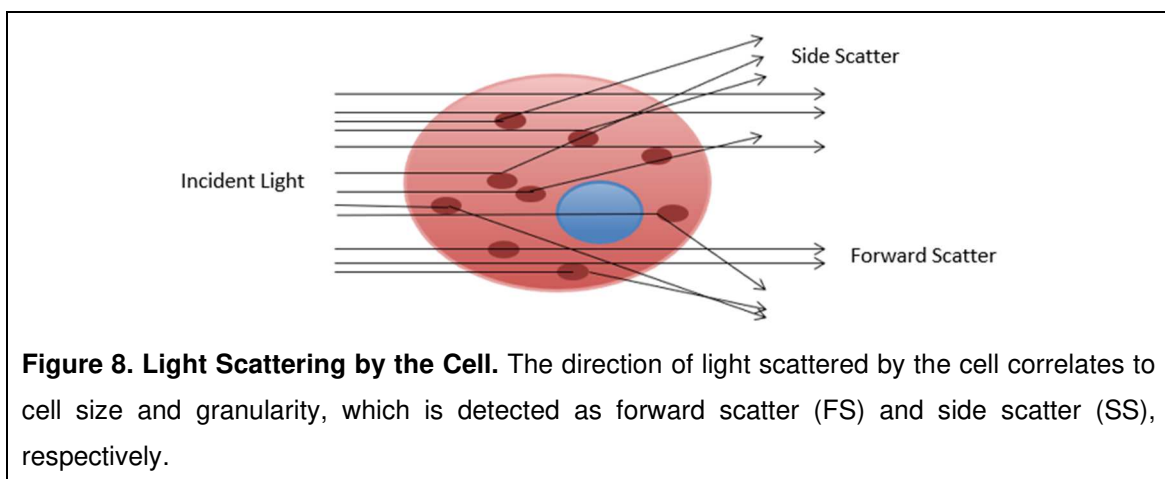
4.2.2 Growth Curve and Viability Count

To study the dynamics of cell growth and viability under the treatment with Nilotinib and Mitoxantrone, 0.2 x 10⁶ L1-1 and L3 leukaemic cells were seeded in triplicate in 12-well plates in 1 mL leukaemic cell line medium and treated with increasing concentrations of Nilotinib using 10 nM, 50 nM, 100 nM, 500 nM and 1000 nM Nilotinib or 1 µM Mitoxantrone. An untreated triplicate of both leukaemic cell lines was performed as untreated control. Number and viability of leukaemic cells per well were both monitored using the light microscope and counted by ViCell XR Cell Counter every 24 hours up to five days. To maintain appropriate culture conditions as well as to keep concentrations of Nilotinib and Mitoxantrone effective, every second day leukaemic cells were split at a 1:2 ratio, medium was exchanged and retreatment with Nilotinib or Mitoxantrone was performed at indicated concentrations in the respective wells.

4.2.3 Flow Cytometry

Flow cytometry is a method to detect the expression of cell surface and intracellular molecules.

The functional principle is based on the detection of scattered light emitted by cells passing through a light beam. Hydrodynamic focusing by a sheath fluid allows the cells in suspension to pass through the laser beam aligned one cell at a time. Light emitted by a laser light source and scattered by the passing cells is sensed by distinct detectors. A detector in front of the light beam facilitates the measurement of forward scatter (FS) and several detectors to the side of side scatter (SS) (Figure 8). As FS is proportional to cell size and SS correlates with cell granularity, cell populations can be distinguished by differences in their size and granularity in this manner (Figure 9). Next to determine cells based on FS and SS, cells can be analysed by their expression of particular proteins. For this, a fluorochrome-conjugated antibody stains the cell by binding to the referring protein of interest. The fluorescent stained cells are able to be detected individually by the emitted light of the fluorochrome when excited by a laser with the corresponding excitation wavelength. This signal of emission is converted to a voltage pulse, known as event, and amplified linearly or logarithmically. The total event height and area is measured by the flow cytometer whereby the measured event area correlates directly to the intensity of fluorescence (Figure 10).



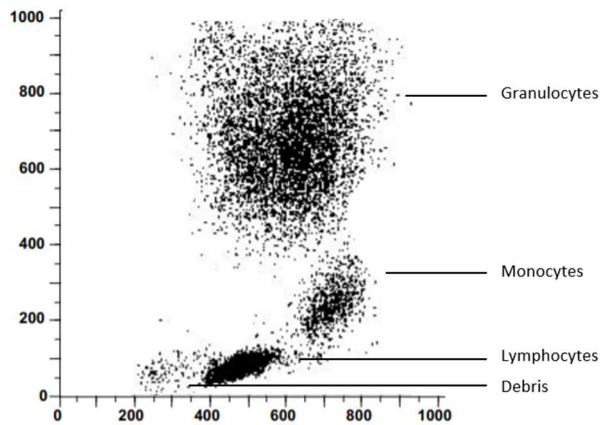


Figure 9. Determination of the Cell Population based on FS and SS in a flow cytometric Data Analysis. Dot plot of forward scatter versus side scatter of a bone marrow sample showing the characteristic position of different cell populations. Each dot represents a single cell analysed by the flow cytometer. Adapted from Riley R. S. Principles and Applications of Flow Cytometry. <http://www.flowlab-childrens-harvard.com>. Accessed January 10, 2020.

The process of using fluorochrome-labelled antibodies is called direct staining. In contrast to this, in indirect staining an antibody without fluorochrome conjugation binds to the target protein and is then detected by a fluorochrome-labelled secondary antibody. Flow cytometry can be used to perform extracellular staining of surface proteins as well as to run intracellular staining of proteins within the cell after fixation and permeabilization with specific agents.

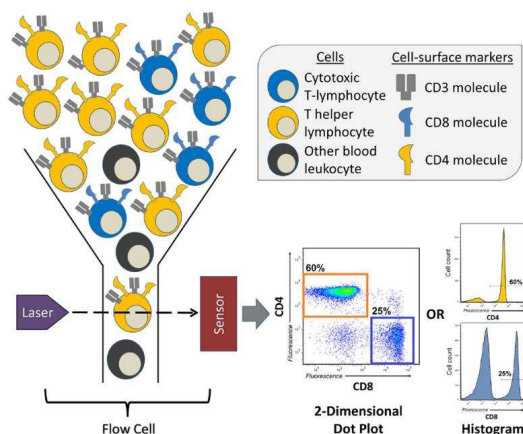


Figure 10. Set-up and functional Principle of Flow Cytometry and Data Analysis. Cells pass through the laser beam focused by a sheath fluid one cell at a time. Both forward and side scattered light as well as fluorescence emitted from stained cells are detected by a sensor. The derived information is visualised digitally as two-dimensional dot plots or one-dimensional histograms allowing the quantification of frequency of the analysed cells. From Verschoor *et al.*, 2015 (1).

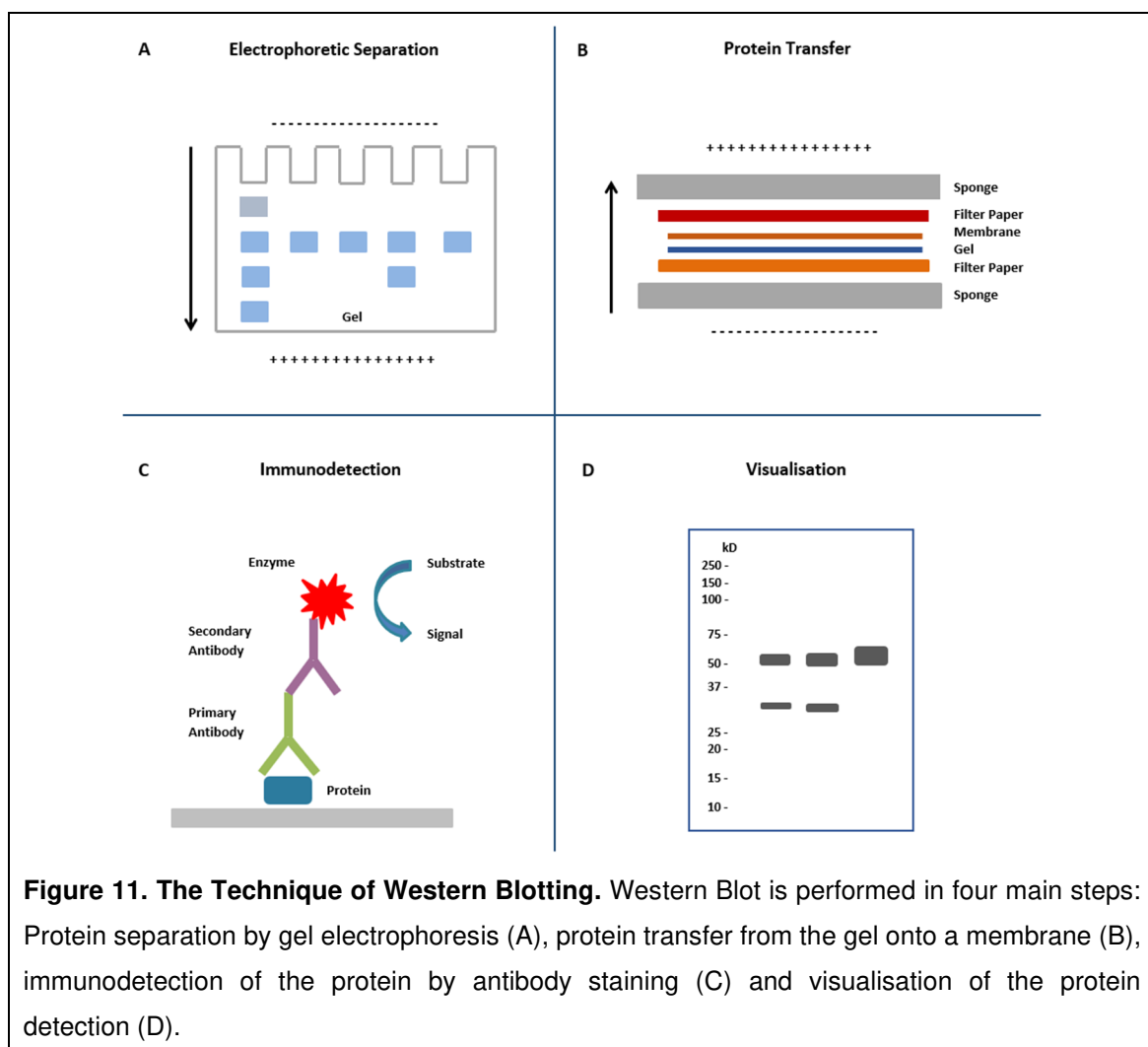
Taking into account the mentioned aspects about flow cytometry, this method was used to analyse different cell types in heterogenous cell populations of different experiments. Thereby, cells were classified within a specific gating strategy regarding not only FS and SS but also their fluorescence. In order to correct the signal overlap between the channels of the emission spectra of different fluorochromes, compensation was performed for all experiments. To avoid non-specific binding all samples were incubated with an Fc receptor blocking antibody. Antibodies with respective dilutions used in the experiments are listed in Table 8. All antibody-mixes were prepared on ice using DPBS containing 2 % FBS as staining buffer. To each sample 50 μ L of antibody-mix were applied for staining, that was performed at room temperature in the dark. Before and after staining as well as between different staining steps, cells were washed twice with DPBS by spinning down for 5 minutes at 1500 revolutions per minute (rpm) at 4 °C and discarding the supernatant. For flow cytometry analysis cells were then re-suspended in FACS buffer using 300 μ L of DPBS supplemented with 2 % FBS. Flow cytometry data were acquired on a BD LSRFortessa Flow Cytometer and analysed using FlowJo software. At least 10000 events were acquired per sample.

4.2.4 Western Blot

Western Blot is a technique to detect a protein of interest in a complex protein mixture by specific antibody-antigen interactions that allows a qualitative and semi-quantitative analysis of the target protein.

The first step in a western blotting procedure is the sample preparation including the lysis in an appropriate lysis buffer as well as the reduction in sample buffer and the following heat denaturation. Thereafter, proteins are separated by gel electrophoresis commonly using polyacrylamide gel electrophoresis (PAGE). While native PAGE separates proteins according to their mass-charge ratios, sodium dodecyl sulphate-PAGE (SDS-PAGE) separates proteins based on their mass only by masking the endogenous protein charge with a negative charge. Thus, upon application of an electric field, proteins of lower molecular weight run faster towards the positive cathode.

Following electrophoresis, proteins are transferred from the gel onto a membrane generally made of nitrocellulose or polyvinylidene difluoride (PVDF). Electrophoretic transfer, performed as wet or semi-dry transfer, is the most used transfer method allowing the negatively charged proteins to move out of the polyacrylamide gel towards the positive cathode and onto the membrane when an electric field is applied. In order to prevent non-specific binding and to reduce background interference, the free sites on the membrane are blocked with a blocking buffer before antibody staining. The process of immunodetection is performed by probing the blocked membrane in a first step with a primary antibody that binds to the protein of interest and in a second step with an enzyme-conjugated secondary antibody. Finally, adding chromogenic, fluorogenic or chemiluminescent substrates allows the visualisation of signal development that is based on the enzyme-substrate reaction and detected with a suitable detection system.



To check for equal loading of the gel and a correct transfer of the proteins onto the membrane, ideally, a loading control is done when running a Western Blot. Hence, antibodies used for loading controls target housekeeping proteins showing a ubiquitous and consistently high level of expression. The technique of Western blotting is illustrated in Figure 11.

4.2.5 Cell Death Assay

In order to assess the modality of Nilotinib-induced cell death in leukaemic cell lines, 1×10^6 L1-1 and L3 leukaemic cells were plated in 12-well plates in 2 mL leukaemic cell line medium and treated with Nilotinib at increasing concentrations of 10 nM, 50 nM or 100 nM for 4, 8, 12 and 48 hours, respectively. To compare with a positive and negative control, same conditions were tested using 1 μ M Mitoxantrone or leaving cells untreated. After incubation at 37 °C in a 5 % CO₂ incubator at indicated concentrations and time, leukaemic cells were harvested and stained for cell death markers Annexin V and Propidium iodide together with B cell surface marker B220. After 30 minutes of incubation at room temperature in the dark, cells were analysed by flow cytometry.

4.2.6 Determination of ICD Markers

4.2.6.1 Calreticulin Exposure

To determine CALR exposure under treatment with Nilotinib, 1×10^6 L1-1 and L3 leukaemic cells were seeded in duplicate in 12-well plates in 1 mL leukaemic cell line medium and treated with 10 nM or 50 nM of Nilotinib for 4 and 6 hours, respectively. Under same conditions an untreated negative control as well as a positive control treated with 1 μ M Mitoxantrone were performed. After incubation, cells were first stained with an anti-CALR primary antibody for 30 minutes and then, in a second step, with an Alexa Fluor 594-conjugated IgG secondary antibody for 15 minutes at room temperature in the dark. In order to detect non-specific background staining, secondary controls were carried out for all conditions. Finally, samples were analysed using flow cytometry.

4.2.6.2 Extracellular ATP Release

Nilotinib-induced release of extracellular ATP was quantified using an ENLITEN ATP Assay System Bioluminescence Detection Kit for ATP Measurement according to the manufacturer's instructions.

In the experiment 2.5×10^3 L1-1 leukaemic cells were plated in triplicate in a 96-well plate in 50 μ L leukaemic cell line medium. Nilotinib was added at concentrations of 10 nM or 50 nM and untreated triplicates as negative control as well as triplicates treated with 1 μ M Mitoxantrone as positive control were performed. To examine the dynamics of extracellular ATP release over the time during treatment, conditions mentioned above were tested for 4, 6, 8, 12 and 24 hours. In order to determine possible effects of the sample buffer (= leukaemic cell line medium) on the luciferase reaction, an ATP standard curve in the range of 10^{-18} M ATP to 10^{-10} M ATP was run in duplicate. Furthermore, both a triplicate with leukaemic cell line medium only and a triplicate with ATP-free water were carried out to quantify background luminescence.

ATP-derived chemoluminescence was detected on a LUMIstar OPTIMA Microplate Luminometer with an automatic reagent delivery system applying 50 μ L of recombinant Luciferin/Luciferase-reagent (rL/L-reagent) to each sample. The measurement was run with a 2-second delay time after reagent injection and a 10-second luminescence signal integration.

4.2.6.3 HMGB1 Release

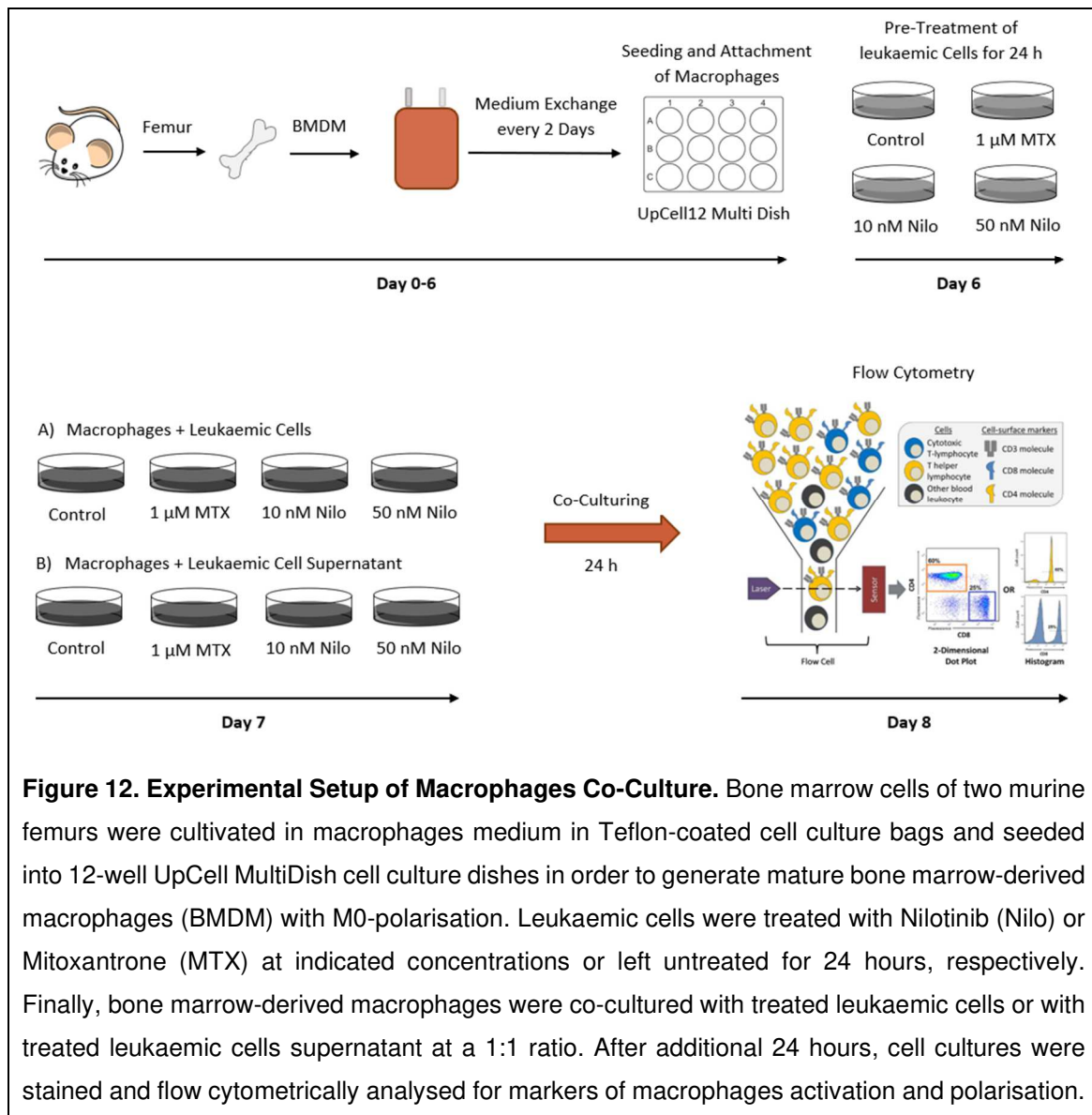
Aiming to investigate the release of HMGB1 under the treatment with Nilotinib, Western Blotting was performed. Therefore, 10×10^6 L1-1 leukaemic cells were seeded into tissue culture flasks in 20 mL leukaemic cell line medium. Nilotinib at the concentrations of 10 nM or 50 nM was added and cells were incubated for 8 hours. Next to that, a positive control treated with 1 μ M Mitoxantrone as well as an untreated negative control were performed under the same conditions. To determine cytosolic HMGB1, whole-cell extracts were prepared by lysing cells with RIPA lysis buffer (10 μ L/1 $\times 10^6$ cells) supplemented with protease inhibitor (10 μ L/1 mL lysis buffer) and phosphatase inhibitor (10 μ L/1 mL lysis buffer). In order to assess extracellular HMGB1 release, 5 mL of cell culture supernatants

were collected, and proteins precipitated using the method of acetone precipitation. Then, samples were reduced and denatured by adding 4x Laemli sample buffer and heating at 95 °C for 5 minutes. After loading of 20 µL of cytosolic extracts and 10 µL of precipitated cell culture supernatants together with a molecular weight marker, proteins were separated by 15 % SDS-PAGE running 30 minutes at 80 V and 1 hour at 100 V in running buffer. Thereafter, proteins were transferred from the gel onto a 0.2 µm nitrocellulose blotting membrane in a wet transfer system in transfer buffer at 250 mA for 1.5 hours at 4 °C on ice. To reduce non-specific binding, the membrane was placed in blocking buffer containing 5 % skimmed milk overnight at 4 °C before immunodetection. The latter was performed by probing the blocked membrane with an anti-HMGB1 primary antibody overnight at 4 °C followed by the incubation with an HRP-conjugated secondary IgG antibody for 1 hour at room temperature with both antibodies diluted in blocking buffer containing 2.5 % skimmed milk. Before and after every step of antibody incubation, the membrane was washed with TBS-T buffer three times for 5 minutes. For visualization, the chemiluminescent ECL Prime Western Blotting Detection Reagent with a final volume of 0.1 mL/cm² membrane was added onto the probed membrane, incubating for 5 minutes. Then, the membrane was exposed to an X-ray film in a dark room for 30 seconds to detect cytosolic HMGB1 protein bands and for 90 seconds to visualise extracellular HMGB1 from cell culture supernatants. Finally, the film was developed immediately in the X-ray film developer machine XR24 Pro to acquire the western blot images. An α -Tubulin loading control was performed for cytosolic HMGB1.

4.2.7 Macrophages Co-Culture

In the purpose of examining the effects of Nilotinib-treated leukaemic cells on macrophages activation and polarisation in an in-vitro setting, bone marrow cells were harvested from the femurs of a 12-week-old female C57BL/6 wild-type mouse and cultured in 30 mL of macrophages medium in Teflon-coated cell culture bags for 7 days at 37 °C in a 5 % CO₂ humidified incubator to generate mature CD11b⁺F4/80⁺ M0-polarised macrophages. Macrophages medium containing DMEM Medium supplemented with 10 % FBS, 1 % L-Glutamine (200 mM) and 1 % Pen Strep (10000 U/mL Penicillin, 10000 µg/nL Streptomycin) in the presence of recombinant mouse macrophage colony-stimulating factor (M-CSF, 100 µg/mL) was exchanged every second day.

On day 6, 0.5×10^6 macrophages were plated into 12-well UpCell MultiDish cell culture dishes in 1 mL macrophages medium for optimal attachment. Next to that, 1×10^6 L1-1 and L3 leukaemic cells were seeded in 6-well plates in 2 mL leukaemic cell line medium and treated with Nilotinib at concentrations of 10 nM or 50 nM for 24 hours. For a positive and negative control, same conditions were performed using 1 µM Mitoxantrone or leaving leukaemic cells untreated for 24 hours, respectively. On day 7, bone marrow-derived macrophages (BMDM) were then co-cultured with 0.5×10^6 treated leukaemic cells in 1 mL macrophages medium (1:1 ratio) or with 500 µL of treated leukaemic cells medium (= supernatant) in 500 µL macrophages medium (1:1 ratio) for additional 24 hours, respectively. Moreover, bone marrow-derived macrophages without co-culturing were cultured in duplicate for control. Finally, after incubation with 30 µL of Brilliant Stain Buffer for 15 minutes at room temperature in the dark, cell cultures were stained with fluorescence-labelled antibodies against CD45, CD11b, F4/80, CD80, CD86, CD206 and MHCII and analysed by flow cytometry (Figure 12).



4.2.8 Vaccination Assay

In order to evaluate Nilotinib-induced immunogenic cell death in-vivo, L1-1 leukaemic cells were incubated with 100 nM Nilotinib for 72 hours or with 1 µM Mitoxantrone for 24 hours. Then 10×10^3 treated leukaemic cells were inoculated subcutaneously into the left flanks of eight-week-old female C57BL/6 wild-type and Gas6 knockout mice. After two weeks, mice were challenged with 1×10^3 living L1-1 leukaemic cells injected with a viability of 96 % into the tail vein. Thereafter, mice were monitored routinely for the incidence of leukaemic burden. When both clinical symptoms of progressing leukaemia and high leukaemic

burden of the peripheral blood in flow cytometry analysis were displayed, mice were sacrificed for a final analysis (Figure 13). Extent and procedure of the final analysis are described in Table 13.

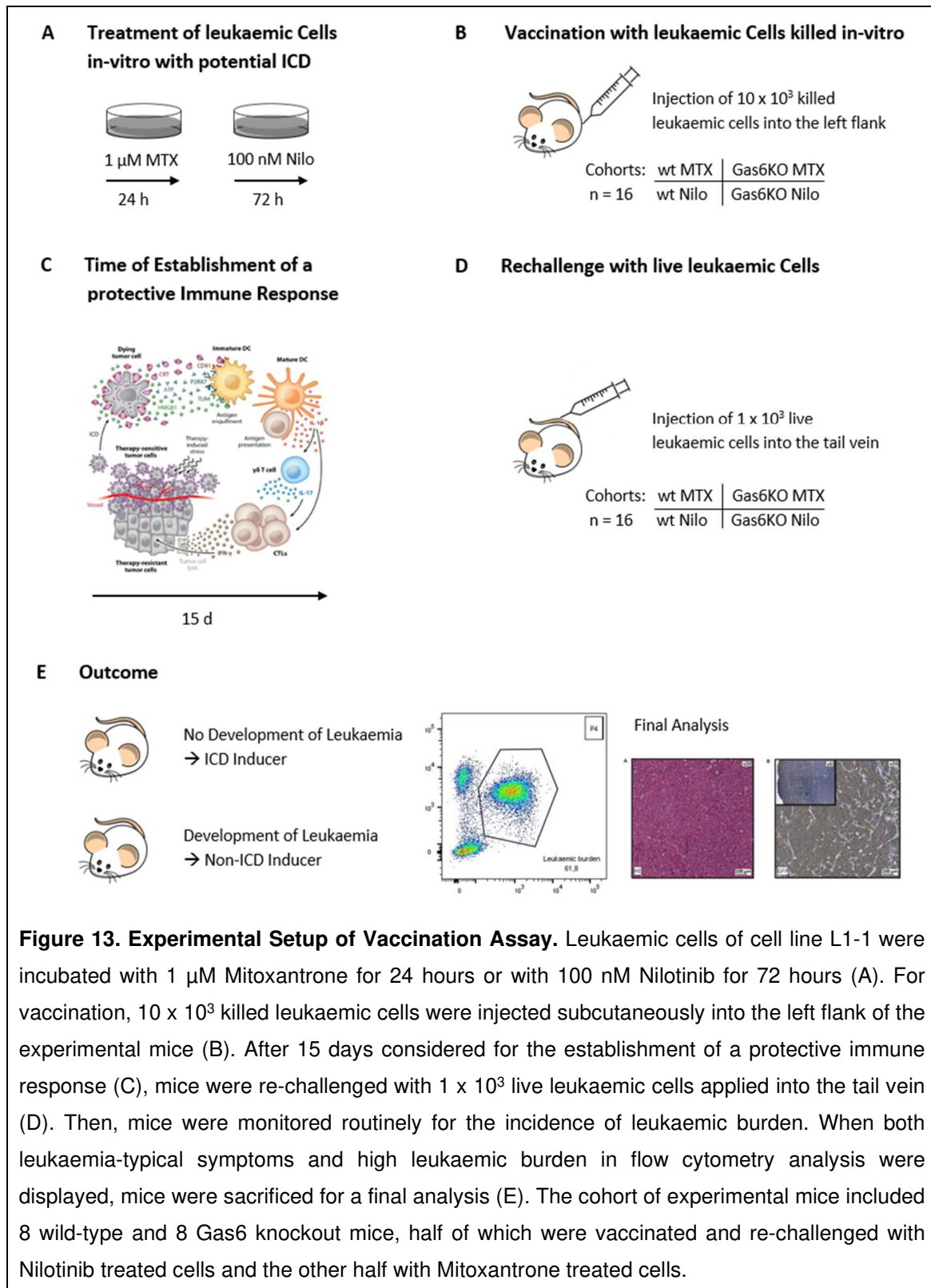






Figure 13. Experimental Setup of Vaccination Assay. Leukaemic cells of cell line L1-1 were incubated with $1 \mu\text{M}$ Mitoxantrone for 24 hours or with 100 nM Nilotinib for 72 hours (A). For vaccination, 10×10^3 killed leukaemic cells were injected subcutaneously into the left flank of the experimental mice (B). After 15 days considered for the establishment of a protective immune response (C), mice were re-challenged with 1×10^3 live leukaemic cells applied into the tail vein (D). Then, mice were monitored routinely for the incidence of leukaemic burden. When both leukaemia-typical symptoms and high leukaemic burden in flow cytometry analysis were displayed, mice were sacrificed for a final analysis (E). The cohort of experimental mice included 8 wild-type and 8 Gas6 knockout mice, half of which were vaccinated and re-challenged with Nilotinib treated cells and the other half with Mitoxantrone treated cells.

Table 13: Extent and Procedure of Final Analysis

<u>Nilotinib cohort:</u>		n = 8, including 4 wt and 4 Gas6KO mice Final analysis on day 8
<u>Mitoxantrone cohort:</u>		n = 8, including 4 wt and 4 Gas6KO mice Final analysis on day 13
Femur + Tibia 	<ul style="list-style-type: none"> IHC (GFP) Flow cytometry analysis of leukaemic burden 	Bones were harvested. Femur was fixed for Immunohistochemistry (IHC) and tibia was crushed to stain cells with PI for dead cell exclusion and B-cell surface marker B220. Leukaemic burden was quantified by the frequency of GFP+B220+ cells using flow cytometry analysis.
Blood 	<ul style="list-style-type: none"> White Blood Count Flow cytometry analysis of leukaemic burden 	Blood was taken from the submandibular vein. White Blood Count was performed using scil Vet abc hematology analyzer. Blood lysed with lysing buffer was stained with PI for dead cell exclusion and B-cell surface marker B220. Leukaemic burden was quantified by the frequency of GFP+B220+ cells using flow cytometry analysis.
Spleen 	<ul style="list-style-type: none"> Spleen weight IHC (GFP) Flow cytometry analysis of leukaemic burden 	Spleen was harvested and weighted. Half of the spleen was fixed for Immunohistochemistry (IHC). The remaining half of the spleen was smashed to stain cells with PI for dead cell exclusion and B-cell surface marker B220. Leukaemic burden was quantified by the frequency of GFP+B220+ cells using flow cytometry analysis.
Tumour 	<ul style="list-style-type: none"> HE stain and IHC (GFP) 	All mice of the Nilotinib cohort developed subcutaneous tumours at the injection site. Tumours were harvested and a piece was fixed for Haematoxylin-Eosin (HE) stain and Immunohistochemistry (IHC).

4.2.9 Haematoxylin-Eosin Stain and Immunohistochemistry

Collected tissues from the vaccination experiment were prepared for Immunohistochemistry. Therefore, tissues were fixed with Roti-Histofix for 24 hours and then washed with DPBS for another 24 hours. In addition to this, femurs were decalcified in decalcification buffer for 14 days. To permit sectioning, samples were dehydrated and paraffin embedded. Dehydration was done in a Leica ASP300 S Tissue Processor by passing the samples through a series of alcohol solutions in ascending concentrations (70 %, 80 %, 96 %, 96 %, 100 %, 100 %, 100 % ethanol) and by clearing with Xylene to remove the ethanol prior to paraffin-embedding. After immersion and blocking in paraffin wax, tissues were sectioned at 3 μm with a Leica RM2235 Manual Rotary Microtome and then transferred onto glass slides. Haematoxylin-Eosin stain was performed using Leica ST5010 Autostainer XL. Leica BOND-MAX was used for fully automated GFP-immunostaining applying 150 μL of antibody diluted with Bond Primary Antibody Diluent per slide. After staining, slides were dehydrated in Leica ST5010 Autostainer XL through an ascending series of alcohol (50 %, 70 % and 96 % ethanol, 100 % isopropanol) and cleared with Xylene to then get cover-slipped with Leica CV5030 Glass Coverslipper using CellTexx mounting medium. Finally, slides were examined under an Axio Imager 2 Research Microscope and imaged using the AxioVision SE64 Microscopy software.

4.2.10 Statistical Analysis

Statistical analysis was performed using GraphPad Prism software. Results are expressed as mean \pm standard deviation (SD). Significant difference between two groups was analysed by unpaired, two-tailed Student t-tests. Statistical significance was determined by a value of $p < 0.05$ for all analyses. P values are presented in the figures as * $p < 0.05$, ** $p < 0.01$, *** $p < 0.001$, **** $p < 0.0001$.

5 Results

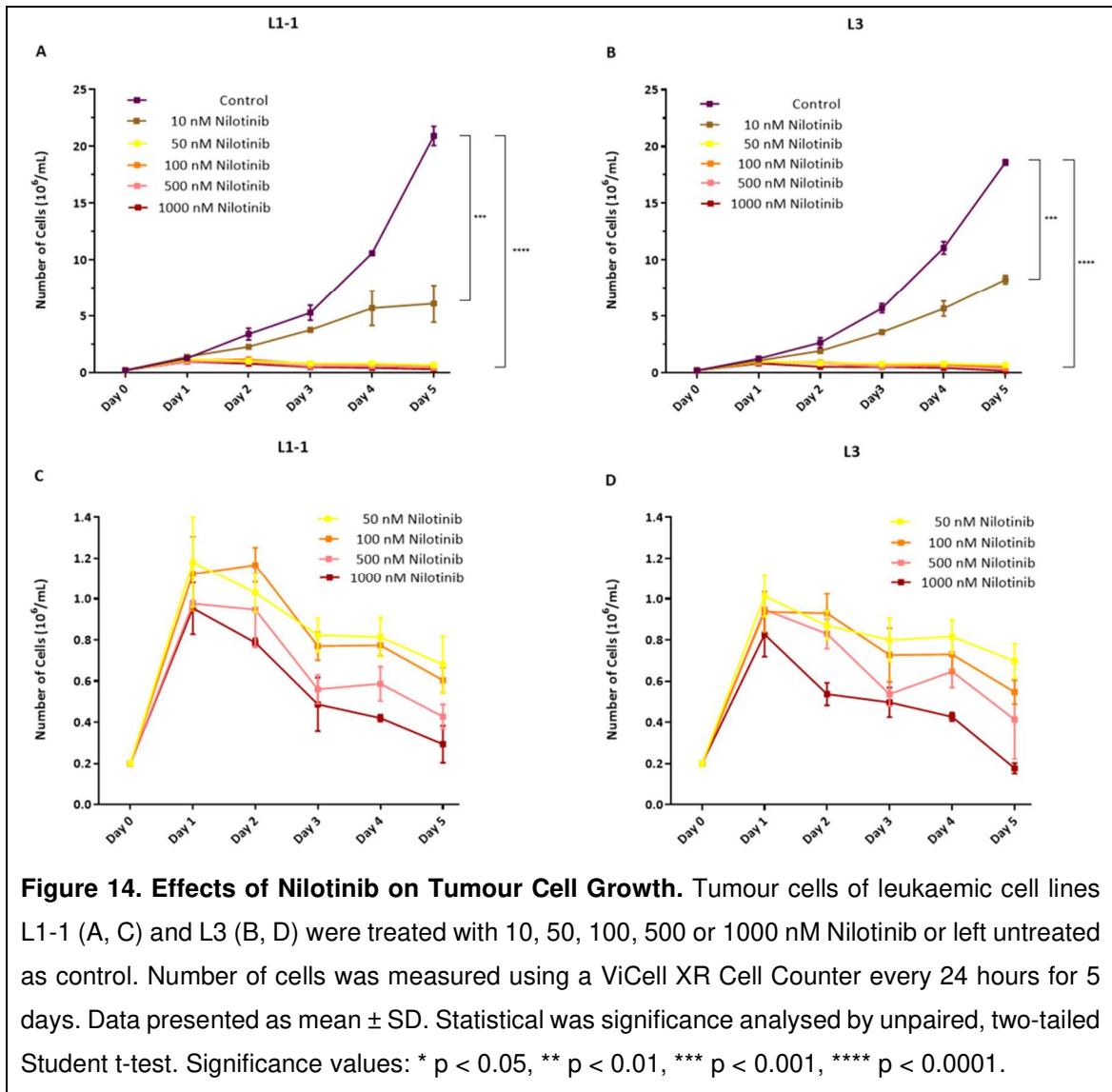
5.1 Effects of Nilotinib on Tumour Cell Growth and Viability

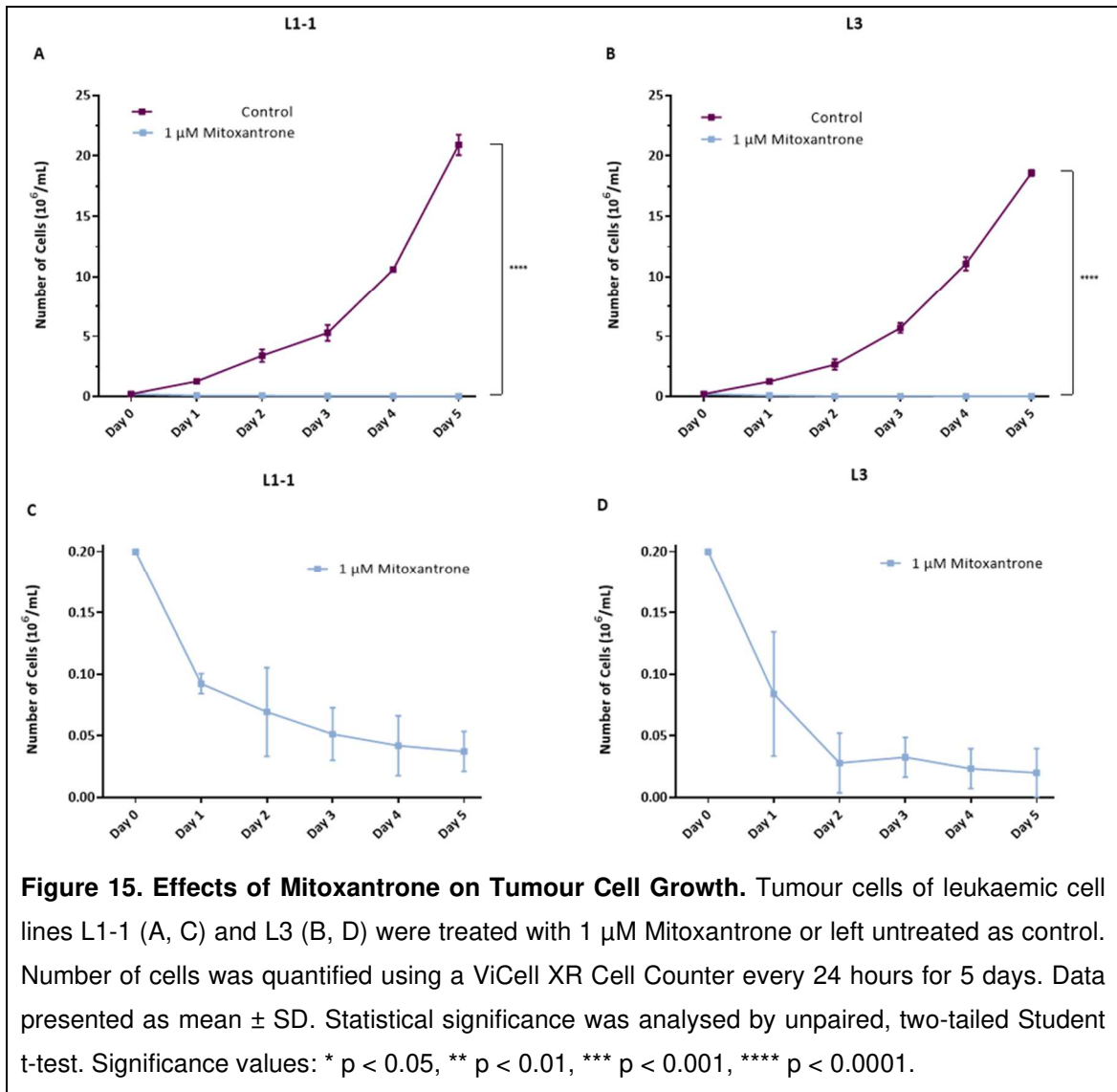
To study the effects of Nilotinib on both growth trends and viability of leukaemic tumour cells in concentration-dependent manner, cells of the leukaemic cell lines L1-1 and L3 were treated in-vitro with increasing doses of Nilotinib between 10 nM and 1000 nM. The number and viability of cells were monitored every 24 hours for 5 days.

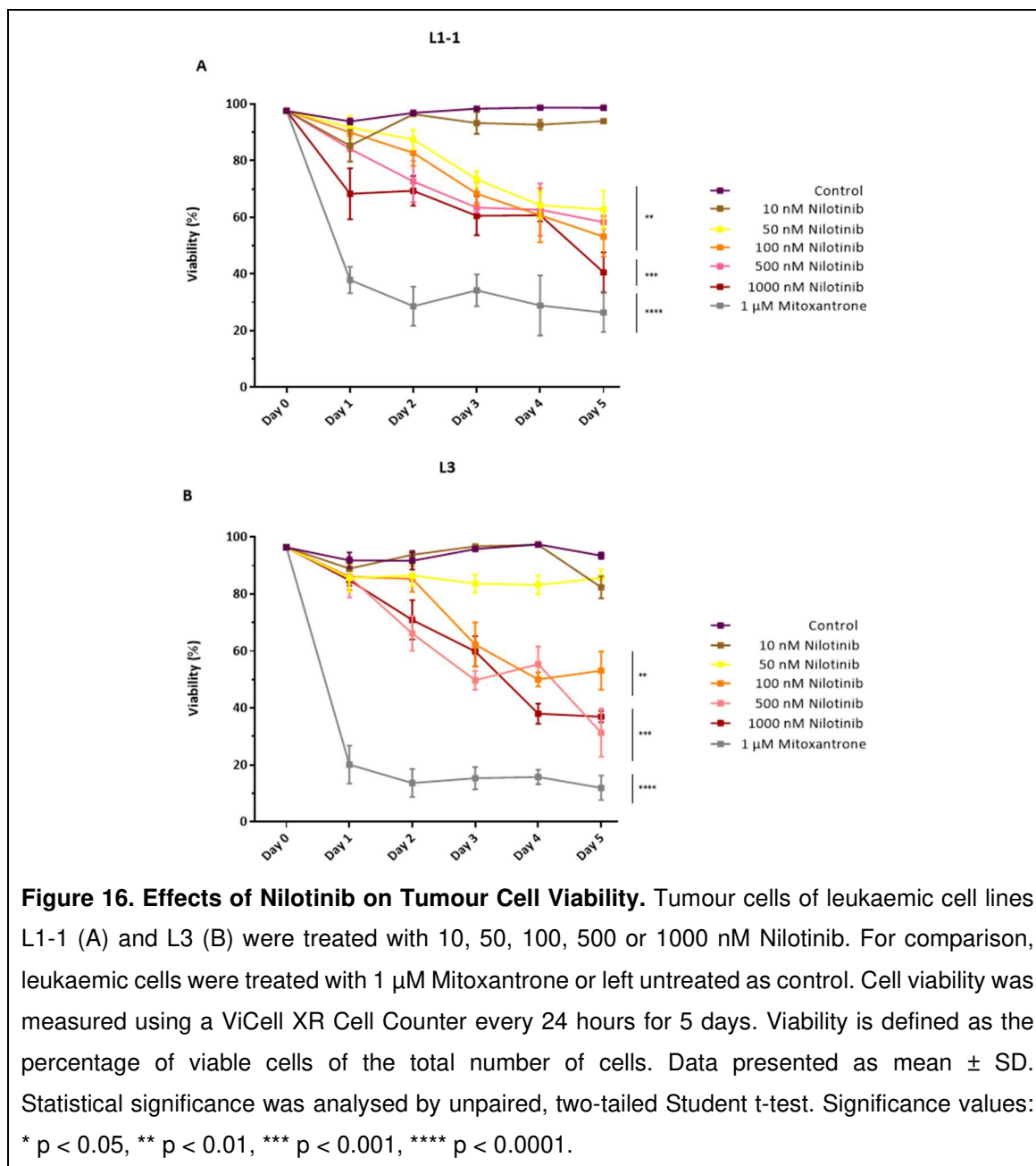
While untreated tumour cells showed unrestrained positive accelerated growth, Nilotinib significantly inhibited growth at all concentrations (Figure 14A and 14B). Here, a higher efficacy was seen at the concentrations greater than 10 nM Nilotinib, as at those concentrations there was an overall decreasing cell count after an initial increase, whereas leukaemic cells treated with 10 nM Nilotinib showed a constantly increasing number of cells despite inhibited growth. However, there were no significant differences in efficacy between the concentrations of Nilotinib greater than 10 nM (Figure 14C and 14D). Next to that, the two leukaemic cell lines exhibited no statistically different sensitivities to Nilotinib exposure.

As Nilotinib, Mitoxantrone was potent to inhibit tumour cell growth significantly compared to the untreated control (Figure 15A and 15B). In contrast, the growth-inhibiting effect of Mitoxantrone was not delayed as with Nilotinib, resulting in an immediately decreasing number of cells (Figure 15C and 15D). Likewise, the leukaemic cell lines L1-1 and L3 were similar in their sensitivity referring to the treatment with Mitoxantrone.

In terms of viability, effects were seen with concentration of Nilotinib greater than 10 nM for leukaemic cell line L1-1 and above 50 nM for L3, while untreated cells maintained a high viability of in average 97 % (L1-1) or 94 % (L3). In comparison to Mitoxantrone, that exposed high and prompt cytotoxicity, cell viability was gradually decreasing with Nilotinib over the time (Figure 16A and 16B).







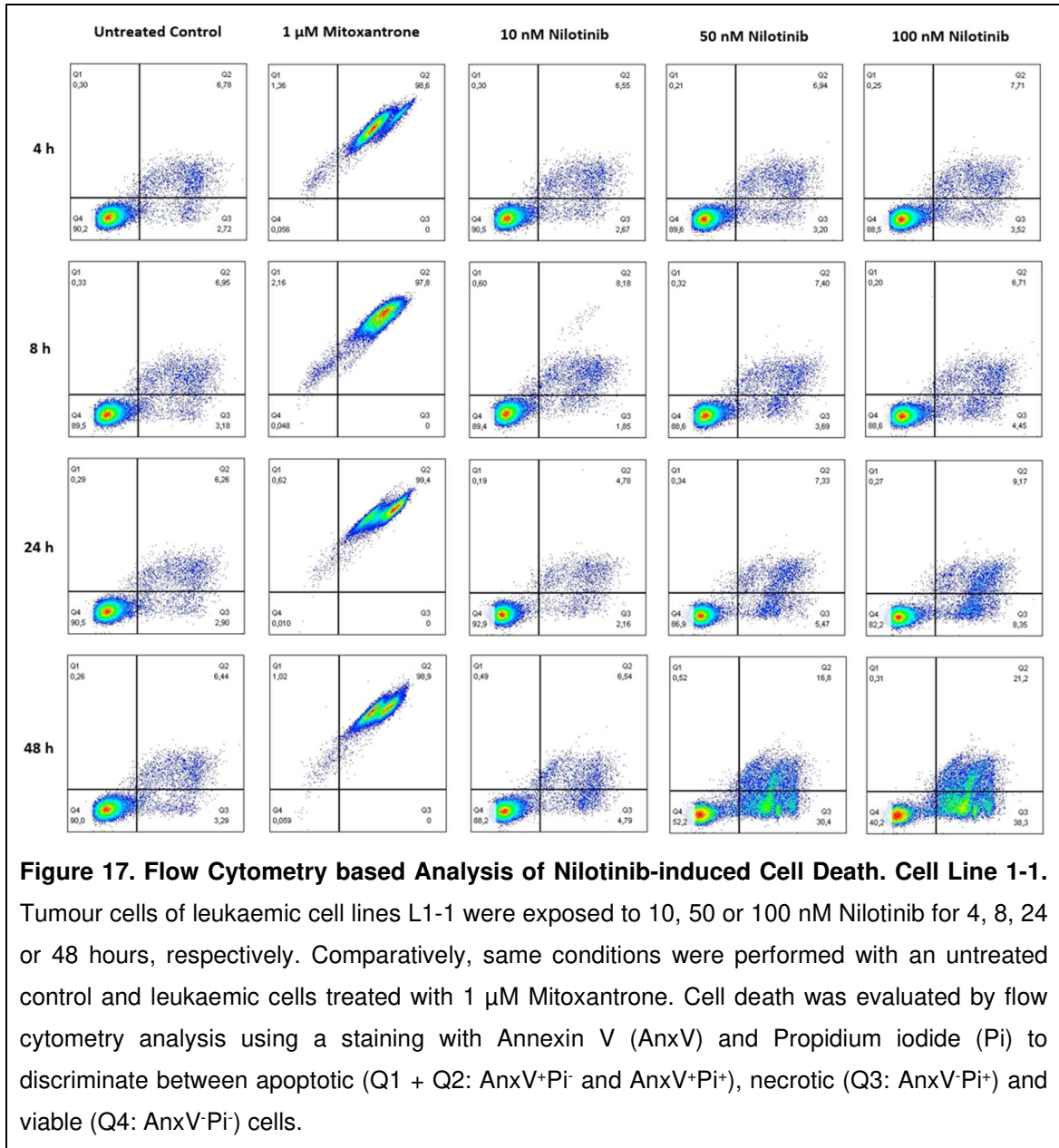
5.2 Characterisation of Nilotinib-induced Cell Death

To further determine the process of Nilotinib-induced cell death, an in-vitro Annexin V/ Propidium iodide cell death assay was performed. This assay allows not only to quantify the extent of cell death but also to distinguish between the cell death modality ranging from apoptosis to necrosis. Therefore, Nilotinib-treated leukaemic cells of both cell lines were stained with Annexin V (AnxV) and Propidium iodide (Pi) in order to qualify cell death by a flow cytometry-based

analysis. With the help of the a gating strategy (Supplementary Figure S2, page 98), cells were finally categorized on the one hand into viable cells (AnxV⁻Pi⁻) and on the other hand into dead apoptotic cells (AnxV⁺Pi⁻ and AnxV⁺Pi⁺) as well as dead necrotic cells (AnxV⁻Pi⁺). Flow cytometry data with all concentrations and different times of incubations are presented in Figure 17 (L1-1) and Figure 18 (L3). In addition to that, data are figured as bar diagrams in Figure 19.

Both types of figure show that after 4 and 8 hours of Nilotinib treatment leukaemic cells were mainly viable and displayed a distribution similar to the untreated control. Depending on the dose, slightly more dead cells compared to the control were found after 24 hours. While Nilotinib at a concentration of 10 nM had no more considerable effect on cell death after another 24 hours, 48 % of the L1-1 and 34 % of the L3 leukaemic cells treated with 50 nM Nilotinib and 60 % of the L1-1 and 40 % of the L3 leukaemic cells treated with 100 nM Nilotinib were dead after 48 hours. Notably, referring to the cell death modality, Nilotinib induced a bimodal cell death, that was predominantly necrotic in L1-1 and apoptotic in L3 leukaemic cells.

In comparison, Mitoxantrone-treated cells of both leukaemic cell lines displayed a nearly complete apoptotic cell death within 4 hours.



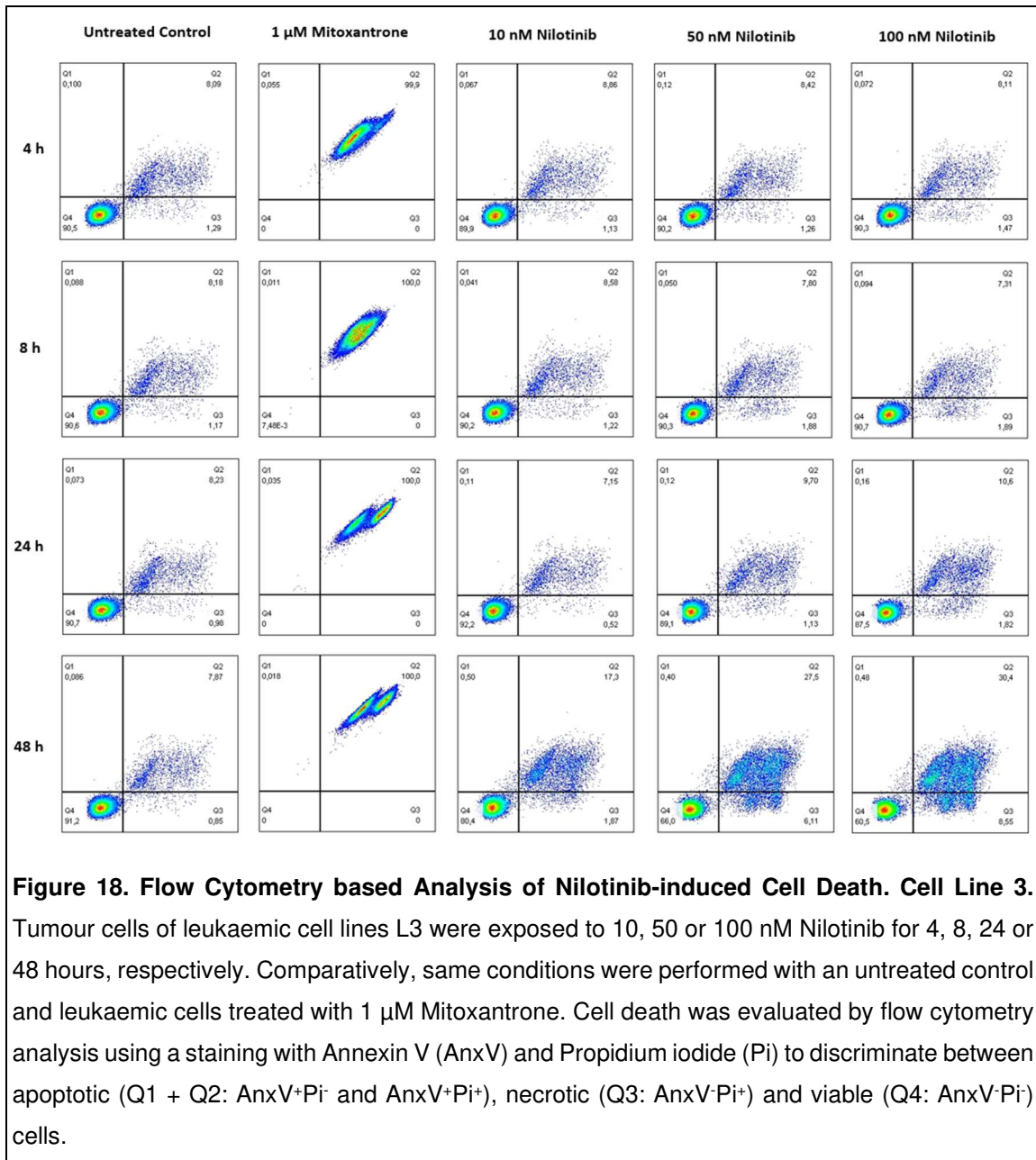


Figure 18. Flow Cytometry based Analysis of Nilotinib-induced Cell Death. Cell Line 3. Tumour cells of leukaemic cell lines L3 were exposed to 10, 50 or 100 nM Nilotinib for 4, 8, 24 or 48 hours, respectively. Comparatively, same conditions were performed with an untreated control and leukaemic cells treated with 1 μM Mitoxantrone. Cell death was evaluated by flow cytometry analysis using a staining with Annexin V (AnxV) and Propidium iodide (Pi) to discriminate between apoptotic (Q1 + Q2: AnxV+Pi⁻ and AnxV+Pi⁺), necrotic (Q3: AnxV-Pi⁺) and viable (Q4: AnxV-Pi⁻) cells.

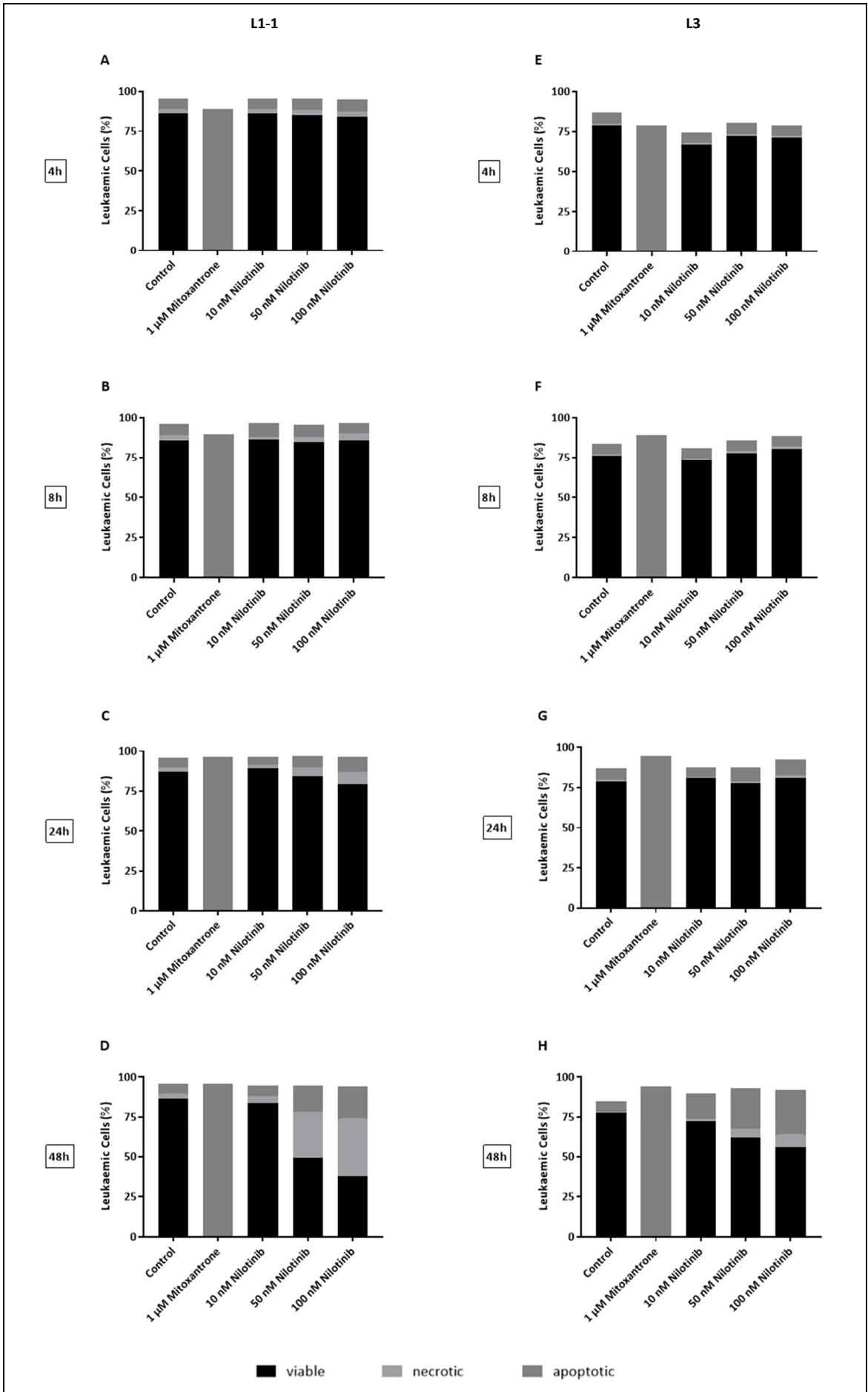


Figure 19. Cell Death Assay. Tumour cells of leukaemic cell lines L1-1 (A-D) and L3 (E-H) were exposed to 10, 50 or 100 nM Nilotinib for 4, 8, 24 or 48 hours, respectively. Comparatively, same conditions were performed with an untreated control and leukaemic cells treated with 1 μ M Mitoxantrone. Cell death was evaluated by flow cytometry analysis using a staining with Annexin V and Propidium iodide to discriminate between viable, apoptotic and necrotic cells. Note: In the bar diagrams 100 % of leukaemic cells were not reached in total due to the exclusion of debris and doublets from the cell population.

5.3 Molecular Determinants of Immunogenic Cell Death.

ICD Marker Analysis

5.3.1 Calreticulin Exposure

In order to investigate a Nilotinib-triggered cell surface exposure of Calreticulin, leukaemic cells of both cell lines were stained for Calreticulin by flow cytometry after treatment with Nilotinib. The flow cytometry-based analysis was performed using a gating strategy, in which the positive gating region for the expression of Calreticulin was constituted with the aid of unstained controls (Supplementary Figure S3, page 99).

The results are illustrated in Figure 20, where Calreticulin expressing cells are given as frequency of total. Here, only the percentage increase in Calreticulin expression compared to the untreated control was evaluated as drug-induced expression, considering the background staining of the target antibody, since the unstimulated control should not be expressing the target.

Accordingly, cell line L1-1 exhibited no Calreticulin exposure after 4 hours and only 2 % after 6 hours, while an exposure of Calreticulin in cell line L3 was detected neither after 4 hours nor after 6 hours of Nilotinib treatment. In contrast, a Mitoxantrone-induced Calreticulin exposure of 8 % in cell line L1-1 after 6 hours and of 6 % in cell line L3 after 4 hours was noted.

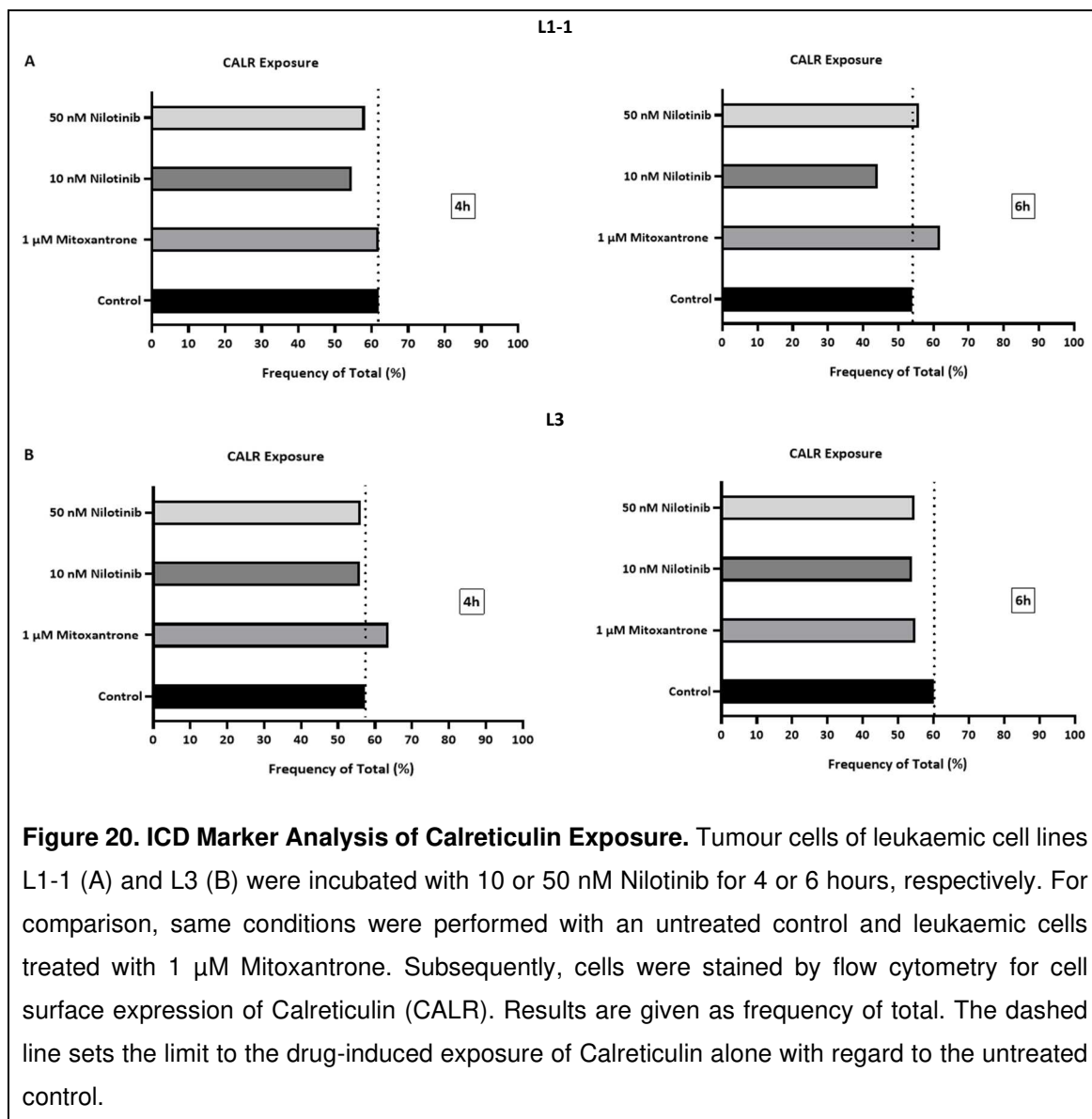


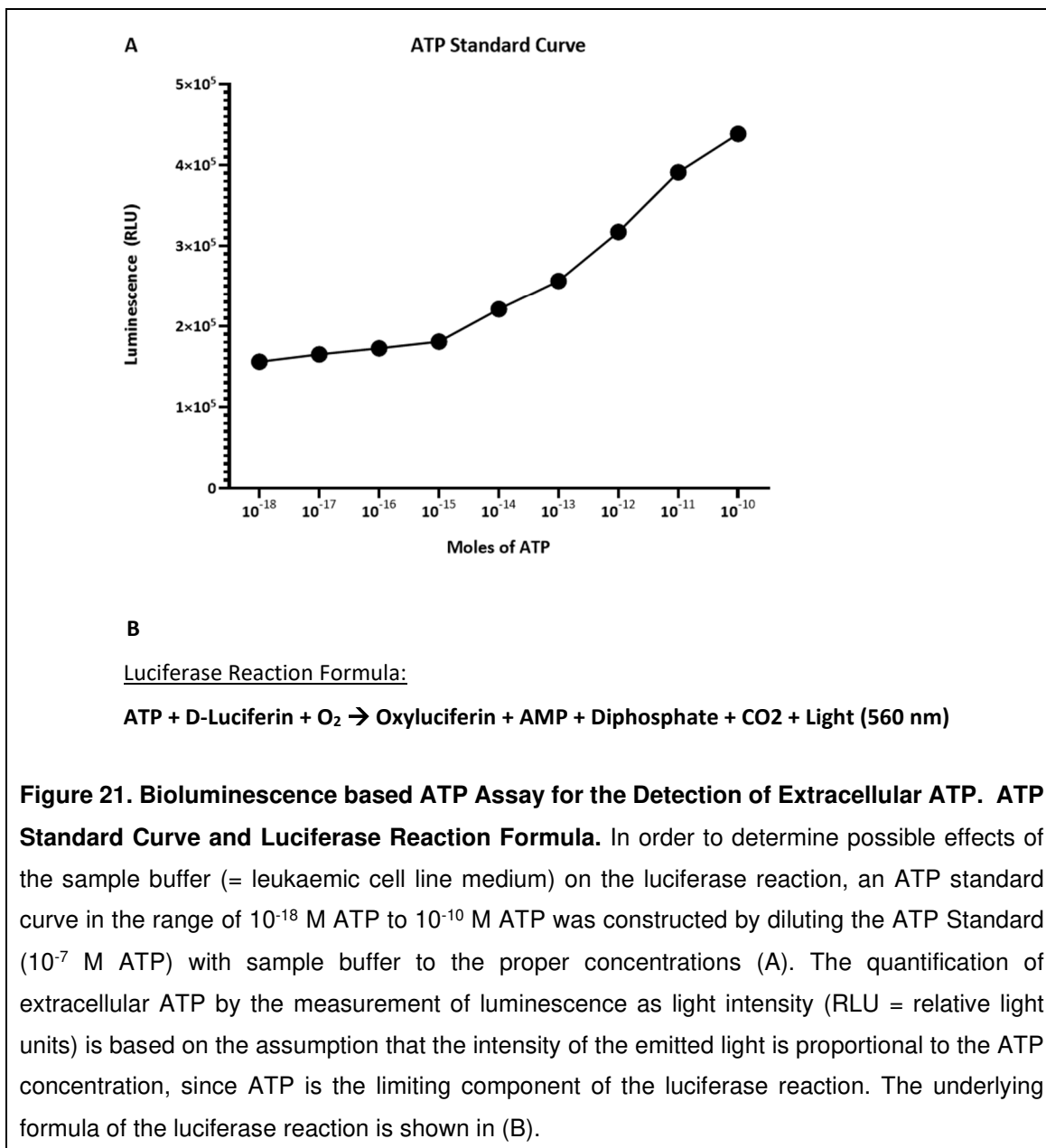
Figure 20. ICD Marker Analysis of Calreticulin Exposure. Tumour cells of leukaemic cell lines L1-1 (A) and L3 (B) were incubated with 10 or 50 nM Nilotinib for 4 or 6 hours, respectively. For comparison, same conditions were performed with an untreated control and leukaemic cells treated with 1 μM Mitoxantrone. Subsequently, cells were stained by flow cytometry for cell surface expression of Calreticulin (CALR). Results are given as frequency of total. The dashed line sets the limit to the drug-induced exposure of Calreticulin alone with regard to the untreated control.

5.3.2 Extracellular ATP Release

For the quantification of Nilotinib-induced release of extracellular ATP a bioluminescence-based ATP assay was used. Therefore, leukaemic cells of cell line L1-1 were exposed to Nilotinib and ATP-derived luminescence was measured at different points of time on a luminometer.

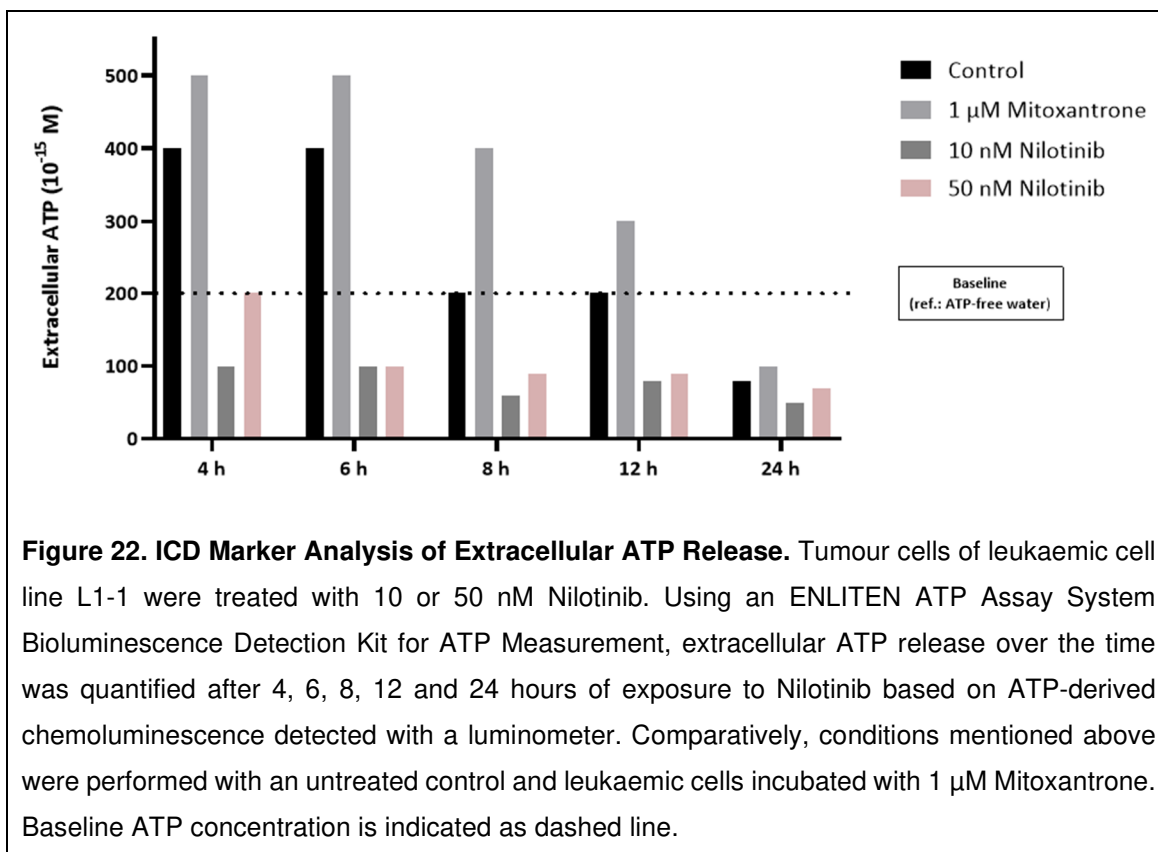
The principle of quantifying extracellular ATP by the measurement of luminescence is based on the assumption that the intensity of the emitted light is proportional to the ATP concentration, since ATP is the limiting component of the luciferase reaction (Figure 21B). To take into account possible effects of the sample buffer, here leukaemic cell line medium, on the luciferase reaction, an

ATP standard curve was prepared (Figure 21A). Thus, the concentration of ATP was determined by comparing to the standard curve. In fact, luminescence was generally lower in the sample buffer as FBS-supplemented media is known to inhibit ATP availability for luciferase reaction.¹⁰² Consequently, the buffer inhibition of light output was corrected by a correction factor.



Data of the analysis of extracellular ATP release are presented in Figure 22. At any time point, there was effectively no release of ATP under the exposure of either 10 nM or 50 nM Nilotinib. In contrast, a significant release of ATP from leukaemic cells under treatment with Mitoxantrone was measured with absolute

peak levels of 500×10^{-15} M ATP after 4 and 6 hours and, in relation to the untreated control, a relative peak level of 400×10^{-15} M ATP after 8 hours, which were gradually decreasing within 24 hours. Results were evaluated considering both the baseline and the untreated control. The baseline indicates the baseline ATP concentration and was set with respect to ATP concentrations measured in ATP-free water, which is why only values above the baseline were assessed as specific.



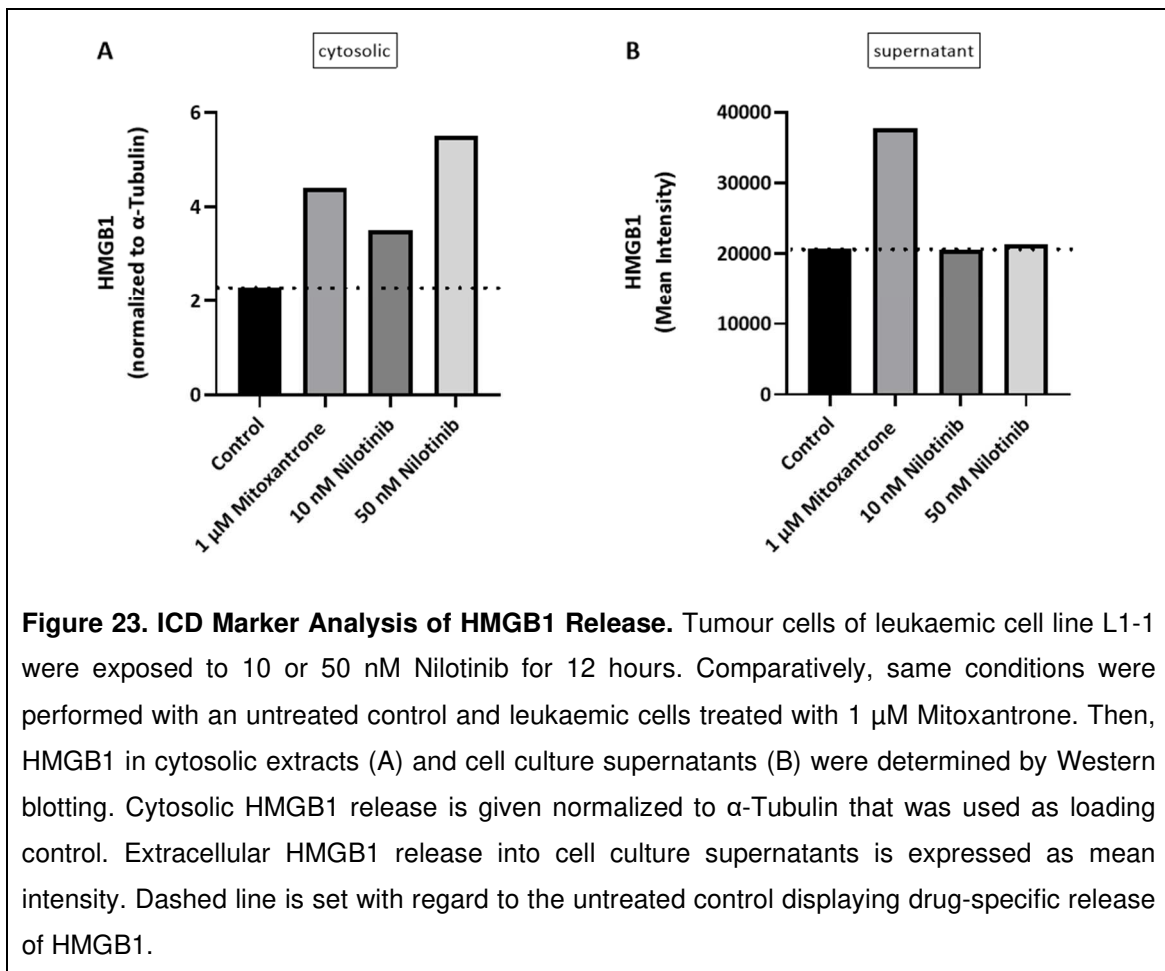
5.3.3 HMGB1 Release

Nilotinib-induced release of HMGB1 from leukaemic cells was assessed by Western blotting. Therefore, HMGB1 in both cytosolic extracts and cell culture supernatants of Nilotinib-exposed leukaemic cells of cell line L1-1 was determined after 12 hours of incubation. For cytosolic HMGB1 release, a loading control using α -Tubulin was performed.

Graphical data of Western blotting indicated a dose-dependent release of cytosolic HMGB1 from leukaemic cells challenged with 10 nM or 50 nM Nilotinib.

Likewise, cytosolic HMGB1 release under treatment with Mitoxantrone was found to be between the two levels of Nilotinib. Hence, in comparison to the untreated control, a drug-specific release of cytosolic HMGB1 was approved for Nilotinib and Mitoxantrone (Figure 23A).

Taking into account that the release of HMGB1 is the process of HMGB1 translocation from the nucleus via the cytosol to the extracellular space during cell death, there was not yet an extracellular HMGB1 release into cell culture supernatants from leukaemic cells exposed to Nilotinib. In contrast to that, a Mitoxantrone-induced release of extracellular HMGB1 was already detected (Figure 23B).



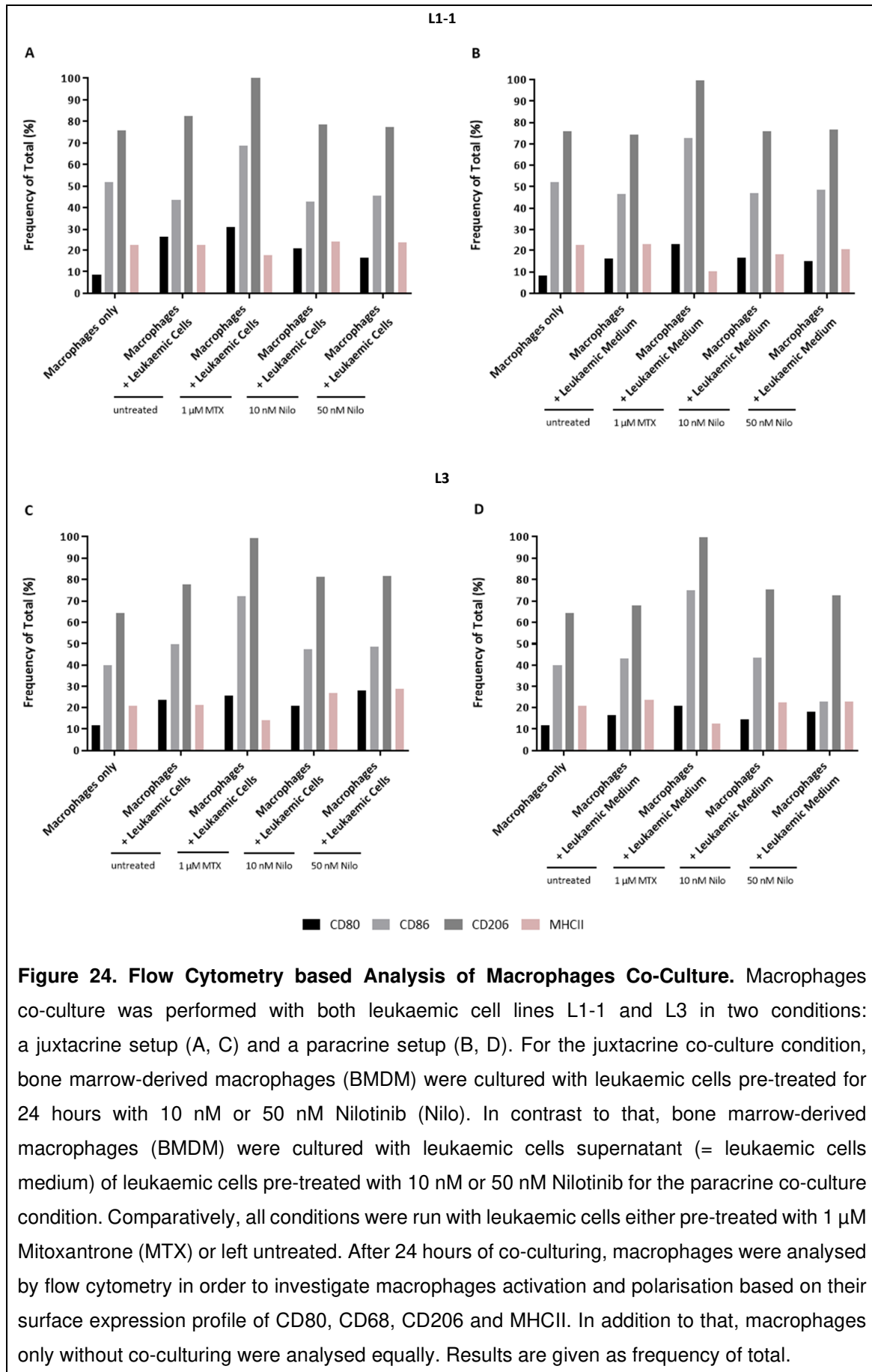
5.4 Immunological Determinants of Immunogenic Cell Death

5.4.1 Macrophages Co-Culture

In order to examine the immunological effects of Nilotinib on macrophages activation and polarisation, macrophages were co-cultured on the one hand side with Nilotinib pre-treated leukaemic cells in a juxtacrine setup and on the other hand side with leukaemic cells supernatant of Nilotinib pre-treated leukaemic cells in a paracrine setup. Therefore, leukaemic cells of both leukaemic cell lines L1-1 and L3 were pre-treated with 10 nM or 50 nM Nilotinib for 24 hours and subsequently co-culturing with bone marrow-derived macrophages was performed for another 24 hours. Finally, macrophages were analysed by flow cytometry with the help of a gating strategy (Supplementary Figure S4, page 100) investigating macrophages activation and polarisation based on their surface expression of CD80, CD86, CD206 and MHCII.

Data of the flow cytometry-based analysis of macrophages co-culture presented in Figure 24 did not reveal a relevant shift in macrophages activation and polarisation in the juxta- and paracrine co-culture conditions with Nilotinib pre-treated leukaemic cells of both cell lines compared to the corresponding co-culture conditions with untreated leukaemic cells. More precisely, the shift of the surface expression profile regarding CD80, CD86, CD206 and MHCII was less than 5 % on total average and with partly opposing changes among the juxta- and paracrine co-culture conditions as well as between the two cell lines L1-1 and L3 (Table 14 and 15, page 101-102).

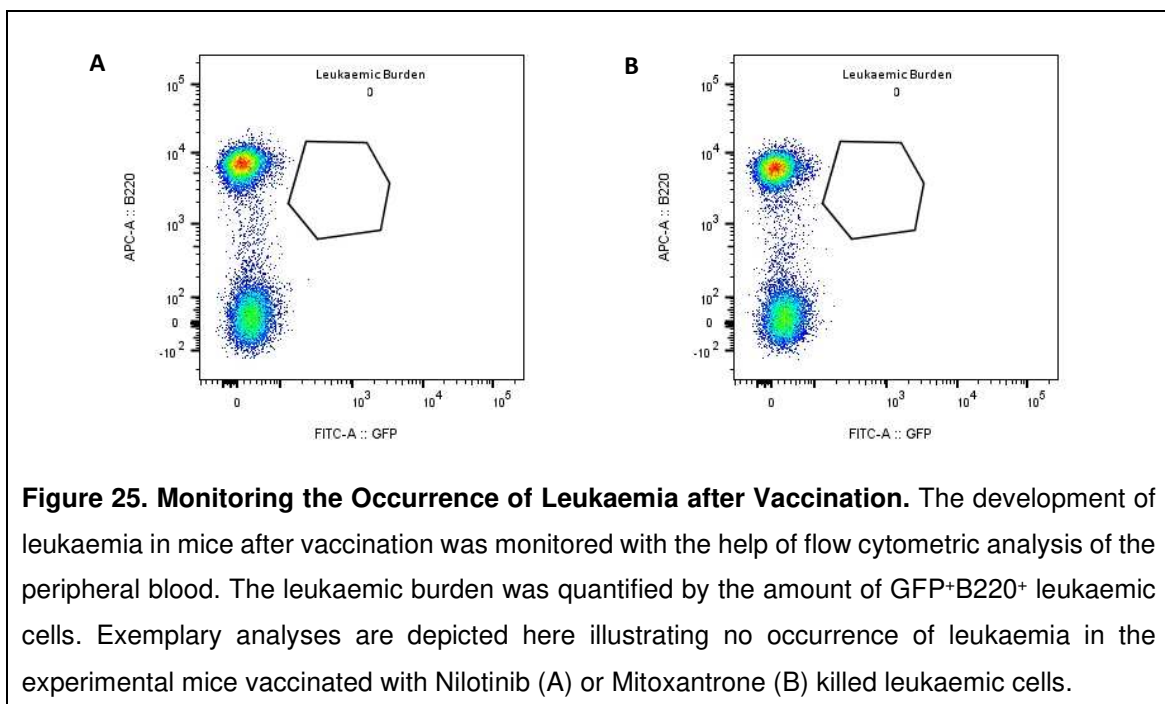
In contrast to that, there were effects on macrophages activation and polarisation in the co-culture conditions with Mitoxantrone pre-treated leukaemic cells in comparison with the corresponding co-culture conditions of untreated leukaemic cells involving an average upregulation of CD80 by 4.4 %, of CD86 by 26.5 % and of CD206 of 24.1 % besides a downregulation of MHCII by 9.0 %. Here, the changes in the surface expression profile of the two cell lines were similar, but more pronounced by an average of 58.0 % in the paracrine setup comparing the two co-culture conditions (Table 16, page 103).



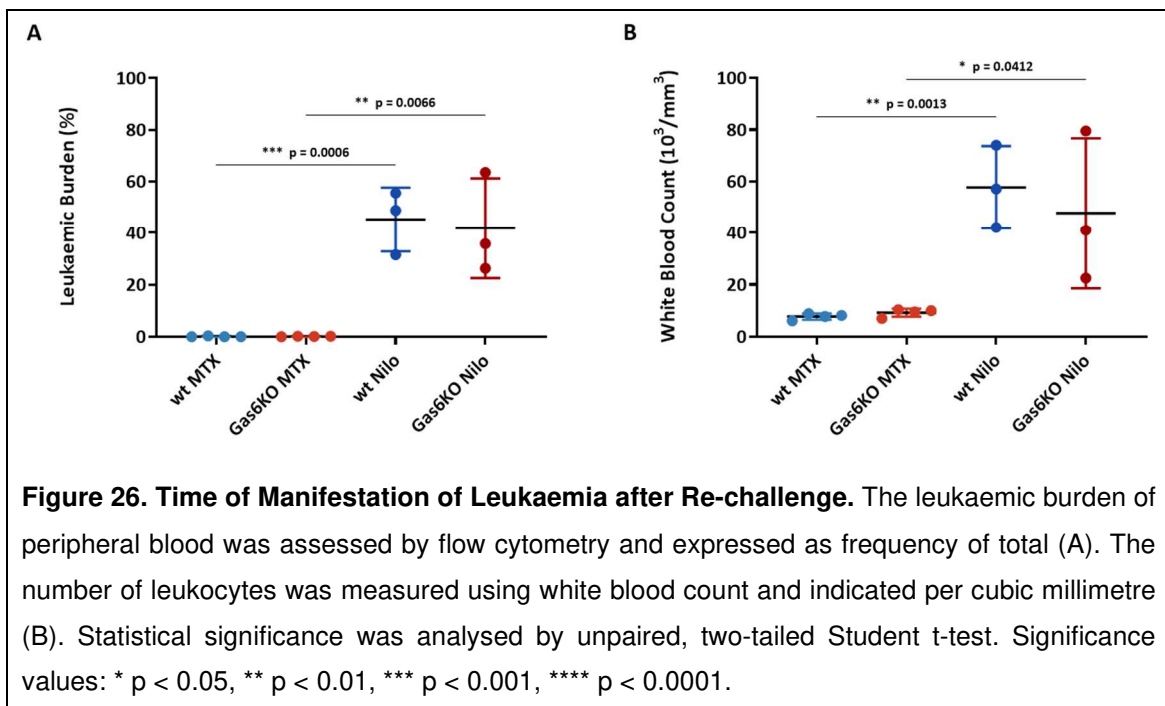
5.4.2 Vaccination Assay

A vaccination assay was performed to examine the potential of Nilotinib to induce immunogenic cell death in-vivo. The first step within the experiment involved the vaccination of mice with killed leukaemic cells functioning as vaccine in order to elicit a protective immune system. For this purpose, leukaemic cells of the cell line L1-1 were incubated with 100 nM Nilotinib for 72 hours or with 1 μ M Mitoxantrone for 24 hours and then injected subcutaneously into the left flank of mice. In a second step, after 15 days those mice were re-challenged with live leukaemic cells injected into the tail vein. Thereafter, mice were regularly checked for the development of leukaemia manifesting both as clinical symptoms and as high leukaemic burden of the peripheral blood in flow cytometry (Supplementary Figure S5, page 104). The cohort of experimental mice included 8 wild-type and 8 Gas6 knockout mice, half of which were vaccinated and re-challenged with Nilotinib treated cells and the other half with Mitoxantrone treated cells. The injection of live leukaemic cells failed in a wild-type and a Gas6 knockout mouse from the Nilotinib cohort, which is why these 2 mice were excluded from the final analysis.

As shown in Figure 25, there was no development of leukaemia in the mice after vaccination, confirmed by the lack of leukaemia-typical symptoms and the absent detection of leukaemic cells in the peripheral blood by flow cytometry.



Thus, mice were re-challenged with live leukaemic cells in a second step of the vaccination assay. Under regular clinical and flow cytometric monitoring, a development of leukaemia was observed in both cohorts, notably, with leukaemia manifesting more rapidly in the Nilotinib cohort within 8 days than in the Mitoxantrone cohort within 13 days. More detailed, while there were no leukaemic cells detected in the peripheral blood of the Mitoxantrone cohort on day 8, a leukaemic burden of 45.3 % (wt) and 41.9 % (Gas6KO) was found in the peripheral blood of the Nilotinib cohort. In accordance with that, the Nilotinib cohort displayed a distinctly elevated white blood count of $57.7 \times 10^3/\text{mm}^3$ (wt) and $47.7 \times 10^3/\text{mm}^3$ (Gas6KO) leukocytes, whereas in the Mitoxantrone cohort a normal white blood count of $7.8 \times 10^3/\text{mm}^3$ (wt) and $9.2 \times 10^3/\text{mm}^3$ (Gas6KO) leukocytes was obtained (Figure 26). So once leukaemia occurred in a cohort, all mice of that cohort were sacrificed for a final analysis comprising (1) the flow cytometric assessment of leukaemic burden in bone marrow, peripheral blood and spleen, (2) immunohistochemistry of femur, spleen and subcutaneous tumours, (3) white blood count of peripheral blood and (4) spleen weight.



The final analysis revealed lower infiltration of leukaemic cells in the Nilotinib cohort as opposed to the Mitoxantrone cohort with respect to the leukaemic burden in all three compartments, bone marrow (wt MTX: 36.6 %, wt Nilo:

32.5 %; Gas6KO MTX: 40.2 %, Gas6KO Nilo: 34.5 %), peripheral blood (wt MTX: 49.3 %, wt Nilo: 45.3 %; Gas6KO MTX: 45.5 %, Gas6KO Nilo: 41.9 %) and spleen (wt MTX: 56.1 %, wt Nilo: 47.5 %; Gas6KO MTX: 31.1 %, Gas6KO Nilo: 11.7 %), which was significant in terms of leukaemic burden of the spleen in the Gas6KO group (Figure 27-29). In terms of the white blood count, a higher number of leukocytes was found in the Nilotinib cohort compared to the Mitoxantrone cohort, as depicted in Figure 28 (wt MTX: $42.7 \times 10^3/\text{mm}^3$, wt Nilo: $57.7 \times 10^3/\text{mm}^3$; Gas6KO MTX: $28.0 \times 10^3/\text{mm}^3$, Gas6KO Nilo: $47.7 \times 10^3/\text{mm}^3$). Considering the lower infiltration of peripheral blood with leukaemic cells as described above, this indicated an increased fraction of normal leukocytes. In a comparison of the two cohorts regarding spleen weight as a correlate of leukaemic spread, lower spleen weights were measured in the Nilotinib cohort (wt MTX: 0.50 g, wt Nilo: 0.44 g; Gas6KO MTX: 0.47 g, Gas6KO Nilo: 0.34 g), which was significant in the Gas6KO group (Figure 29). Furthermore, all mice of the Nilotinib cohort developed subcutaneous tumours at the injection site in the left flank. To further investigate the consistency of those tumours, histological samples were prepared and stained for HE and GFP revealing a tumour mass of densely packed GFP-positive leukaemic cells, as illustrated in Figure 30.

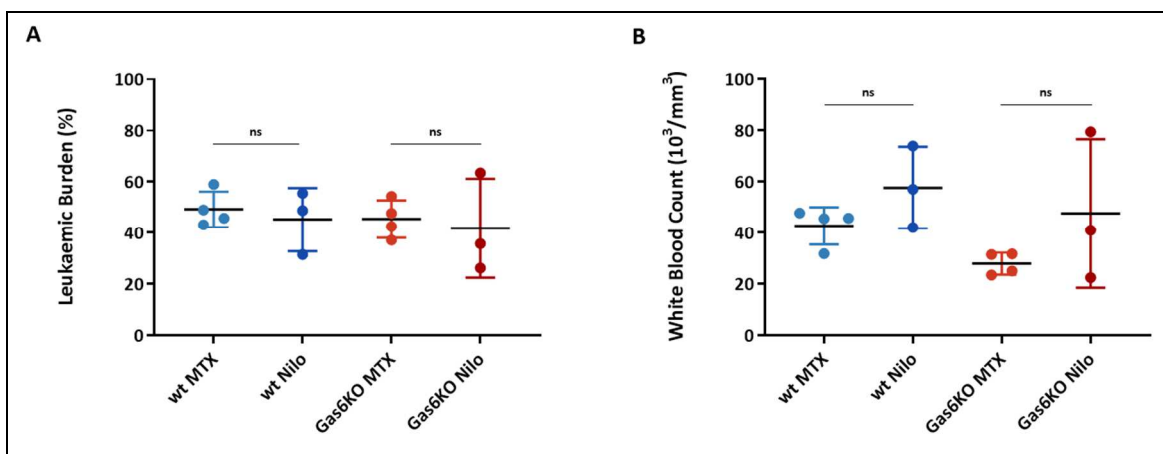
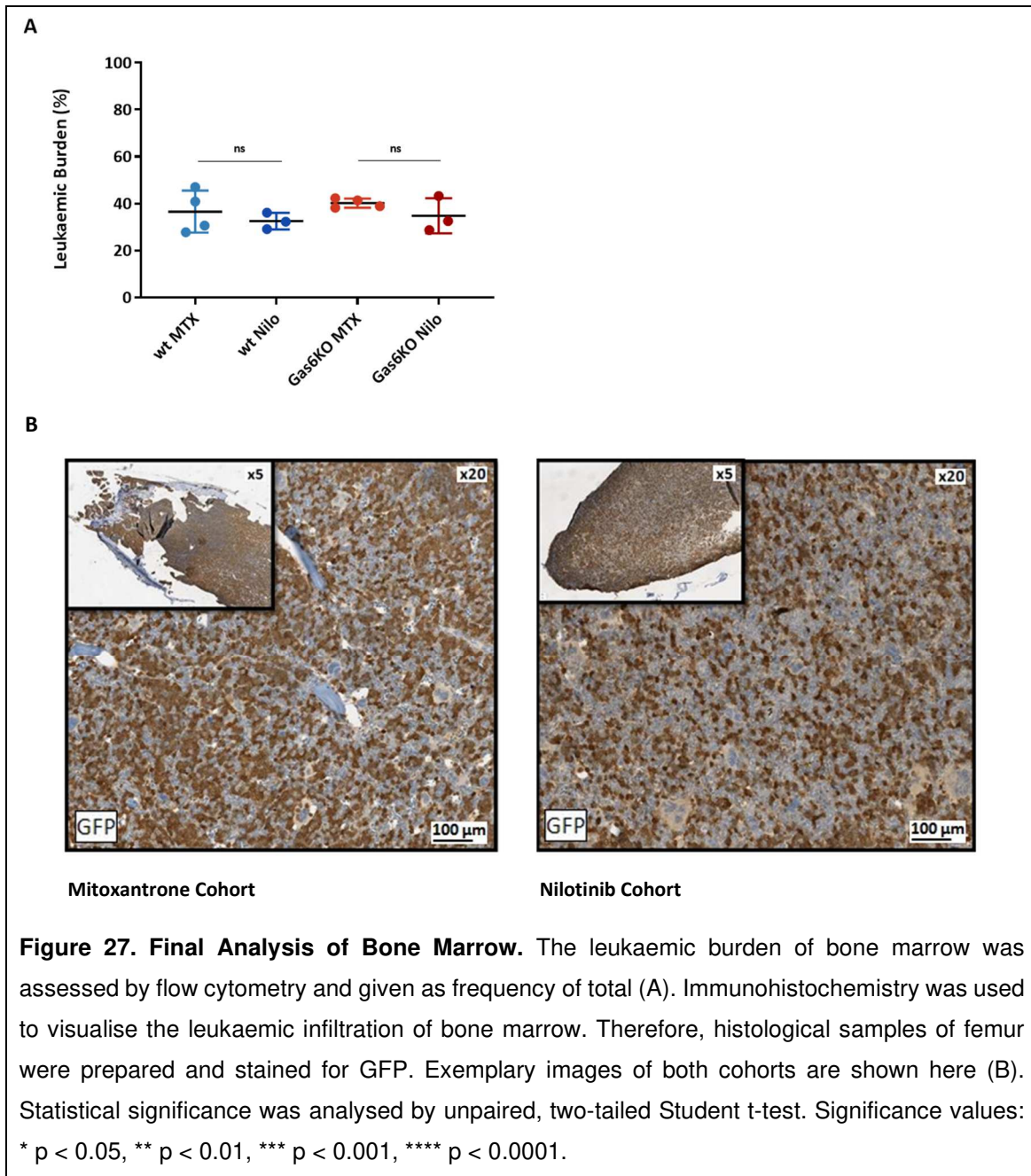


Figure 28. Final Analysis of Peripheral Blood. The leukaemic burden of peripheral blood was assessed by flow cytometry and expressed as frequency of total (A). The number of leukocytes was measured using white blood count and indicated per cubic millimetre (B). Statistical significance was analysed by unpaired, two-tailed Student t-test. Significance values: * $p < 0.05$, ** $p < 0.01$, *** $p < 0.001$, **** $p < 0.0001$.

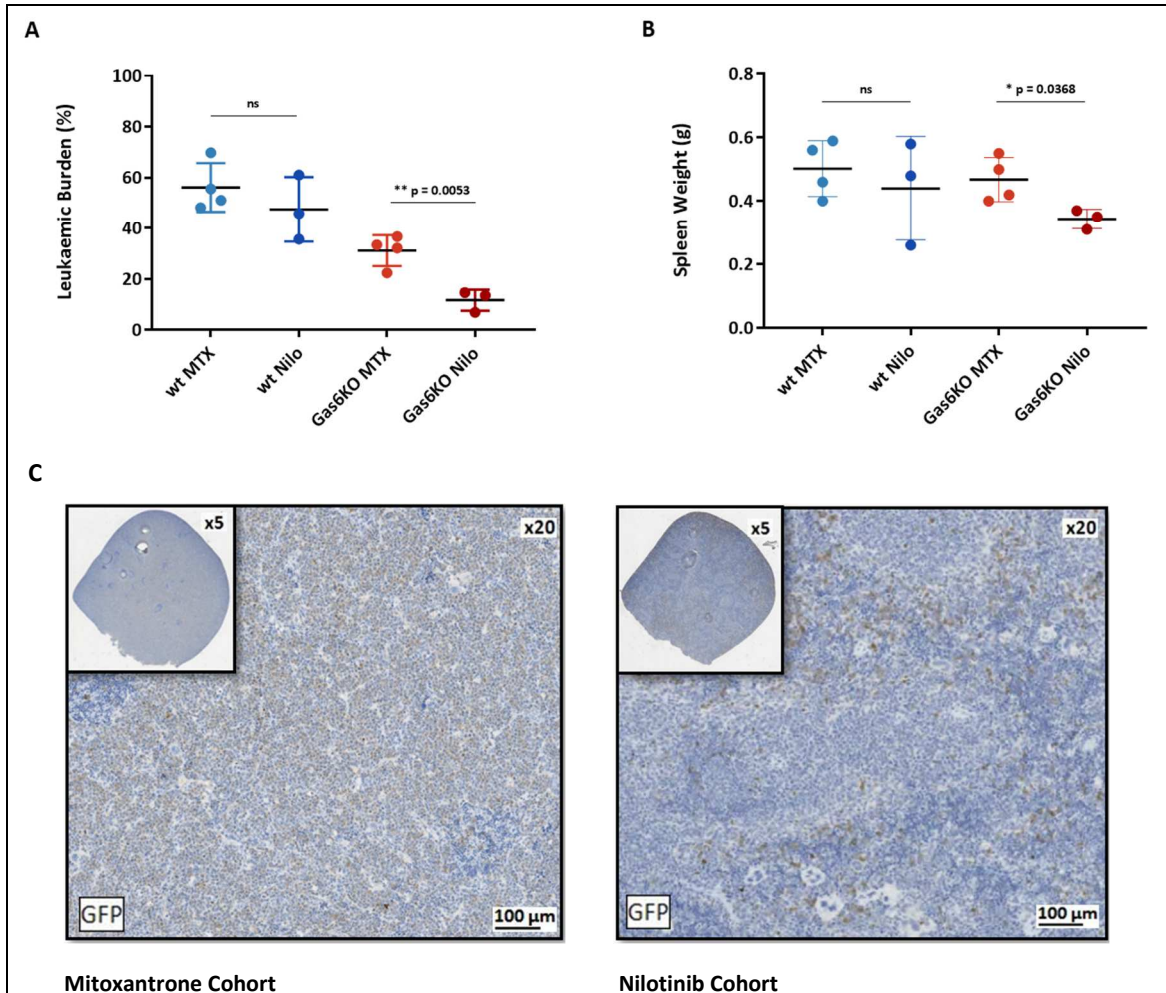
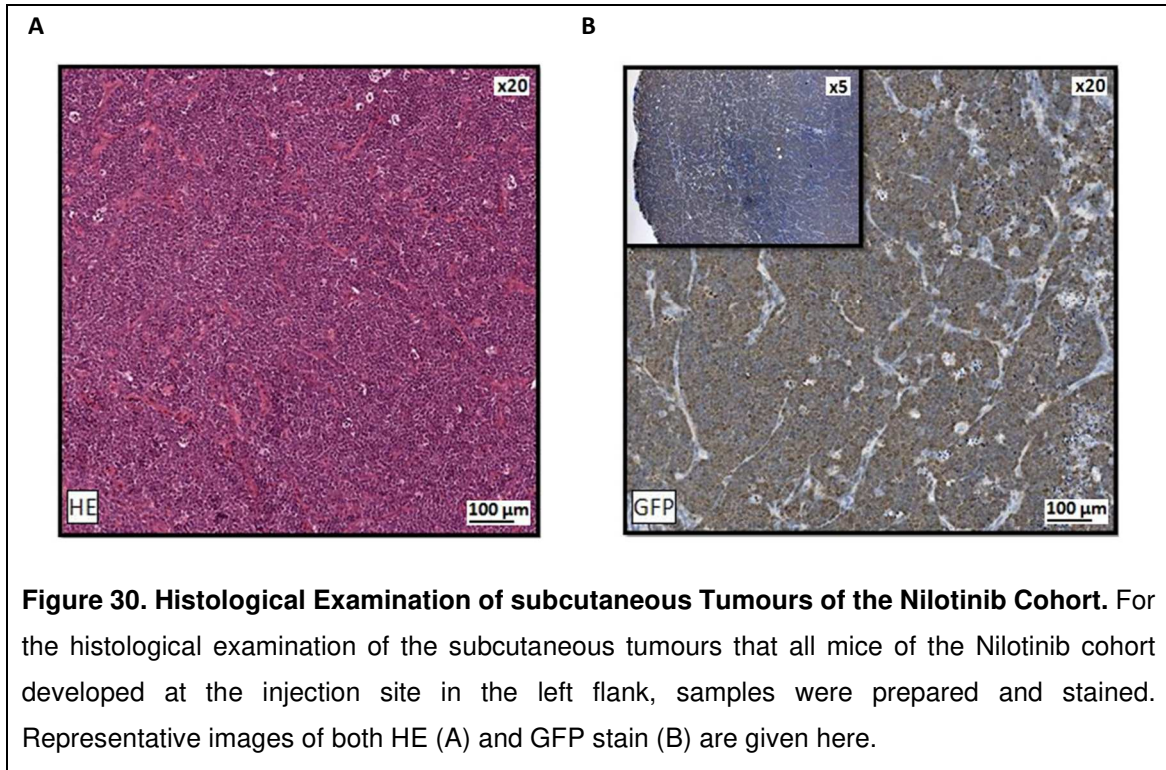


Figure 29. Final Analysis of Spleen. The leukaemic burden of spleen was assessed by flow cytometry and quoted as frequency of total (A). Spleen weight was determined and given in grams (B). To visualise the leukaemic infiltration of spleen, histological samples were prepared and stained for GFP. Representative images of both cohorts are presented here (C). Statistical significance was analysed by unpaired, two-tailed Student t-test. Significance values: * $p < 0.05$, ** $p < 0.01$, *** $p < 0.001$, **** $p < 0.0001$.



6 Discussion

6.1 Results on Interpretation and Discussion

6.1.1 Growth Inhibition and Viability Assay

At first, the effects of Nilotinib on cell growth and viability of Ph⁺ B-ALL cells were studied in a concentration-dependent manner. It was shown that Nilotinib inhibited cell growth in all tested concentrations ranging between 10 nM and 1000 nM, whereby a concentration of 10 nM appeared to be a threshold dose, since at this concentration the cell number continued to increase constantly despite decelerated growth. This was consistent with the effects on cell viability, which dropped significantly above a concentration of 10 nM (L1-1) and 50 nM (L3). However, when exposed to the highest concentration of Nilotinib, neither cell count was below baseline nor viability declined below 37 % implying, especially in comparison with Mitoxantrone, which showed strong and prompt cytotoxicity, that Nilotinib exerts more cytostatic than cytotoxic activity on the leukaemic cells. These results are in accordance with the known pharmacological properties of both drugs. Nilotinib exhibits anti-proliferative properties by competitively binding to the ATP binding site of the BCR-ABL1 kinase¹⁰³, thereby inhibiting cell proliferation¹⁰⁴, whereas Mitoxantrone displays cytotoxic effects by DNA intercalation and inhibition of topoisomerase II.^{105,106} In other studies investigating the effects of Nilotinib on BCR-ABL1⁺ cells, both similar concentrations were tested, and consistent results were obtained.¹⁰⁷⁻¹⁰⁹ Additionally, in other Ph⁺ B-ALL models, including the BV-173 cell line, and in Ba/F3, that is a popular tool in kinase drug discovery¹¹⁰, a half maximal inhibitory concentration (IC₅₀) of ≤ 12 nM Nilotinib was evaluated,¹⁰⁸ corresponding to the concentration of 10 nM Nilotinib determined in the experiments of this work.

6.1.2 Cell Death Assay

Although Nilotinib predominantly exhibited cytostatic properties, it also appeared to have cytotoxic potential to some extent. To both quantify the extent of cell death and to assess the cell death modality ranging between apoptosis and

necrosis, an Annexin V/Propidium iodide cell death assay was performed. The Annexin V/PI protocol is a commonly used approach for investigating cell death,¹¹¹ which allows to distinguish between viable, apoptotic and necrotic cells based on the differences in plasma membrane integrity and permeability.^{112,113} Annexin V detects apoptotic cells by its ability to bind to phosphatidylserine, which is translocated from the intracellular side of the plasma membrane to the surface during apoptosis.¹¹⁴ PI is a nucleic acid intercalator that can enter and stain only permeable cells, that is why it is used for the detection of late apoptotic and necrotic cells with decreased membrane integrity.¹¹⁵ The cell death assay showed that after 24 hours Nilotinib treated leukaemic cells began to undergo cell death, which was increasing as a function of concentration and exposure time. In terms of cell death modality, Nilotinib induced a bimodal cell death, which was predominantly necrotic in cell line L1-1 and apoptotic in cell line L3. In contrast, apoptosis was triggered in nearly all cells within 4 hours in response to Mitoxantrone exposure. Taken together, these findings are in line with the results observed in the cell growth inhibition and viability assay. Other studies have also demonstrated that inhibition of cell growth by Nilotinib is associated with the induction of cell death, with varying degrees within different BCR-ABL⁺ cell lines.^{108,116} As one aspect of the potential causes for that, cell maturity is cited.¹¹⁷ In this context, it has been reported that CD34⁺ hematopoietic stem and progenitor cells do not respond with cell death even at very high concentrations of 5 μ M Nilotinib, whereas more mature cells start to undergo cell death.^{117,118} Of note, this fact is considered a contributing factor to disease persistence, minimal residual disease and relapse.^{119,120} So far, classical mechanisms of resistance, such as point mutations, inadequate active drug uptake or enhanced drug efflux have been disproved to explain the different sensitivity of Ph⁺ cell lines to Nilotinib and other TKIs.^{117,118} Interestingly, studies suggested an interrelation between the expression level of mouse double minute 2 homolog (MDM2) and drug sensitivity, with Nilotinib displaying stronger cytotoxic effects in Ph⁺ cells with MDM2 overexpression. At this, it is reported that both the tumour suppressor p53 is activated and the anti-apoptotic X-linked inhibitor of apoptosis protein (XIAP) is suppressed by Nilotinib-induced inhibition of MDM2, leading to the induction of apoptotic cell death in BCR-ABL⁺ cells.^{116,121} Moreover, high-dose TKI (HD-TKI) pulse-exposure represents a further aspect regarding Nilotinib-induced cell death

in leukaemic cells. Cytotoxic activity of TKIs was found to be enhanced by HD-TKI pulse-exposure due to prolonged intracellular TKI accumulation and retention resulting in an increased fraction of cancer cells initiating apoptosis.^{122,123}

Besides the aspect of the initiation of cell death per se, which is an obligatory requirement for the induction of ICD, considerations in terms of cell death modality have been controversially discussed. Morphologically, apoptosis is characterized by progressive cell condensation and nuclear fragmentation resulting in the formation of apoptotic bodies surrounded by membranes, whereas necrosis is defined by rupture of the plasma membrane as a result of cell swelling without displaying hallmarks of apoptosis.¹²⁴ According to the Nomenclature Committee on Cell Death (NCCD), the definitions of cell death modalities were adjusted from a morphologic to a molecular one.¹²⁵ Thereby, apoptosis represents a programmed cell death modality mediated by caspase activation in contrast to necrosis, which is an unregulated, caspase independent form of cell death.¹²⁵ Moreover, it was found that necrosis can also occur in a regulated manner, termed necroptosis, involving active disintegration of cellular membranes with limited compartmentalisation of organelles and requiring the activation of receptor-interacting protein kinases 1 (RIPK1) and 3 (RIPK3).^{126,127} Initially, when efforts were made to determine the characteristics of ICD, the occurrence of an apoptotic cell death was assumed to be necessary for the immunogenic potential of ICD.⁹¹ This might seem peculiar, since on the one hand side apoptotic cell death has long been hypothesised to be of low immunogenicity,¹²⁸ and on the other hand side, necrosis is known to be accompanied by the release of DAMPs¹²⁷, which have been identified to actually evoke the immunogenic effects of ICD.¹²⁹ Current data indicate that both regulated necrosis and apoptosis play an important role in immunological processes⁸⁸ and may promote analogous effect in the tumour microenvironment including in terms of ICD.¹²⁷ Therefore, it is suggested that different cell death modalities are capable to induce ICD.^{84,97,101,127} Notably, this assumption seems to be plausible considering that cell death modalities can both occur simultaneously within a cell and merge into each other, as it is known in the form of apoptosis-necrosis switch.^{130,131} Even though the exact signalling pathways that determine immunogenic and non-immunogenic cell death have not yet been fully explored, the capacity to elicit ICD seems to be based on the induction of

ER stress response.^{97,127} However, it remains to be investigated which modality of cell death maximises the immunogenicity of dying cancer cells within the TME.¹²⁷

6.1.3 ICD Marker Analysis

Next, Nilotinib-treated leukaemic cells were examined for the exhibition of molecular ICD hallmarks. According to the criteria for the assessment of ICD, those comprise translocation of CALR to the cell surface, extracellular secretion of ATP and release of HMGB1 from the nucleus.^{91,95,96} The ICD marker analysis was performed with concentrations of Nilotinib at 10 nM and 50 nM. The former to study a possible influence on the level of ICD marker expression at half maximal inhibition, and the latter to investigate potential ICD marker expression at the lowest concentration tested as fully inhibitory. Regarding CALR cell surface exposure, no exposure in Nilotinib-treated leukaemic cells could be detected by flow cytometry. In contrast to that, CALR surface exposure was observed in leukaemic cells exposed to Mitoxantrone after 4 (L3) and 6 (L1-1) hours. Also, in terms of ATP, Nilotinib did not induce extracellular ATP release measured in a bioluminescence-based ATP assay. On the other hand, extracellular ATP release was observed under exposure to Mitoxantrone with absolute peak levels after 4 and 6 hours and, in relation to the untreated control, with relative peak levels after 8 hours. Considering that ATP is released both in the absence of external stimuli and in response to physiological stimuli,¹⁰² this is most likely to give the reason that ATP release was also measured in the untreated controls at early measurement time points. ATP release is seen during mechanical stress, as is the case in experimental manoeuvres.¹³² Therefore, conclusions regarding the effective ATP release under exposure to a drug have to be made both in respect to an evaluated baseline (ATP-free water) and in comparison to an untreated negative control, as performed in the ATP assay of this work. In addition, the fact that the levels of ATP release of Nilotinib-treated leukaemic cells were below baseline may not to be considered significant but rather stochastically random in the scope of technical inaccuracy, since the quantified values lay within the 95 % confidence interval. In order to assess HMGB1 release from the nucleus, HMGB1 was determined in both cytosolic extracts and cell culture supernatants of

Nilotinib-exposed leukaemic cells by Immunoblotting. Thereby a concentration-dependent release of HMGB1 into the cytosol but not into the cell culture supernatant was found. In the case of leukaemic cells exposed to Mitoxantrone, HMGB1 release was not only observed in the cytosol but also in the supernatant. This is consistent with the results from the cell death assay taking into account that the release of HMGB1 is the process of passive translocation from the nucleus via the cytosol into the extracellular space in response to several forms of cell death, including apoptosis, necrosis and necroptosis by dying or dead cells.¹³³⁻¹³⁵ It seems that HMGB1 release from Nilotinib exposed cells has not yet progressed as far after 12 hours as in those cells the initiation of cell death was just beginning, which is why HMGB1 was only detected in the cytosol and not yet extracellularly. In contrast, the leukaemic cells treated with Mitoxantrone were already completely succumbed to cell death at this time, so that HMGB1 was found in both the cytosol and the supernatant.

Taken together, the results support the assumption that Nilotinib is not capable of inducing immunogenic cell death in Ph⁺ leukaemic cells in-vitro considering the use of techniques referred as standard⁹¹ as well as by comparison with Mitoxantrone as a positive control. In fact, the orchestration of all three molecular determinants together is considered a required condition for the eligibility of ICD, whereas the exposure of only one or two determinants is viewed as insufficient.^{91,95,96} However, the different requirements for the immunogenicity of cell death have not been fully investigated. Although CALR, ATP and HMGB1 are considered key hallmarks, several other processes have been linked to the immunogenicity of cell death, involving release of the heat shock proteins (HSP) 70 and 90, unfolded protein response, secretion of CXC motif chemokine ligand 10 (CXCL10), autophagy induction, release of annexin A1 (ANXA1) as well as inflammasome and TLR3 signalling.⁸⁴ Besides, the exact mechanisms that underlie the release of the immunogenic hallmarks remain to be completely elucidated.⁹⁷ The process of CALR exposure to the cell surface is suggested to take place in dependence of the stage of cell death, via secretory pathway, phosphatidylserine-based or as a result of a general exposure of chaperons from the ER.¹³⁶ In terms of ATP, the release is reported to occur by secretory pathway, pannexin 1- or autophagy-based secretion or as passive release due to plasma membrane permeabilisation.¹³⁶ The release of HMGB1 is revealed least so far

and is considered to be operated in autophagy- or caspase activity-dependent manner next to a passive release during plasma membrane permeabilisation.¹³⁷ Moreover, the full spectrum of aspects regarding the effects exhibited by the molecular ICD determinants within ICD are still under investigation, especially in terms of the role of HMGB1.^{136,137} HMGB1 shows cytokine, chemokine and growth factor activity that acts in multiple biological processes, thus making HMGB1 an important target in inflammatory diseases, cancer and immune response.¹³⁸⁻¹⁴⁰ Remarkably, HMGB1 has been found to cause different and even adverse effects within the immune system depending on the redox state induced by the cell or the extracellular environment.^{141,142} Referring to this, the activity of HMGB1 shifts between chemoattractant (reduced redox state), cytokine-inducing (intermediate redox state) and nonimmune activity (oxidised redox state).¹⁴³

6.1.4 Macrophages Co-Culture

To further assess Nilotinib for its functional potential in inducing ICD, a macrophage co-culture was performed, as macrophages play a key role in mediating the immunological effects of ICD by antigen presentation and T cell activation.⁹⁵ The prerequisite for this is the activation and maturation of macrophages towards an immune-stimulating phenotype.^{95,96} Therefore, bone marrow-derived macrophages were investigated for their activation and polarisation in response to co-cultivation with Nilotinib pre-treated leukaemic cells in both a juxtacrine and paracrine setup. The experiment was set on the background that macrophages display polarisation in reaction to environmental stimuli towards an M1 or M2 phenotype, that differ in immunogenic function and is characterised by a specific cytokine and surface expression profile.⁶⁷ Referring to this, M1 macrophages represent an immune-stimulating, tumour-suppressive phenotype with pro-inflammatory cytokine production, while M2 macrophages exhibit immune-suppressive, tumour-promoting features associated with an anti-inflammatory cytokine profile.⁶⁸⁻⁷⁰

Regarding macrophages co-culture with Nilotinib-treated leukaemic cells, no relevant shift in terms of macrophages activation and polarisation was observed in either the juxtacrine or paracrine setup compared to the corresponding co-culture conditions of untreated leukaemic cells. In contrast to that, macrophages

co-cultured with Mitoxantrone-incubated leukaemic cells were found to exhibit an average upregulation of CD80, CD86 and of CD206 next to a downregulation of MHCII. The findings of this more functional approach are in line with the results of the molecular ICD marker analysis suggesting that leukaemic cells exposed to Mitoxantrone but not to Nilotinib exhibit increased immunogenicity indicated by the upregulated expression of CD80 and CD86 in macrophages co-cultured with Mitoxantrone-treated leukaemic cells, as CD80 and CD86 represent costimulatory molecules on activated macrophages mediating activation of cytotoxic T cells.¹⁴⁴ However, with regard to macrophage polarisation, the results are not as distinct as in terms of macrophage activation. In the context of macrophage polarisation, CD80 and CD86 are related to a M1 phenotype, while CD206 is considered a typical marker for M2 macrophages.⁶⁸ The simultaneous upregulation of CD206 might therefore initially seem surprising but may be explained by the fact that tumour-associated macrophages are assumed to be not explicitly attributable to either phenotype by expressing overlapping M1/M2 properties.^{71-74,145} This fact becomes evident with respect to MHCII, which is not only a marker of macrophage activation but also of macrophage polarisation, where it is attributed to both the M1 and M2 phenotype.^{72,145} Furthermore, in the context of macrophage polarisation, not only the coexistence of M1 and M2 macrophages within the TME but also the shift in macrophages polarisation status over the time in response to the TME have been observed.^{145,146} Moreover, TAMs are found to exist in distinct TAM subsets residing in different tumour compartments, exerting specialised functions and displaying a certain surface expression profile.¹⁴⁷ Taken together, these aspects underline both the heterogeneity and the plasticity of TAMs emphasising the approach of classifying different TAMs subsets according to their function within the TME rather than in terms of their M1/M2 phenotype.¹⁴⁸⁻¹⁵⁰ As an example, the observation that hypoxia modifies macrophages polarisation and function can be cited. TAMs in hypoxic areas, such as the tumour-stroma border or the tumour centre, are sessile and pro-angiogenic macrophages that are CD206⁺MHCII^{low} and in general more M2-like orientated, while TAMs in oxygen-rich, perivascular areas exhibit migratory and pro-metastatic features associated with an CD206⁻MHCII^{high} expression profile and a rather M1-like phenotype.^{147,151}

In terms of the co-culture setup, effects on activation and polarisation of macrophages co-cultured with Mitoxantrone-treated leukaemic cells were found both in the juxtacrine and the paracrine co-culture condition. Juxtacrine signalling represents a direct signalling mechanism via close cell-cell interaction, whereas paracrine signalling is an indirect signalling mechanism that is mediated by the secretion of signalling molecules from neighbouring cells reaching the target cells via diffusion.¹⁵² The paracrine co-culture condition was performed with the aim to demonstrate that the effects on macrophage activation and polarisation are not only based on unspecific cell-cell contact between leukaemic cells and macrophages but in fact are due to the release of DAMPs from dying tumour cells succumbing to ICD. Interestingly, the effects were more pronounced in the paracrine than in the juxtacrine setup. Concerning this observation, there are almost no data available. In the study of Chang et al.¹⁵³ it was seen that the effects on macrophage activation were more distinct in the paracrine setup at early time points of co-culture, while juxtacrine signalling dominated at later time suggesting that the predominant mechanism of signalling might be in relation to the duration of co-cultivation. This may appear plausible considering that once the process of cell death is completed the release of DAMPs dries up.

6.1.5 Vaccination Assay

Finally, to evaluate the potential of Nilotinib to induce immunogenic cell death in-vivo, a vaccination assay was performed that is defined as gold-standard approach to assess bona fide ICD.⁹⁸ Therefore, leukaemic cells were treated with the drug in-vitro and then injected into the left flank of mice for vaccination. After 15 days, mice were re-challenged with live leukaemic cells injected into the tail vein. In the vaccination assay a vaccination in the sense of an active immunisation is aimed to be evoked. Thereby, in response to immortalised pathogens, the immune system is stimulated to build up a pathogen-specific immunocompetence with an immune memory so that a subsequent exposure to living pathogens leads to an effective elimination based on the established immune response.¹⁵⁴

In order to make leukaemic cells immortalised and potentially immunogenic by the induction of ICD, they were exposed to Nilotinib and Mitoxantrone,

respectively. After vaccination, leukaemia did not occur in mice as expected, but all mice of the Nilotinib cohort developed subcutaneous tumours at the injection site. Histological staining revealed tumours of densely packed leukaemic cells, indicating that Nilotinib was not sufficient to completely kill the leukaemic cells. This was to be assumed considering that Nilotinib predominantly exerts antiproliferative rather than cytotoxic effects unlike Mitoxantrone.

After rechallenge with live leukaemic cells, leukaemia occurred in both cohorts manifesting more rapidly in the Nilotinib cohort within 8 days than in the Mitoxantrone cohort within 13 days. This suggests that Nilotinib is not potent in eliciting an anti-leukaemic immune response by the induction of ICD in-vivo reinforcing the observations of the in-vitro experiments in which Nilotinib was shown to not meet the criteria of a bona fide ICD inducer. With regard to Mitoxantrone as a well-known inducer of ICD, the following considerations may be mentioned to explain why leukaemia developed in mice after rechallenge. One aspect is that Ph⁺ B-ALL is a highly aggressive leukaemia model, which is clinically emphasised by the fact that Philadelphia chromosome positive B-ALL is the most aggressive ALL subtype with a long-term survival rate in the range of only 30 %.¹⁵⁵ Therefore, the effects of ICD induction by Mitoxantrone might not be sufficient to prevent but at least delay the occurrence of leukaemia as seen in the vaccination assay. Furthermore, the in-vivo vaccination assay is designed for the application in solid tumours and has not yet been investigated in the context of non-solid leukaemia according to current data, rendering its implementation and interpretation challenging.

Notably, lower leukaemic burden was observed in the Nilotinib cohort compared to the Mitoxantrone cohort with respect to all three compartments involving bone marrow, peripheral blood and spleen. Additionally, in accordance with this, lower spleen weights were found in the Nilotinib cohort. These findings regarding leukaemic spread were most pronounced in spleen and here were found significant in the Gas6KO but not in the wild-type group. This may support the observations consistently seen in the in-vivo experiments of our research group, that Nilotinib synergizes with a Gas6-deficient environment. Moreover, it was observed by our group that the anti-leukaemic effects of Gas6 deletion in the microenvironment diminish with progression of leukaemia, initially at the site of origin in the bone marrow and finally in peripheral organs such as the spleen.

This might be the reason why in the vaccination assay the synergistic impact between Gas6KO and Nilotinib was found to be significant only in spleen, considering that leukaemia was already quite progressed in the mice with an infiltration of 35 % in bone marrow and 42 % in peripheral blood.

Besides, in white blood count a higher number of leukocytes was measured in the Nilotinib cohort compared to the Mitoxantrone cohort, indicating an increased fraction of normal leukocytes taking into account the lower leukaemic burden in peripheral blood. This finding could be interesting to be further investigated, taking into consideration that, as mentioned before, in several studies chemotherapeutic agents including TKIs have been reported to improve anti-tumour immune response by modulating the tumour immune microenvironment, such as by increasing the infiltration of cytotoxic CD8⁺ T cells.⁷⁸

6.1.6 Conclusion

In the in-vivo experiments of our research group it has been consistently observed that the use of Nilotinib but not of other chemotherapeutic agents enhances the anti-leukaemic immunity mediated by a deletion of Gas6 in the TME, which is why I was assigned to examine this observation in the present work. Against the background of increasing importance of chemotherapeutic agents as potent modulators of a dysregulated TME, it was hypothesized that Nilotinib may synergize with a Gas6-deficient environment by inducing ICD. Thus, according to the criteria for the assessment of a potential ICD inducer, Nilotinib was evaluated for the molecular and functional determinants of ICD in in-vitro and in-vivo experiments.

So far, the induction of ICD in leukaemic cells has been found in several studies.¹⁵⁶⁻¹⁶² However, there is no data available investigating the induction of ICD in leukaemic cells by Nilotinib. In the present work it was shown that Nilotinib induces cell death in leukaemic cells in concentration-dependent manner that occurs bimodally in terms of cell death modality ranging between apoptosis and necrosis. Furthermore, it was found that Nilotinib-induced cell death is not accompanied by CALR exposure and ATP release, but is associated with the release of HMGB1. No relevant shift in terms of macrophages activation and polarisation was observed in either a juxtacrine or paracrine setup of a

macrophages co-culture experiment with Nilotinib-treated leukaemic cells. In consistency with the results obtained in the in-vitro experiments, Nilotinib was not potent to elicit a protective immune response in the in-vivo vaccination assay. Conclusively, Nilotinib was identified to not qualify as a bona fide ICD inducer. This gives rise to the question by which mechanism Nilotinib instead synergistically contributes the anti-leukaemic effects of a Gas6-deficient environment. In this context, the role of Nilotinib-induced cell death and HMGB1 release may be of relevance for further investigation.

6.2 Limitations and Options

A critical review of the used methods and the obtained results is crucial to ensure quality and reliability of scientific work. Therefore, it is necessary to examine one's own work with respect to this.

By growth inhibition and viability assay it was shown that Nilotinib displays concentration- and exposure time-dependent efficacy. This relation to concentration and exposure time was further affirmed in the cell death assay. To assess Nilotinib as a potential ICD inducer under strict experimental conditions, the experiments were performed using Nilotinib at a concentration of 50 nM, which gives the lowest concentration tested with full inhibitory activity. Additionally, experiments were carried out using 10 nM Nilotinib to study a possible influence on the level of ICD hallmark expression at half maximal inhibition. As Nilotinib could not be identified as a bona fide inducer of ICD, this should be confirmed for both higher concentrations and longer exposure times in order to validate this finding.

To examine the capacity of Nilotinib to induce ICD in-vitro, ICD marker analysis was performed using techniques referred as standard according to the consensus guidelines for the detection of immunogenic cell death.⁹¹ Nonetheless, the use of additional methods allows the results obtained to be substantiated. In this respect, the evaluation of CALR exposure and HMGB1 release can be complemented by fluorescence microscopy. Moreover, extracellular HMGB1 can be assessed using enzyme-linked immunosorbent assay (ELISA). Regarding CALR, exposure to the cell surface in leukaemic cells incubated with

Mitoxantrone as positive control was not pronounced in flow cytometry indicating that the staining protocol may be optimized. In this context, modifications in terms of antibody dilution and exposure time, as well as the testing of other secondary antibodies, with which fewer non-specific background staining is obtained, could improve the experimental design.

Antigen presenting cells, including dendritic cells and macrophages, play a key role in ICD, as CALR, ATP and HMGB1 released by dying tumour cells succumbing to ICD bind to those cells mediating anti-tumour immune response.⁹⁵ The studies of our research group suggested that TAM-expressing macrophages are the essential mediators of Gas6 immune effects. For this reason, in the co-culture experiment the effects of Nilotinib in the context of ICD were assessed on macrophages and not, as primarily common, on dendritic cells. Based on the surface expression profile macrophages were investigated for their activation and polarisation. As discussed above, an evaluation concerning macrophage polarisation by surface expression markers alone is not sufficient, as in this way TAMs cannot be assigned to an M1/M2 phenotype due to overlapping characteristics.⁷¹⁻⁷⁴ Therefore, a cytokine profile assay including IL-1 β , IL-6, TNF- α , IL-10 and TGF- β performed by ELISA may provide a helpful contribution. Besides, both phagocytosis and antigen presentation capacity of macrophages could be studied by flow cytometry using DiO-labelled or OVA peptide SIINFEKL-expressing leukaemic cells, respectively. In addition, methods and addressed aspects of the macrophage co-culture experiment can be transferred to the investigation of dendritic cells for completing the picture.

Finally, the potential of Nilotinib to induce ICD in-vivo was evaluated in a vaccination assay. Unlike in the other experiments, no negative control with mice vaccinated and re-challenged using untreated leukaemic cells was performed from questions of rational resource management. With regards to the intention to elicit a protective immune response by vaccination with killed leukaemic cells that have succumbed to ICD, the question arises about how many cells have to be applied. Moreover, the efficacy of vaccination needs to be examined for a dependence on the time point of rechallenge in order to ensure optimal conditions. As outlined above, the in-vivo vaccination assay is designed for the application in solid tumours rendering its implementation and interpretation challenging in terms of leukaemia. In addition to that, all mice of the Nilotinib

cohort developed tumours at the injection site because Nilotinib was insufficient to completely kill leukemic cells due to displaying predominantly antiproliferative rather than cytotoxic activity. In order to circumvent these issues, an ex-vivo immune stimulation approach may be suggested. In this case, instead of the vaccination with leukaemic cells killed by the potential ICD inducer, bone marrow-derived macrophages and/or dendritic cells including their supernatant would be applied, which have been co-cultured with leukaemic cells pre-treated with the drug of interest. In the final analysis of the vaccination assay leukaemic burden was assessed. Considering that chemotherapeutic agents have been shown to promote anti-tumour immune response by modulating the tumour immune microenvironment,⁷⁶⁻⁷⁸ studying the impact on the immune cell infiltrate could be a contributing addition to the final analysis. Since the induction of ICD results in a tumour antigen-specific T cell immune response, the frequency of both total and INF- γ producing T cells as well as the CD8⁺/CD4⁺ and CD8⁺/Treg ratio might be an investigation of interest.

6.3 Perspectives

Besides cardiovascular disease, cancer is one of the major causes of death.¹ Therefore, highest efforts are required concerning effective treatment of cancer. Since conventional therapy concepts remain suboptimal, alternative approaches need to be investigated. Tumour cells display various mechanisms to promote tumour growth and metastasis including tumour immune escape. In this way cancer evades immunosurveillance and cannot be detected and eliminated by the immune system.⁸² The efficacy of chemotherapy has long been mainly attributed to tumour cell toxicity while immune modulating effects were neglected. But in fact, recent advances emphasise the use of chemotherapeutic agents, including TKIs, for normalising or re-educating the dysfunctional TME in the context of cancer treatment.⁷⁸ Accumulating evidence suggests that reactivation of comprised immunosurveillance in the tumour microenvironment is a critical approach for improved disease outcome and patient survival that can be achieved by the use of agents inducing immunogenic cell death in tumour cells.¹⁰⁰ However, the majority of chemotherapeutic agents are incapable of inducing ICD.

In order to restore immunogenicity of cell death, the co-administration of chemicals is conceived that convert non-ICD inducer into bona fide inducer of ICD by boosting, eliciting or substituting hallmarks of ICD, such as tumour cell death, CALR exposure, ATP secretion, HMGB1 release and Type I IFN production (Figure 31).^{96,101} Optimising the immunological potential of conventional chemotherapy is of particular importance in view of the acquired resistance to TKIs that represent the major clinical challenge of TKI treatment, as rapid but not durable tumour response is achieved.⁷⁸

In conclusion, emerging evidence supports the concept that conventional chemotherapeutic agents can display immunomodulatory effects within the TME and synergise with immunotherapeutic approaches. Testing anticancer drugs for their capability to induce ICD and establishing optimized combinatorial therapeutic regimes is a promising strategy to enhance anti-tumour immunity and to improve therapeutic efficacy with the aim of providing cancer patients with the best possible treatment in the future.

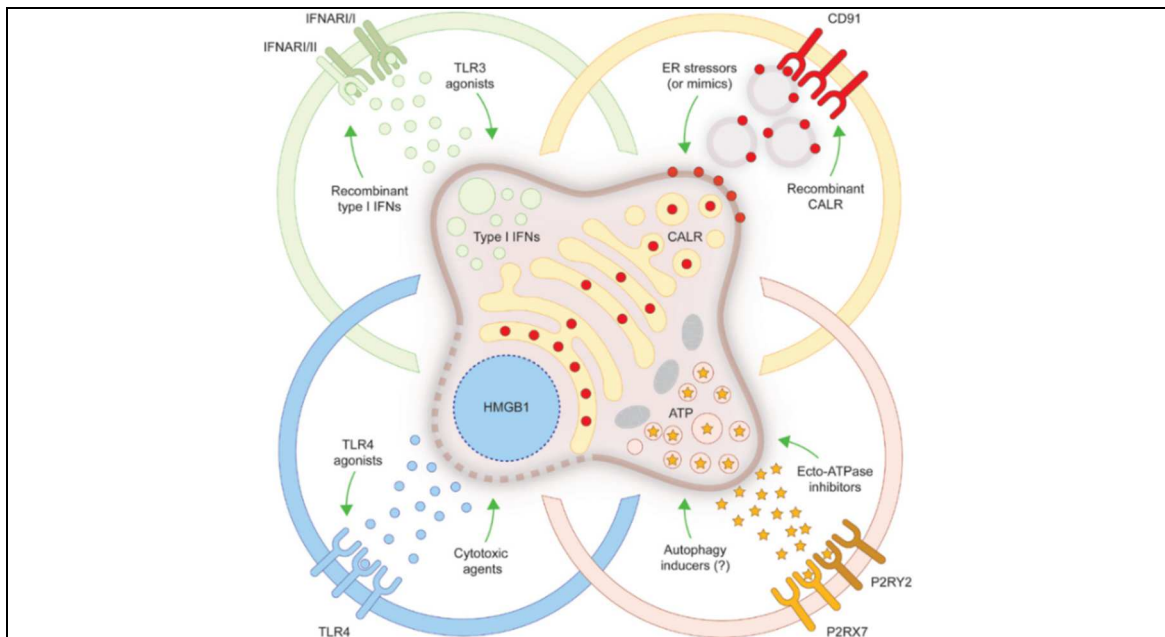


Figure 31. Strategies for the Induction of ICD. The induction of ICD relies on the release of DAMPs from dying tumour cells succumbing to ICD. CALR exposure, ATP secretion and HMGB1 release are considered key hallmarks of ICD mediating anti-tumour immunity upon binding to antigen presenting immune cells, which results in an INF- γ -mediated tumour antigen-specific T cell response. If any of these DAMPs is not released, dying cancer cells cannot be perceived as immunogenic by the immune system. Several strategies have been conceived aiming to convert non-immunogenic cell death into bona fide ICD in order to restore immunogenicity. From Bezu *et al.*, 2015 (101).

7 References

1. Siegel RL, Miller KD, Jemal A. Cancer statistics, 2019. *CA Cancer J Clin.* 2019;69(1):7-34. doi:10.3322/caac.21551.
2. Gesellschaft für Pädiatrische Onkologie und Hämatologie. S1-Leitlinie 025/014: Akute lymphoblastische- (ALL) Leukämie im Kindesalter. Updated April 11, 2016. Accessed January 13, 2020.
3. An Q, Fan C-H, Xu S-M. Recent perspectives of pediatric leukemia - an update. *Eur Rev Med Pharmacol Sci.* 2017;21(4 Suppl):31-36.
4. Poplack DG, Helman L, Pizzo PA, Adamson PC, Blaney SM, eds. *Principles and practice of pediatric oncology.* Philadelphia, PA: Wolters Kluwer; 2016.
5. Zuckerman T, Rowe JM. Pathogenesis and prognostication in acute lymphoblastic leukemia. *F1000Prime Rep.* 2014;6:59. doi:10.12703/P6-59.
6. Deutsche Gesellschaft für Hämato-Onkologie. Leitlinie Akute Lymphatische Leukämie (ALL). Updated February 2018. Accessed January 13, 2020.
7. Bene MC, Castoldi G, Knapp W, et al. Proposals for the immunological classification of acute leukemias. European Group for the Immunological Characterization of Leukemias (EGIL). *Leukemia.* 1995;9(10):1783-1786.
8. Firkin B, Moore CV. Clinical manifestations of leukemia. *The American Journal of Medicine.* 1960;28(5):764-776. doi:10.1016/0002-9343(60)90133-9.
9. Moorman AV, Ensor HM, Richards SM, et al. Prognostic effect of chromosomal abnormalities in childhood B-cell precursor acute lymphoblastic leukaemia: results from the UK Medical Research Council ALL97/99 randomised trial. *Lancet Oncol.* 2010;11(5):429-438. doi:10.1016/S1470-2045(10)70066-8.

10. Moorman AV, Harrison CJ, Buck GAN, et al. Karyotype is an independent prognostic factor in adult acute lymphoblastic leukemia (ALL): analysis of cytogenetic data from patients treated on the Medical Research Council (MRC) UKALLXII/Eastern Cooperative Oncology Group (ECOG) 2993 trial. *Blood*. 2007;109(8):3189-3197. doi:10.1182/blood-2006-10-051912.
11. Rowley JD. Letter: A new consistent chromosomal abnormality in chronic myelogenous leukaemia identified by quinacrine fluorescence and Giemsa staining. *Nature*. 1973;243(5405):290-293. doi:10.1038/243290a0.
12. Kurzrock R, Gutterman JU, Talpaz M. The molecular genetics of Philadelphia chromosome-positive leukemias. *N Engl J Med*. 1988;319(15):990-998. doi:10.1056/NEJM198810133191506.
13. Li S, Ilaria RL, Million RP, Daley GQ, van Etten RA. The P190, P210, and P230 forms of the BCR/ABL oncogene induce a similar chronic myeloid leukemia-like syndrome in mice but have different lymphoid leukemogenic activity. *J Exp Med*. 1999;189(9):1399-1412. doi:10.1084/jem.189.9.1399.
14. Bernt KM, Hunger SP. Current concepts in pediatric Philadelphia chromosome-positive acute lymphoblastic leukemia. *Front Oncol*. 2014;4:54. doi:10.3389/fonc.2014.00054.
15. Roberts KG, Mullighan CG. Genomics in acute lymphoblastic leukaemia: insights and treatment implications. *Nat Rev Clin Oncol*. 2015;12(6):344-357. doi:10.1038/nrclinonc.2015.38.
16. Ravandi F. Current management of Philadelphia chromosome positive ALL and the role of stem cell transplantation. *Hematology Am Soc Hematol Educ Program*. 2017;2017(1):22-27.
17. Chalandon Y, Thomas X, Hayette S, et al. Randomized study of reduced-intensity chemotherapy combined with imatinib in adults with Ph-positive acute lymphoblastic leukemia. *Blood*. 2015;125(24):3711-3719. doi:10.1182/blood-2015-02-627935.

18. Kang Z-J, Liu Y-F, Xu L-Z, et al. The Philadelphia chromosome in leukemogenesis. *Chin J Cancer*. 2016;35:48. doi:10.1186/s40880-016-0108-0.
19. Ravandi F, Kebriaei P. PHILADELPHIA CHROMOSOME POSITIVE ACUTE LYMPHOBLASTIC LEUKEMIA. *Hematol Oncol Clin North Am*. 2009;23(5):1043-vi. doi:10.1016/j.hoc.2009.07.007.
20. Hochhaus A, Kreil S, Corbin AS, et al. Molecular and chromosomal mechanisms of resistance to imatinib (STI571) therapy. *Leukemia*. 2002;16(11):2190-2196. doi:10.1038/sj.leu.2402741.
21. Gorre ME, Mohammed M, Ellwood K, et al. Clinical resistance to STI-571 cancer therapy caused by BCR-ABL gene mutation or amplification. *Science*. 2001;293(5531):876-880. doi:10.1126/science.1062538.
22. Shah NP, Nicoll JM, Nagar B, et al. Multiple BCR-ABL kinase domain mutations confer polyclonal resistance to the tyrosine kinase inhibitor imatinib (STI571) in chronic phase and blast crisis chronic myeloid leukemia. *Cancer Cell*. 2002;2(2):117-125. doi:10.1016/S1535-6108(02)00096-X.
23. Redaelli S, Mologni L, Rostagno R, et al. Three novel patient-derived BCR/ABL mutants show different sensitivity to second and third generation tyrosine kinase inhibitors. *Am J Hematol*. 2012;87(11):E125-8. doi:10.1002/ajh.23338.
24. Zhang H, Chen J. Current status and future directions of cancer immunotherapy. *J Cancer*. 2018;9(10):1773-1781. doi:10.7150/jca.24577.
25. Kruger S, Ilmer M, Kobold S, et al. Advances in cancer immunotherapy 2019 - latest trends. *J Exp Clin Cancer Res*. 2019;38(1):268. doi:10.1186/s13046-019-1266-0.
26. Whiteside TL, Demaria S, Rodriguez-Ruiz ME, Zarour HM, Melero I. Emerging Opportunities and Challenges in Cancer Immunotherapy. *Clin Cancer Res*. 2016;22(8):1845-1855. doi:10.1158/1078-0432.CCR-16-0049.

27. Li Y, Liu S, Margolin K, Hwu P. Summary of the primer on tumor immunology and the biological therapy of cancer. *J Transl Med.* 2009;7:11. doi:10.1186/1479-5876-7-11.
28. Dougan M, Dranoff G, Dougan SK. Cancer Immunotherapy: Beyond Checkpoint Blockade. *Annu. Rev. Cancer Biol.* 2019;3(1):55-75. doi:10.1146/annurev-cancerbio-030518-055552.
29. Dougan M, Dranoff G. Immune therapy for cancer. *Annu Rev Immunol.* 2009;27:83-117. doi:10.1146/annurev.immunol.021908.132544.
30. Junttila MR, Sauvage FJ de. Influence of tumour micro-environment heterogeneity on therapeutic response. *Nature.* 2013;501(7467):346-354. doi:10.1038/nature12626.
31. Klemm F, Joyce JA. Microenvironmental regulation of therapeutic response in cancer. *Trends Cell Biol.* 2015;25(4):198-213. doi:10.1016/j.tcb.2014.11.006.
32. Yu Y, Cui J. Present and future of cancer immunotherapy: A tumor microenvironmental perspective. *Oncol Lett.* 2018;16(4):4105-4113. doi:10.3892/ol.2018.9219.
33. Wang M, Zhao J, Zhang L, et al. Role of tumor microenvironment in tumorigenesis. *J Cancer.* 2017;8(5):761-773. doi:10.7150/jca.17648.
34. Chen F, Zhuang X, Lin L, et al. New horizons in tumor microenvironment biology: challenges and opportunities. *BMC Med.* 2015;13. doi:10.1186/s12916-015-0278-7.
35. Tang H, Qiao J, Fu Y-X. Immunotherapy and tumor microenvironment. *Cancer Lett.* 2015;370(1):85-90. doi:10.1016/j.canlet.2015.10.009.
36. Devaud C, John LB, Westwood JA, Darcy PK, Kershaw MH. Immune modulation of the tumor microenvironment for enhancing cancer immunotherapy. *Oncoimmunology.* 2013;2(8). doi:10.4161/onci.25961.

37. Binnewies M, Roberts EW, Kersten K, et al. Understanding the tumor immune microenvironment (TIME) for effective therapy. *Nat Med*. 2018;24(5):541-550. doi:10.1038/s41591-018-0014-x.
38. Markman JL, Shiao SL. Impact of the immune system and immunotherapy in colorectal cancer. *J Gastrointest Oncol*. 2015;6(2):208-223. doi:10.3978/j.issn.2078-6891.2014.077.
39. Quail DF, Joyce JA. Microenvironmental regulation of tumor progression and metastasis. *Nat Med*. 2013;19(11):1423-1437. doi:10.1038/nm.3394.
40. Swartz MA, Iida N, Roberts EW, et al. Tumor microenvironment complexity: emerging roles in cancer therapy. *Cancer Res*. 2012;72(10):2473-2480. doi:10.1158/0008-5472.CAN-12-0122.
41. Kerkar SP, Restifo NP. Cellular constituents of immune escape within the tumor microenvironment. *Cancer Res*. 2012;72(13):3125-3130. doi:10.1158/0008-5472.CAN-11-4094.
42. Roma-Rodrigues C, Mendes R, Baptista PV, Fernandes AR. Targeting Tumor Microenvironment for Cancer Therapy. *Int J Mol Sci*. 2019;20(4). doi:10.3390/ijms20040840.
43. Valkenburg KC, Groot AE de, Pienta KJ. Targeting the tumour stroma to improve cancer therapy. *Nat Rev Clin Oncol*. 2018;15(6):366-381. doi:10.1038/s41571-018-0007-1.
44. Lemke G. Biology of the TAM receptors. *Cold Spring Harb Perspect Biol*. 2013;5(11):a009076. doi:10.1101/cshperspect.a009076.
45. Sasaki T, Knyazev PG, Clout NJ, et al. Structural basis for Gas6-Axl signalling. *EMBO J*. 2006;25(1):80-87. doi:10.1038/sj.emboj.7600912.
46. Axelrod H, Pienta KJ. Axl as a mediator of cellular growth and survival. *Oncotarget*. 2014;5(19):8818-8852. doi:10.18632/oncotarget.2422.
47. Gustafsson A, Boström A-K, Ljungberg B, Axelson H, Dahlbäck B. Gas6 and the receptor tyrosine kinase Axl in clear cell renal cell carcinoma. *PLoS ONE*. 2009;4(10):e7575. doi:10.1371/journal.pone.0007575.

48. Lee C-H, Yen C-Y, Liu S-Y, et al. Axl is a prognostic marker in oral squamous cell carcinoma. *Ann Surg Oncol*. 2012;19 Suppl 3:S500-8. doi:10.1245/s10434-011-1985-8.
 49. Sainaghi PP, Castello L, Bergamasco L, Galletti M, Bellosta P, Avanzi GC. Gas6 induces proliferation in prostate carcinoma cell lines expressing the Axl receptor. *J Cell Physiol*. 2005;204(1):36-44. doi:10.1002/jcp.20265.
 50. Song X, Wang H, Logsdon CD, et al. Overexpression of receptor tyrosine kinase Axl promotes tumor cell invasion and survival in pancreatic ductal adenocarcinoma. *Cancer*. 2011;117(4):734-743. doi:10.1002/cncr.25483.
 51. Buehler M, Tse B, Leboucq A, et al. Meta-analysis of microarray data identifies GAS6 expression as an independent predictor of poor survival in ovarian cancer. *Biomed Res Int*. 2013;2013:238284. doi:10.1155/2013/238284.
 52. Demarest SJ, Gardner J, Vendel MC, et al. Evaluation of Tyro3 expression, Gas6-mediated Akt phosphorylation, and the impact of anti-Tyro3 antibodies in melanoma cell lines. *Biochemistry*. 2013;52(18):3102-3118. doi:10.1021/bi301588c.
 53. Whitman SP, Kohlschmidt J, Maharry K, et al. GAS6 expression identifies high-risk adult AML patients: potential implications for therapy. *Leukemia*. 2014;28(6):1252-1258. doi:10.1038/leu.2013.371.
 54. Ben-Batalla I, Schultze A, Wroblewski M, et al. Axl, a prognostic and therapeutic target in acute myeloid leukemia mediates paracrine crosstalk of leukemia cells with bone marrow stroma. *Blood*. 2013;122(14):2443-2452. doi:10.1182/blood-2013-03-491431.
 55. Lee-Sherick AB, Eisenman KM, Sather S, et al. Aberrant Mer receptor tyrosine kinase expression contributes to leukemogenesis in acute myeloid leukemia. *Oncogene*. 2016;35(48):6270. doi:10.1038/onc.2016.29
- 5.

56. Han J, Tian R, Yong B, et al. Gas6/Axl mediates tumor cell apoptosis, migration and invasion and predicts the clinical outcome of osteosarcoma patients. *Biochem Biophys Res Commun.* 2013;435(3):493-500. doi:10.1016/j.bbrc.2013.05.019.
57. Linger RMA, Cohen RA, Cummings CT, et al. Mer or Axl receptor tyrosine kinase inhibition promotes apoptosis, blocks growth and enhances chemosensitivity of human non-small cell lung cancer. *Oncogene.* 2013;32(29):3420-3431. doi:10.1038/onc.2012.355.
58. Lee Y, Lee M, Kim S. Gas6 induces cancer cell migration and epithelial-mesenchymal transition through upregulation of MAPK and Slug. *Biochem Biophys Res Commun.* 2013;434(1):8-14. doi:10.1016/j.bbrc.2013.03.082.
59. Rothlin CV, Ghosh S, Zuniga EI, Oldstone MBA, Lemke G. TAM receptors are pleiotropic inhibitors of the innate immune response. *Cell.* 2007;131(6):1124-1136. doi:10.1016/j.cell.2007.10.034.
60. Rothlin CV, Carrera-Silva EA, Bosurgi L, Ghosh S. TAM receptor signaling in immune homeostasis. *Annu Rev Immunol.* 2015;33:355-391. doi:10.1146/annurev-immunol-032414-112103.
61. Wu G, Ma Z, Cheng Y, et al. Targeting Gas6/TAM in cancer cells and tumor microenvironment. *Mol Cancer.* 2018;17(1):20. doi:10.1186/s12943-018-0769-1.
62. Wu G, Ma Z, Hu W, et al. Molecular insights of Gas6/TAM in cancer development and therapy. *Cell Death Dis.* 2017;8(3):e2700. doi:10.1038/cddis.2017.113.
63. Paolino M, Choidas A, Wallner S, et al. The E3 ligase Cbl-b and TAM receptors regulate cancer metastasis via natural killer cells. *Nature.* 2014;507(7493):508-512. doi:10.1038/nature12998.
64. Harris W. *TAM RTK Inhibition Causes Different Effects in Myeloid-Derived Suppressor Cells and Dendritic Cells*; 2017.

65. Chiu K-C, Lee C-H, Liu S-Y, et al. Polarization of tumor-associated macrophages and Gas6/Axl signaling in oral squamous cell carcinoma. *Oral Oncol.* 2015;51(7):683-689. doi:10.1016/j.oraloncology.2015.04.004.
66. Akalu YT, Rothlin CV, Ghosh S. TAM receptor tyrosine kinases as emerging targets of innate immune checkpoint blockade for cancer therapy. *Immunol Rev.* 2017;276(1):165-177. doi:10.1111/imr.12522.
67. Yao Y, Xu X-H, Jin L. Macrophage Polarization in Physiological and Pathological Pregnancy. *Front Immunol.* 2019;10:792. doi:10.3389/fimmu.2019.00792.
68. Mills CD. Anatomy of a discovery: m1 and m2 macrophages. *Front Immunol.* 2015;6:212. doi:10.3389/fimmu.2015.00212.
69. Mills CD. M1 and M2 Macrophages: Oracles of Health and Disease. *Crit Rev Immunol.* 2012;32(6):463-488. doi:10.1615/critrevimmunol.v32.i6.10.
70. Biswas SK, Mantovani A. Macrophage plasticity and interaction with lymphocyte subsets: cancer as a paradigm. *Nat Immunol.* 2010;11(10):889-896. doi:10.1038/ni.1937.
71. Hamilton JA. Colony-stimulating factors in inflammation and autoimmunity. *Nat Rev Immunol.* 2008;8(7):533-544. doi:10.1038/nri2356.
72. Mantovani A, Marchesi F, Malesci A, Laghi L, Allavena P. Tumour-associated macrophages as treatment targets in oncology. *Nat Rev Clin Oncol.* 2017;14(7):399-416. doi:10.1038/nrclinonc.2016.217.
73. Aras S, Zaidi MR. TAMEless traitors: macrophages in cancer progression and metastasis. *Br J Cancer.* 2017;117(11):1583-1591. doi:10.1038/bjc.2017.356.
74. Lin Y, Xu J, Lan H. Tumor-associated macrophages in tumor metastasis: biological roles and clinical therapeutic applications. *J Hematol Oncol.* 2019;12(1):76. doi:10.1186/s13045-019-0760-3.

75. Belvin MP, Luoh S-M, Cheung J, McNamara E, Cubas R, Kim J. Abstract 4898: Effects of chemotherapeutic agents on the tumor immune microenvironment. In: Immunology: American Association for Cancer Research; 07152016:4898.
76. Zitvogel L, Kepp O, Kroemer G. Immune parameters affecting the efficacy of chemotherapeutic regimens. *Nat Rev Clin Oncol*. 2011;8(3):151-160. doi:10.1038/nrclinonc.2010.223.
77. Tsuchikawa T, Takeuchi S, Nakamura T, Shichinohe T, Hirano S. Clinical impact of chemotherapy to improve tumor microenvironment of pancreatic cancer. *World J Gastrointest Oncol*. 2016;8(11):786-792. doi:10.4251/wjgo.v8.i11.786.
78. Tan H-Y, Wang N, Lam W, Guo W, Feng Y, Cheng Y-C. Targeting tumour microenvironment by tyrosine kinase inhibitor. *Mol Cancer*. 2018;17(1):43. doi:10.1186/s12943-018-0800-6.
79. Galluzzi L, Buqué A, Kepp O, Zitvogel L, Kroemer G. Immunological Effects of Conventional Chemotherapy and Targeted Anticancer Agents. *Cancer Cell*. 2015;28(6):690-714. doi:10.1016/j.ccell.2015.10.012.
80. Galluzzi L, Senovilla L, Zitvogel L, Kroemer G. The secret ally: immunostimulation by anticancer drugs. *Nat Rev Drug Discov*. 2012;11(3):215-233. doi:10.1038/nrd3626.
81. Swann JB, Smyth MJ. Immune surveillance of tumors. *J Clin Invest*. 2007;117(5):1137-1146. doi:10.1172/JCI31405.
82. Dunn GP, Bruce AT, Ikeda H, Old LJ, Schreiber RD. Cancer immunoediting: from immunosurveillance to tumor escape. *Nat Immunol*. 2002;3(11):991-998. doi:10.1038/ni1102-991.
83. Garg AD, Dudek AM, Agostinis P. Cancer immunogenicity, danger signals, and DAMPs: what, when, and how? *Biofactors*. 2013;39(4):355-367. doi:10.1002/biof.1125.

84. Galluzzi L, Buqué A, Kepp O, Zitvogel L, Kroemer G. Immunogenic cell death in cancer and infectious disease. *Nat Rev Immunol*. 2017;17(2):97-111. doi:10.1038/nri.2016.107.
85. Garg AD, More S, Rufo N, et al. Trial watch: Immunogenic cell death induction by anticancer chemotherapeutics. *Oncoimmunology*. 2017;6(12):e1386829. doi:10.1080/2162402X.2017.1386829.
86. Dudek AM, Garg AD, Krysko DV, Ruyscher D de, Agostinis P. Inducers of immunogenic cancer cell death. *Cytokine Growth Factor Rev*. 2013;24(4):319-333. doi:10.1016/j.cytogfr.2013.01.005.
87. Zitvogel L, Kepp O, Kroemer G. Decoding cell death signals in inflammation and immunity. *Cell*. 2010;140(6):798-804. doi:10.1016/j.cell.2010.02.015.
88. Nagata S, Tanaka M. Programmed cell death and the immune system. *Nat Rev Immunol*. 2017;17(5):333-340. doi:10.1038/nri.2016.153.
89. Bianchi ME. DAMPs, PAMPs and alarmins: all we need to know about danger. *J Leukoc Biol*. 2007;81(1):1-5. doi:10.1189/jlb.0306164.
90. Zitvogel L, Kepp O, Senovilla L, Menger L, Chaput N, Kroemer G. Immunogenic tumor cell death for optimal anticancer therapy: the calreticulin exposure pathway. *Clin Cancer Res*. 2010;16(12):3100-3104. doi:10.1158/1078-0432.CCR-09-2891.
91. Kepp O, Senovilla L, Vitale I, et al. Consensus guidelines for the detection of immunogenic cell death. *Oncoimmunology*. 2014;3(9):e955691. doi:10.4161/21624011.2014.955691.
92. Obeid M, Tesniere A, Ghiringhelli F, et al. Calreticulin exposure dictates the immunogenicity of cancer cell death. *Nat Med*. 2007;13(1):54-61. doi:10.1038/nm1523.
93. Garg AD, Krysko DV, Verfaillie T, et al. A novel pathway combining calreticulin exposure and ATP secretion in immunogenic cancer cell death. *EMBO J*. 2012;31(5):1062-1079. doi:10.1038/emboj.2011.497.

94. Stoetzer OJ, Fersching DMI, Salat C, et al. Circulating immunogenic cell death biomarkers HMGB1 and RAGE in breast cancer patients during neoadjuvant chemotherapy. *Tumour Biol.* 2013;34(1):81-90. doi:10.1007/s13277-012-0513-1.
95. Garg AD, Dudek-Peric AM, Romano E, Agostinis P. Immunogenic cell death. *Int J Dev Biol.* 2015;59(1-3):131-140. doi:10.1387/ijdb.150061pa.
96. Kroemer G, Galluzzi L, Kepp O, Zitvogel L. Immunogenic cell death in cancer therapy. *Annu Rev Immunol.* 2013;31:51-72. doi:10.1146/annurev-immunol-032712-100008.
97. Zhou J, Wang G, Chen Y, Wang H, Hua Y, Cai Z. Immunogenic cell death in cancer therapy: Present and emerging inducers. *J Cell Mol Med.* 2019;23(8):4854-4865. doi:10.1111/jcmm.14356.
98. Green DR, Ferguson T, Zitvogel L, Kroemer G. Immunogenic and tolerogenic cell death. *Nat Rev Immunol.* 2009;9(5):353-363. doi:10.1038/nri2545.
99. Vacchelli E, Galluzzi L, Fridman WH, et al. Trial watch: Chemotherapy with immunogenic cell death inducers. *Oncoimmunology.* 2012;1(2):179-188. doi:10.4161/onci.1.2.19026.
100. Wang Y-J, Fletcher R, Yu J, Zhang L. Immunogenic effects of chemotherapy-induced tumor cell death. *Genes Dis.* 2018;5(3):194-203. doi:10.1016/j.gendis.2018.05.003.
101. Bezu L, Gomes-de-Silva LC, Dewitte H, et al. Combinatorial strategies for the induction of immunogenic cell death. *Front Immunol.* 2015;6:187. doi:10.3389/fimmu.2015.00187.
102. Seminario-Vidal L, Lazarowski ER, Okada SF. Assessment of extracellular ATP concentrations. *Methods Mol Biol.* 2009;574:25-36. doi:10.1007/978-1-60327-321-3_3.

103. Weisberg E, Manley P, Mestan J, Cowan-Jacob S, Ray A, Griffin JD. AMN107 (nilotinib): a novel and selective inhibitor of BCR-ABL. *Br J Cancer*. 2006;94(12):1765-1769. doi:10.1038/sj.bjc.6603170.
104. Blay J-Y, Mehren M von. Nilotinib: a novel, selective tyrosine kinase inhibitor. *Semin Oncol*. 2011;38 Suppl 1:S3-9. doi:10.1053/j.seminoncol.2011.01.016.
105. Bellosillo B, Colomer D, Pons G, Gil J. Mitoxantrone, a topoisomerase II inhibitor, induces apoptosis of B-chronic lymphocytic leukaemia cells. *Br J Haematol*. 1998;100(1):142-146. doi:10.1046/j.1365-2141.1998.00520.x.
106. Seitz M. Molecular and cellular effects of methotrexate. *Curr Opin Rheumatol*. 1999;11(3):226-232. doi:10.1097/00002281-199905000-00012.
107. Kaur P, Feldhahn N, Zhang B, et al. Nilotinib treatment in mouse models of P190 Bcr/Abl lymphoblastic leukemia. *Mol Cancer*. 2007;6:67. doi:10.1186/1476-4598-6-67.
108. Weisberg E, Manley PW, Breitenstein W, et al. Characterization of AMN107, a selective inhibitor of native and mutant Bcr-Abl. *Cancer Cell*. 2005;7(2):129-141. doi:10.1016/j.ccr.2005.01.007.
109. O'Hare T, Walters DK, Stoffregen EP, et al. In vitro activity of Bcr-Abl inhibitors AMN107 and BMS-354825 against clinically relevant imatinib-resistant Abl kinase domain mutants. *Cancer Res*. 2005;65(11):4500-4505. doi:10.1158/0008-5472.CAN-05-0259.
110. Warmuth M, Kim S, Gu X-j, Xia G, Adrián F. Ba/F3 cells and their use in kinase drug discovery. *Curr Opin Oncol*. 2007;19(1):55-60. doi:10.1097/CCO.0b013e328011a25f.
111. Cornelissen M, Philippé J, Sitter S de, Ridder L de. Annexin V expression in apoptotic peripheral blood lymphocytes: an electron microscopic evaluation. *Apoptosis*. 2002;7(1):41-47. doi:10.1023/a:1013560828090.

- 112.** Vermes I, Haanen C, Reutelingsperger C. Flow cytometry of apoptotic cell death. *J Immunol Methods*. 2000;243(1-2):167-190. doi:10.1016/s0022-1759(00)00233-7.
- 113.** Vermes I, Haanen C, Steffens-Nakken H, Reutelingsperger C. A novel assay for apoptosis. Flow cytometric detection of phosphatidylserine expression on early apoptotic cells using fluorescein labelled Annexin V. *J Immunol Methods*. 1995;184(1):39-51. doi:10.1016/0022-1759(95)00072-i.
- 114.** Crowley LC, Marfell BJ, Scott AP, Waterhouse NJ. Quantitation of Apoptosis and Necrosis by Annexin V Binding, Propidium Iodide Uptake, and Flow Cytometry. *Cold Spring Harb Protoc*. 2016;2016(11). doi:10.1101/pdb.prot087288.
- 115.** Rieger AM, Nelson KL, Konowalchuk JD, Barreda DR. Modified Annexin V/Propidium Iodide Apoptosis Assay For Accurate Assessment of Cell Death. *J Vis Exp*. 2011;(50). doi:10.3791/2597.
- 116.** Zhang H, Gu L, Liu T, Chiang K-Y, Zhou M. Inhibition of MDM2 by nilotinib contributes to cytotoxicity in both Philadelphia-positive and negative acute lymphoblastic leukemia. *PLoS ONE*. 2014;9(6):e100960. doi:10.1371/journal.pone.0100960.
- 117.** Jørgensen HG, Allan EK, Jordanides NE, Mountford JC, Holyoake TL. Nilotinib exerts equipotent antiproliferative effects to imatinib and does not induce apoptosis in CD34+ CML cells. *Blood*. 2007;109(9):4016-4019. doi:10.1182/blood-2006-11-057521.
- 118.** Davies A, Jordanides NE, Giannoudis A, et al. Nilotinib concentration in cell lines and primary CD34(+) chronic myeloid leukemia cells is not mediated by active uptake or efflux by major drug transporters. *Leukemia*. 2009;23(11):1999-2006. doi:10.1038/leu.2009.166.
- 119.** Copland M, Hamilton A, Elrick LJ, et al. Dasatinib (BMS-354825) targets an earlier progenitor population than imatinib in primary CML but does not eliminate the quiescent fraction. *Blood*. 2006;107(11):4532-4539. doi:10.1182/blood-2005-07-2947.

120. Reddicono G, Toto C, Palamà I, et al. Targeting of GSK3 β promotes imatinib-mediated apoptosis in quiescent CD34+ chronic myeloid leukemia progenitors, preserving normal stem cells. *Blood*. 2012;119(10):2335-2345. doi:10.1182/blood-2011-06-361261.
121. Carter BZ, Mak PY, Mak DH, et al. Synergistic effects of p53 activation via MDM2 inhibition in combination with inhibition of Bcl-2 or Bcr-Abl in CD34+ proliferating and quiescent chronic myeloid leukemia blast crisis cells. *Oncotarget*. 2015;6(31):30487-30499. doi:10.18632/oncotarget.5890.
122. Wagner M-C, Dziadosz M, Melo JV, Heidel F, Fischer T, Lipka DB. Nilotinib shows prolonged intracellular accumulation upon pulse-exposure: a novel mechanism for induction of apoptosis in CML cells. *Leukemia*. 2013;27(7):1567-1570. doi:10.1038/leu.2012.364.
123. Lipka DB, Wagner M-C, Dziadosz M, et al. Intracellular retention of ABL kinase inhibitors determines commitment to apoptosis in CML cells. *PLoS ONE*. 2012;7(7):e40853. doi:10.1371/journal.pone.0040853.
124. Galluzzi L, Maiuri MC, Vitale I, et al. Cell death modalities: classification and pathophysiological implications. *Cell Death Differ*. 2007;14(7):1237-1243. doi:10.1038/sj.cdd.4402148.
125. Galluzzi L, Vitale I, Abrams JM, et al. Molecular definitions of cell death subroutines: recommendations of the Nomenclature Committee on Cell Death 2012. *Cell Death Differ*. 2012;19(1):107-120. doi:10.1038/cdd.2011.96.
126. Vandenabeele P, Galluzzi L, Vanden Berghe T, Kroemer G. Molecular mechanisms of necroptosis: an ordered cellular explosion. *Nat Rev Mol Cell Biol*. 2010;11(10):700-714. doi:10.1038/nrm2970.
127. Messmer MN, Snyder AG, Oberst A. Comparing the effects of different cell death programs in tumor progression and immunotherapy. *Cell Death Differ*. 2019;26(1):115-129. doi:10.1038/s41418-018-0214-4.

- 128.** Bellamy CO, Malcomson RD, Harrison DJ, Wyllie AH. Cell death in health and disease: the biology and regulation of apoptosis. *Semin Cancer Biol.* 1995;6(1):3-16. doi:10.1006/scbi.1995.0002.
- 129.** Hou W, Zhang Q, Yan Z, et al. Strange attractors: DAMPs and autophagy link tumor cell death and immunity. *Cell Death Dis.* 2013;4:e966. doi:10.1038/cddis.2013.493.
- 130.** Nicotera P, Melino G. Regulation of the apoptosis-necrosis switch. *Oncogene.* 2004;23(16):2757-2765. doi:10.1038/sj.onc.1207559.
- 131.** Nicotera P, Leist M, Ferrando-May E. Apoptosis and necrosis: different execution of the same death. *Biochem Soc Symp.* 1999;66:69-73. doi:10.1042/bss0660069.
- 132.** Burnstock G, Knight GE. Cell culture: complications due to mechanical release of ATP and activation of purinoceptors. *Cell Tissue Res.* 2017;370(1):1-11. doi:10.1007/s00441-017-2618-8.
- 133.** Bell CW, Jiang W, Reich CF, Pisetsky DS. The extracellular release of HMGB1 during apoptotic cell death. *Am J Physiol , Cell Physiol.* 2006;291(6):C1318-25. doi:10.1152/ajpcell.00616.2005.
- 134.** Scaffidi P, Misteli T, Bianchi ME. Release of chromatin protein HMGB1 by necrotic cells triggers inflammation. *Nature.* 2002;418(6894):191-195. doi:10.1038/nature00858.
- 135.** Duprez L, Takahashi N, van Hauwermeiren F, et al. RIP kinase-dependent necrosis drives lethal systemic inflammatory response syndrome. *Immunity.* 2011;35(6):908-918. doi:10.1016/j.immuni.2011.09.020.
- 136.** Krysko DV, Garg AD, Kaczmarek A, Krysko O, Agostinis P, Vandenabeele P. Immunogenic cell death and DAMPs in cancer therapy. *Nat Rev Cancer.* 2012;12(12):860-875. doi:10.1038/nrc3380.
- 137.** Tang D, Kang R. HMGB1 in Cell Death. In: Ntuli TM, ed. *Cell Death - Autophagy, Apoptosis and Necrosis.* [S.l.]: InTech; 2015.

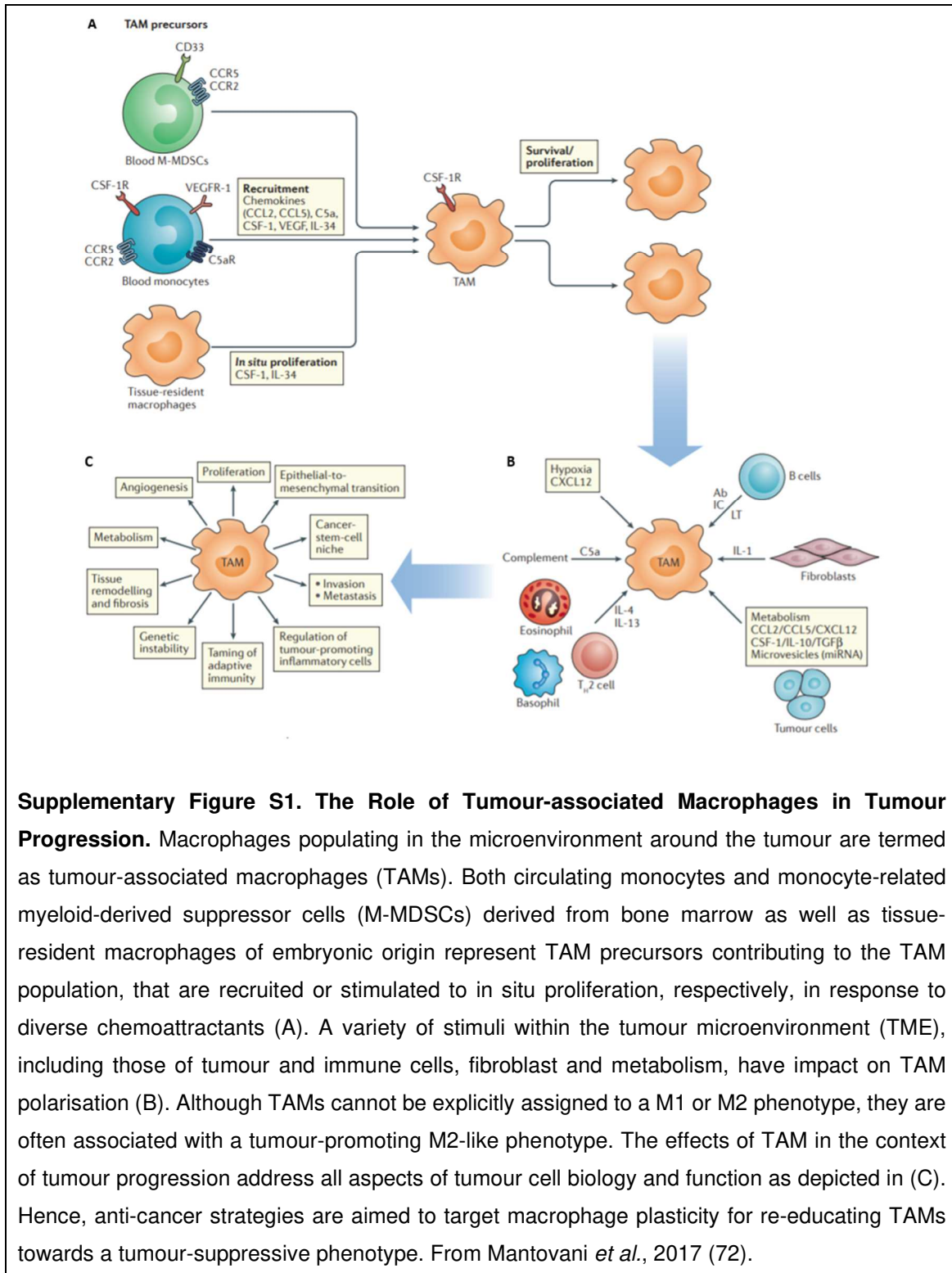
- 138.** Kang R, Chen R, Zhang Q, et al. HMGB1 in health and disease. *Mol Aspects Med.* 2014;40:1-116. doi:10.1016/j.mam.2014.05.001.
- 139.** Lee S-A, Kwak MS, Kim S, Shin J-S. The role of high mobility group box 1 in innate immunity. *Yonsei Med J.* 2014;55(5):1165-1176. doi:10.3349/ymj.2014.55.5.1165.
- 140.** Kang R, Zhang Q, Zeh HJ, Lotze MT, Tang D. HMGB1 in cancer: good, bad, or both? *Clin Cancer Res.* 2013;19(15):4046-4057. doi:10.1158/1078-0432.CCR-13-0495.
- 141.** Venereau E, Casalgrandi M, Schiraldi M, et al. Mutually exclusive redox forms of HMGB1 promote cell recruitment or proinflammatory cytokine release. *J Exp Med.* 2012;209(9):1519-1528. doi:10.1084/jem.20120189.
- 142.** Yang H, Lundbäck P, Ottosson L, et al. Redox modification of cysteine residues regulates the cytokine activity of high mobility group box-1 (HMGB1). *Mol Med.* 2012;18:250-259. doi:10.2119/molmed.2011.00389.
- 143.** Tang D, Billiar TR, Lotze MT. A Janus Tale of Two Active High Mobility Group Box 1 (HMGB1) Redox States. *Mol Med.* 2012;18(1):1360-1362. doi:10.2119/molmed.2012.00314.
- 144.** Subauste CS, Waal Malefyt R de, Fuh F. Role of CD80 (B7.1) and CD86 (B7.2) in the immune response to an intracellular pathogen. *J Immunol.* 1998;160(4):1831-1840.
- 145.** Chávez-Galán L, Olleros ML, Vesin D, Garcia I. Much More than M1 and M2 Macrophages, There are also CD169(+) and TCR(+) Macrophages. *Front Immunol.* 2015;6:263. doi:10.3389/fimmu.2015.00263.
- 146.** Eligini S, Crisci M, Bono E, et al. Human monocyte-derived macrophages spontaneously differentiated in vitro show distinct phenotypes. *J Cell Physiol.* 2013;228(7):1464-1472. doi:10.1002/jcp.24301.
- 147.** Laoui D, Movahedi K, van Overmeire E, et al. Tumor-associated macrophages in breast cancer: distinct subsets, distinct functions. *Int J Dev Biol.* 2011;55(7-9):861-867. doi:10.1387/ijdb.113371dl.

- 148.** Yang M, McKay D, Pollard JW, Lewis CE. Diverse Functions of Macrophages in Different Tumor Microenvironments. *Cancer Res.* 2018;78(19):5492-5503. doi:10.1158/0008-5472.CAN-18-1367.
- 149.** Qian B-Z, Pollard JW. Macrophage diversity enhances tumor progression and metastasis. *Cell.* 2010;141(1):39-51. doi:10.1016/j.cell.2010.03.014.
- 150.** Poh AR, Ernst M. Targeting Macrophages in Cancer: From Bench to Bedside. *Front Oncol.* 2018;8:49. doi:10.3389/fonc.2018.00049.
- 151.** Raggi F, Pelassa S, Pierobon D, et al. Regulation of Human Macrophage M1-M2 Polarization Balance by Hypoxia and the Triggering Receptor Expressed on Myeloid Cells-1. *Front Immunol.* 2017;8:1097. doi:10.3389/fimmu.2017.01097.
- 152.** Alberts B, Johnson A, Lewis J, Raff M, Roberts K, Walter P. *Molecular biology of the cell.* Fourth edition. New York, NY: Garland Science Taylor & Francis Group; 2002. <http://www.loc.gov/catdir/enhancements/fy0652/2001054471-d.html>.
- 153.** Chang DT, Colton E, Anderson JM. Paracrine and juxtacrine lymphocyte enhancement of adherent macrophage and foreign body giant cell activation. *J Biomed Mater Res A.* 2009;89(2):490-498. doi:10.1002/jbm.a.31981.
- 154.** Edsall G. Principles of active immunization. *Annu Rev Med.* 1966;17:39-48. doi:10.1146/annurev.me.17.020166.000351.
- 155.** Fielding AK, Rowe JM, Buck G, et al. UKALLXII/ECOG2993: addition of imatinib to a standard treatment regimen enhances long-term outcomes in Philadelphia positive acute lymphoblastic leukemia. *Blood.* 2014;123(6):843-850. doi:10.1182/blood-2013-09-529008.
- 156.** Ocadlikova D, Lecciso M, Isidori A, et al. Chemotherapy-Induced Tumor Cell Death at the Crossroads Between Immunogenicity and Immunotolerance: Focus on Acute Myeloid Leukemia. *Front Oncol.* 2019;9:1004. doi:10.3389/fonc.2019.01004.

- 157.** Fredly H, Ersvær E, Gjertsen B-T, Bruserud O. Immunogenic apoptosis in human acute myeloid leukemia (AML): primary human AML cells expose calreticulin and release heat shock protein (HSP) 70 and HSP90 during apoptosis. *Oncol Rep.* 2011;25(6):1549-1556. doi:10.3892/or.2011.1229.
- 158.** Fucikova J, Truxova I, Hensler M, et al. Calreticulin exposure by malignant blasts correlates with robust anticancer immunity and improved clinical outcome in AML patients. *Blood.* 2016;128(26):3113-3124. doi:10.1182/blood-2016-08-731737.
- 159.** Wemeau M, Kepp O, Tesnière A, et al. Calreticulin exposure on malignant blasts predicts a cellular anticancer immune response in patients with acute myeloid leukemia. *Cell Death Dis.* 2010;1:e104. doi:10.1038/cddis.2010.82.
- 160.** Fucikova J, Kasikova L, Truxova I, et al. Relevance of the chaperone-like protein calreticulin for the biological behavior and clinical outcome of cancer. *Immunol Lett.* 2018;193:25-34. doi:10.1016/j.imlet.2017.11.006.
- 161.** Fucikova J, Kralikova P, Fialova A, et al. Human tumor cells killed by anthracyclines induce a tumor-specific immune response. *Cancer Res.* 2011;71(14):4821-4833. doi:10.1158/0008-5472.CAN-11-0950.
- 162.** Chen X, Fosco D, Kline DE, Kline J. Calreticulin promotes immunity and type I interferon-dependent survival in mice with acute myeloid leukemia. *Oncoimmunology*2017;6(4):e1278332. doi:10.1080/2162402X.2016.1278332.

8 Appendix

8.1 Supplementary Figure S1: The Role of Tumour-associated Macrophages in Tumour Progression



8.2 Table 1: Consumable Material

<i>Product Name</i>	<i>Manufacturer</i>
BD Microfine+ U100 Insulin Syringes, 0.30 mm x 8 mm, 0.5 mL	BD Bioscience, Franklin Lakes, NJ, US
Cell Culture Multiwell Plate, 6 Well	Greiner Bio-One, Kremsmünster, AT
Cell Culture Multiwell Plate, 12 Well	Greiner Bio-One, Kremsmünster, AT
Cell Culture Multiwell Plate, 96 Well, white	Greiner Bio-One, Kremsmünster, AT
Cellstar Serologic Pipettes, 5 mL, bulk, sterile	Greiner Bio-One, Kremsmünster, AT
Cellstar Serologic Pipettes, 5 mL, single packed, sterile	Greiner Bio-One, Kremsmünster, AT
Cellstar Serologic Pipettes, 10 mL, bulk, sterile	Greiner Bio-One, Kremsmünster, AT
Cellstar Serologic Pipettes, 10 mL, single packed, sterile	Greiner Bio-One, Kremsmünster, AT
Cellstar Serologic Pipettes, 25 mL, bulk, sterile	Greiner Bio-One, Kremsmünster, AT
Cellstar Serologic Pipettes, 25 mL, single packed, sterile	Greiner Bio-One, Kremsmünster, AT
Falcon Conical Centrifuge Tubes, 15 mL	Corning Life Sciences, Amsterdam, NL
Falcon Conical Centrifuge Tubes, 50 mL	Corning Life Sciences, Amsterdam, NL
Filter Cap Cell Culture Flasks, 50 mL, 25 cm ²	Greiner Bio-One, Kremsmünster, AT
Filter Cap Cell Culture Flasks, 250 mL, 75 cm ²	Greiner Bio-One, Kremsmünster, AT
Filter Cap Cell Culture Flasks, 550 mL, 175 cm ²	Greiner Bio-One, Kremsmünster, AT

Teflon Bag, Teflon-Coated Cell Culture Bag	American Durafilm, Holliston, MA, US
TipOne 10 µl Pipette Tips, red	STARLAB, Hamburg, DE
TipOne 200 µl Pipette Tips, yellow	STARLAB, Hamburg, DE
TipOne 1000 µl Pipette Tips, blue	STARLAB, Hamburg, DE
Tubes, 5 ml, 75 mm x 13 mm, PS	Sarstedt, Nümbrecht, DE
UpCell MultiDish Cell Culture Dish, 12 Well	Thermo Fisher Scientific, Waltham, MA, US

8.3 Table 2: Common Reagents and Chemicals

<i>Product Name (Catalogue Number)</i>	<i>Manufacturer</i>
Acetone ≥ 99.5 % (5025)	Carl Roth, Karlsruhe, DE
Ammonium persulfate ≥ 98 % (A3678)	Sigma-Aldrich, St. Louis, MO, US
Dimethyl sulfoxide (472301)	Sigma-Aldrich, St. Louis, MO, US
Disodium hydrogen phosphate ≥ 99.0 % (S7907)	Sigma-Aldrich, St. Louis, MO, US
Ethanol ≥ 99.8 % (9065)	Carl Roth, Karlsruhe, DE
Ethylenediaminetetraacetic acid ≥ 98.5% (ED)	Sigma-Aldrich, St. Louis, MO, US
Glycine ≥ 99 % (G8898)	Sigma-Aldrich, St. Louis, MO, US
Isopropanol ≥ 99.9 % (9781)	Carl Roth, Karlsruhe, DE
Methanol ≥ 99.9 % (0082)	Carl Roth, Karlsruhe, DE

Rotiphorese Gel 30, 30 % acrylamide and bisacrylamide stock solution (ratio 37.5:1) (3029)	Carl Roth, Karlsruhe, DE
Sodium chloride \geq 99 % (S9888)	Sigma-Aldrich, St. Louis, MO, US
Sodium dihydrogen phosphate \geq 99.0 % (S8282)	Sigma-Aldrich, St. Louis, MO, US
Sodium dodecyl sulphate 98 % (862010)	Sigma-Aldrich, St. Louis, MO, US
Tetramethylethylenediamine \sim 99 % (T9281)	Sigma-Aldrich, St. Louis, MO, US
Tris base (TRIS-RO)	Sigma-Aldrich, St. Louis, MO, US
Tween 20, Polyoxyethylene (20) sorbitan monolaurate (P2287)	Sigma-Aldrich, St. Louis, MO, US

8.4 Table 3: Reagents and Chemicals for Cell Culture

<i>Product Name (Catalogue Number)</i>	<i>Manufacturer</i>
Dulbecco's Modified Eagle Medium, DMEM Medium (11960044)	Thermo Fisher Scientific, Waltham, MA, US
Foetal Bovine Serum, FBS (10437028)	Thermo Fisher Scientific, Waltham, MA, US
Leukaemic Cell Line Medium <ul style="list-style-type: none"> • RPMI 1640 Medium • 15 % Foetal Bovine Serum (FBS) • 1 % L-Glutamine (200 mM) • 1 % Pen Strep 	

L-Glutamine (200 mM), 100x (25030081)	Thermo Fisher Scientific, Waltham, MA, US
Macrophages Medium <ul style="list-style-type: none"> • DMEM Medium • 10 % Foetal Bovine Serum (FBS) • 1 % L-Glutamine (200 mM) • 1 % Pen Strep • 100 µg/mL Recombinant Mouse M-CSF 	
Pen Strep, Penicillin (10000 U/mL)- Streptomycin (10000 µg/nL) (15140122)	Thermo Fisher Scientific, Waltham, MA, US
Recombinant Mouse M-CSF (576406)	BioLegend, San Diego, CA, US
RPMI 1640 Medium (21870076)	Thermo Fisher Scientific, Waltham, MA, US
Trypan Blue Solution (T8154)	Sigma-Aldrich, St. Louis, MO, US

8.5 Table 4: Reagents and Chemicals for Flow Cytometry

<i>Product Name (Catalogue Number)</i>	<i>Manufacturer</i>
BD Horizon Brilliant Stain Buffer (563794)	BD Bioscience, Franklin Lakes, NJ, US
BD Pharm Lyse Lysing Buffer (555899)	BD Bioscience, Franklin Lakes, NJ, US
Dulbecco's Phosphate Buffered Saline, 1x, DPBS (14190094)	Thermo Fisher Scientific, Waltham, MA, US
Dulbecco's Phosphate Buffered Saline, 10x, DPBS (14200075)	Thermo Fisher Scientific, Waltham, MA, US

FACS Buffer <ul style="list-style-type: none"> • Dulbecco's Phosphate Buffered Saline (DPBS) • 2 % Foetal Bovine Serum (FBS)
Staining Buffer <ul style="list-style-type: none"> • Dulbecco's Phosphate Buffered Saline (DPBS) • 2 % Foetal Bovine Serum (FBS)

8.6 Table 5: Reagents and Chemicals for Western Blot

<i>Product Name (Catalogue Number)</i>	<i>Manufacturer</i>
Amersham Hyperfilm ECL High performance chemiluminescence film (28906836)	GE Healthcare Life science, Chalfont St Giles, UK
Amersham Protran Premium 0.2 µm NC Nitrocellulose Blotting Membrane (10600001)	GE Healthcare Life science, Chalfont St Giles, UK
Blocking Buffer <ul style="list-style-type: none"> • TBS-T Buffer • 2.5 % or 5 % Skim milk powder 	
Laemmli Sample Buffer, 4x (1610747)	Bio-Rad Laboratories, Hercules, CA, US
Phosphatase Inhibitor Cocktail (78428)	Thermo Fisher Scientific, Waltham, MA, US
Polyacrylamide Gel	
a) 15 % Resolving Gel (10 mL, 1 gel) <ul style="list-style-type: none"> • 5 mL 30 % Acrylamide mix • 2.5 mL 1.5 M Tris base (pH 8.8) • 100µL 10 % Sodium dodecyl sulphate (SDS) • 100 µL 10 % Ammonium persulfate (APS) • 4 µL Tetramethylethylenediamine (TEMED) • 2.3 mL Distilled water 	

b) 5 % Stacking Gel (3 mL, 1 gel) <ul style="list-style-type: none"> • 500 μL 30 % Acrylamide mix • 380 μL 12.5 % 1.0 M Tris base (pH 6.8) • 30 μL 10 % Sodium dodecyl sulphate (SDS) • 30 μL 10 % Ammonium persulfate (APS) • 3 μL Tetramethylethylenediamine (TEMED) • 2.1 mL Distilled water 	
Precision Plus Protein WesternC Blotting Standards (1610376)	Bio-Rad Laboratories, Hercules, CA, US
Protease Inhibitor Cocktail, EDTA-free (78425)	Thermo Fisher Scientific, Waltham, MA, US
RIPA Lysis and Extraction Buffer (89900)	Thermo Fisher Scientific, Waltham, MA, US
Running Buffer (pH 8.3) <ul style="list-style-type: none"> • 25 mM Tris base • 192 mM Glycine • 0.1 % Sodium dodecyl sulphate (SDS) • Distilled water 	
Skim milk powder (1.15363)	Sigma-Aldrich, St. Louis, MO, US
TBS-T Buffer (pH 7.2 - 7.6) <ul style="list-style-type: none"> • 20 mM Tris base • 150 mM Sodium chloride (NaCl) • 0.05 % Tween 20 • Distilled water 	
Wet Transfer Buffer (pH 8.3) <ul style="list-style-type: none"> • 25 mM Tris base • 190 mM Glycine • 20% Methanol • Distilled water 	

Western Blotting Filter Paper (84784)	Thermo Fisher Scientific, Waltham, MA, US
--	--

8.7 Table 6: Reagents and Chemicals for Haematoxylin-Eosin Stain and Immunohistochemistry

<i>Product Name (Catalogue Number)</i>	<i>Manufacturer</i>
BOND Primary Antibody Diluent (AR9352)	Leica Biosystems, Wetzlar, DE
Cover glass (3800145ACS)	Leica Biosystems, Wetzlar, DE
CellTexx Mounting Medium (19360)	Englebrecht Medizin- und Labortechnik, Edermünde, DE
Decalcification Buffer <ul style="list-style-type: none"> • 900 mL 0.5 M Ethylenediaminetetraacetic acid (EDTA, pH 8.0) • 100 mL 10x NaPBS (pH 7.4) <ul style="list-style-type: none"> ○ 150 mM Sodium chloride (NaCl) ○ 10.8 mM Disodium hydrogen phosphate (Na₂HPO₄) ○ 1.6 mM Sodium dihydrogen phosphate (NaH₂PO₄) ○ 100 mL Distilled water 	
EM-400 Embedding Medium Paraffin (3801320)	Leica Biosystems, Wetzlar, DE
IP Cassette III (38440210)	Leica Biosystems, Wetzlar, DE
Roti-Histofix 4 % (P087)	Carl Roth, Karlsruhe, DE
Snowcoat Pearl Microscope Slides (3809299)	Leica Biosystems, Wetzlar, DE

8.8 Table 7: Detection Kit for Extracellular ATP Release

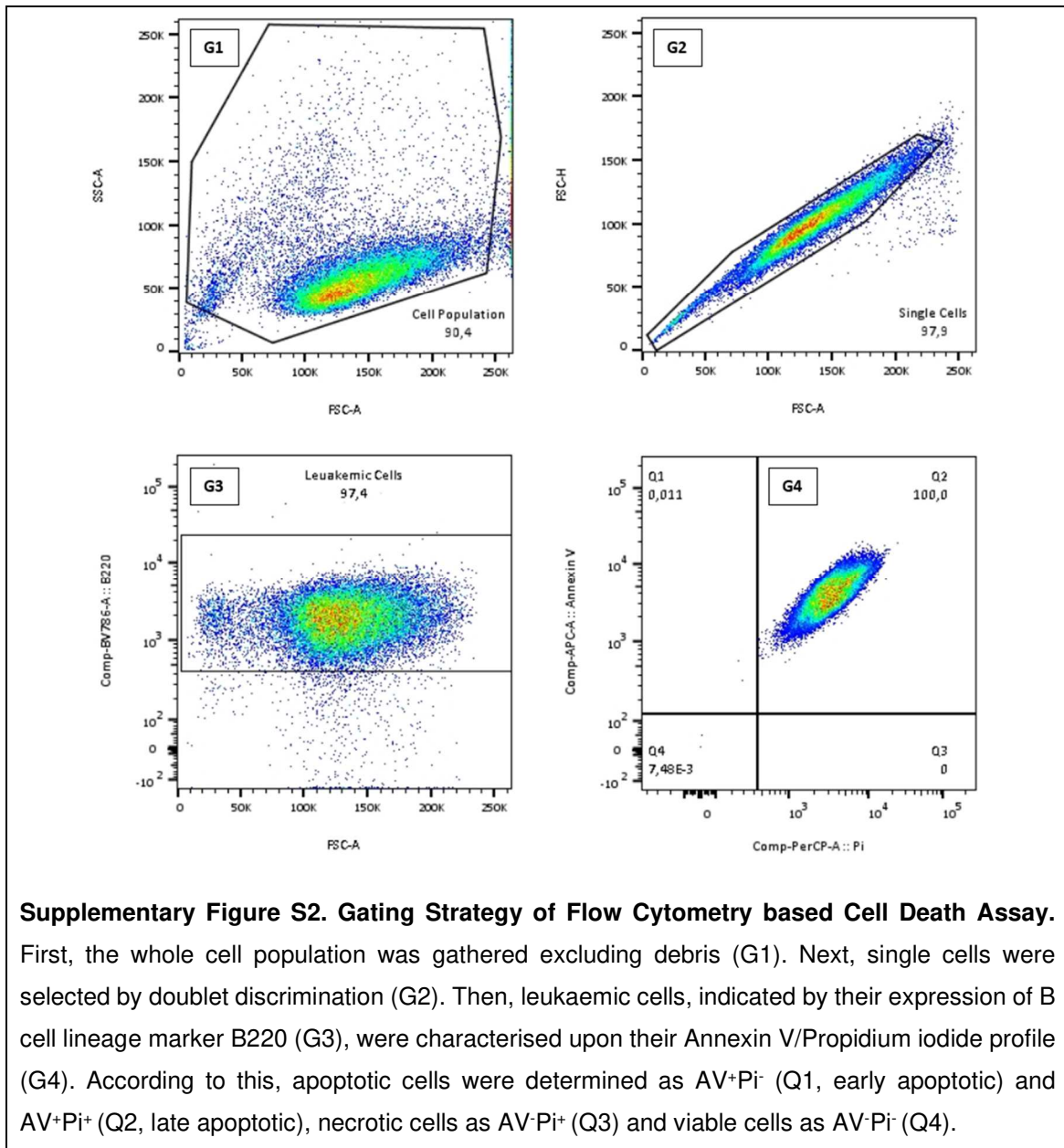
<i>Product Name (Catalogue Number)</i>	<i>Manufacturer</i>
ENLITEN ATP Assay System Bioluminescence Detection Kit for ATP Measurement (FF2000)	Promega, Mannheim, DE

8.9 Table 12: Devices and Software

<i>Product Name</i>	<i>Manufacturer</i>
Axio Imager 2 Research Microscope	Carl Zeiss, Oberkochen, DE
BD LSRFortessa Flow Cytometer	BD Bioscience, Franklin Lakes, NJ, US
BINDER CO ₂ Incubator C170	BINDER, Tuttlingen, DE
Heraeus Megafuge 40R Centrifuge	Thermo Fisher Scientific, Waltham, MA, US
Heraeus Pico 17 Centrifuge	Thermo Fisher Scientific, Waltham, MA, US
Leica ASP300 S Fully Enclosed Tissue Processor	Leica Biosystems, Wetzlar, DE
Leica BOND-MAX Fully Automated IHC and ISH	Leica Biosystems, Wetzlar, DE
Leica CV5030 Fully Automated Glass Coverslipper	Leica Biosystems, Wetzlar, DE
Leica RM2235 Manual Rotary Microtome	Leica Biosystems, Wetzlar, DE
Leica ST5010 Autostainer XL	Leica Biosystems, Wetzlar, DE
LUMIstar OPTIMA Microplate Luminometer	BMG Labtech, Ortenberg, DE
scil Vet abc hematology analyzer	scil animal care company, Gurnee, IL, US
ViCell XR Cell Counter	Beckman Coulter, Brea, CA, US

X-ray film developer machine XR24 Pro	Dürr Dental, Bietigheim-Bissingen, DE
AxioVision Microscopy software Vision SE64 4.9	Carl Zeiss, Oberkochen, DE
BD FACSDiva software Version 8.0.1	BD Bioscience, Franklin Lakes, NJ, US
FlowJo software Version 10.5.3	BD Bioscience, Franklin Lakes, NJ, US
GraphPad Prism software Version 8	GraphPad Software, San Diego, CA, US
Lumistar 32 software Version 1.7	BMG Labtech, Ortenberg, DE
Vi-Cell XR software Version 2.04	Beckman Coulter, Brea, CA, US

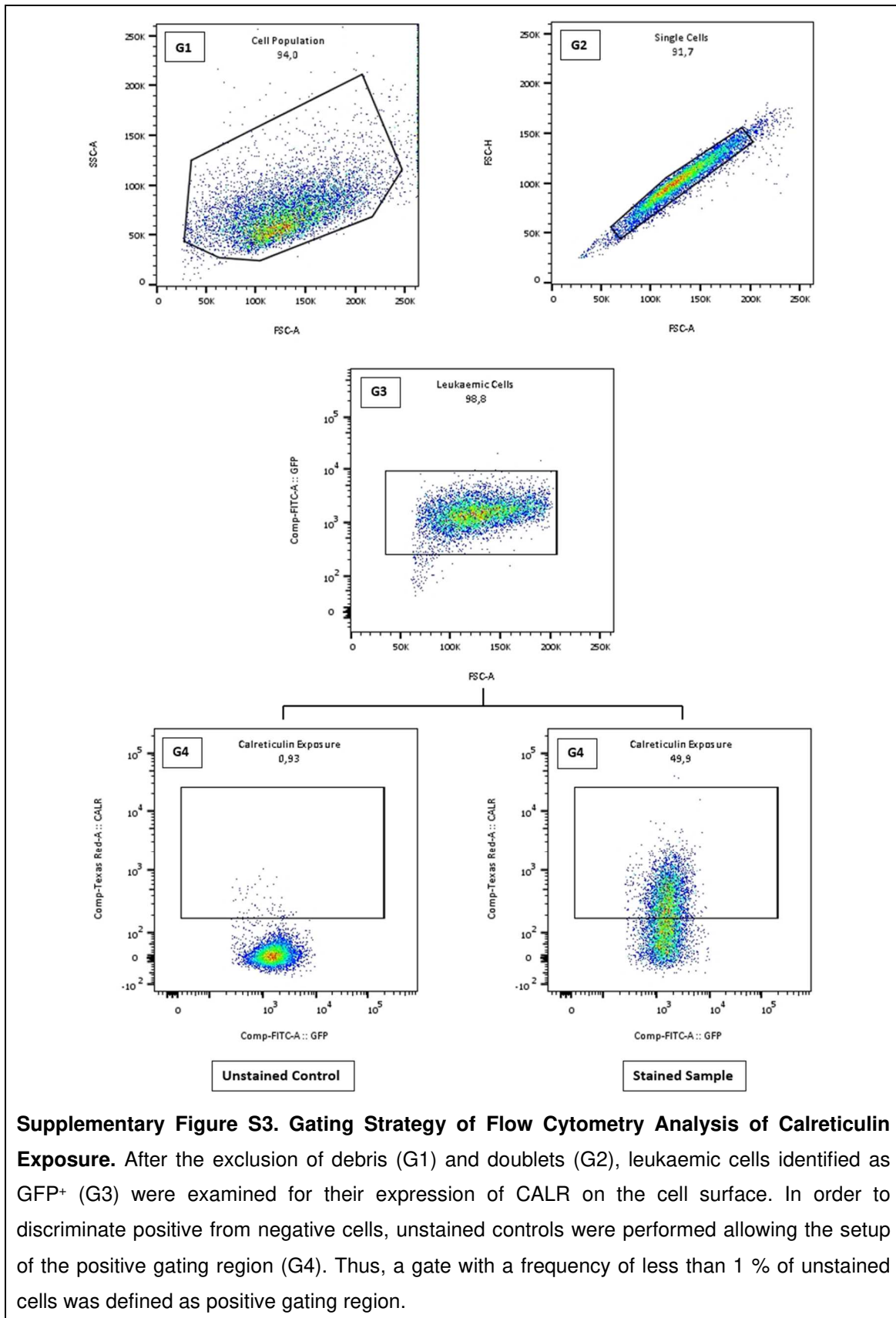
8.10 Supplementary Figure S2: Gating Strategy of Flow Cytometry based Cell Death Assay



Supplementary Figure S2. Gating Strategy of Flow Cytometry based Cell Death Assay.

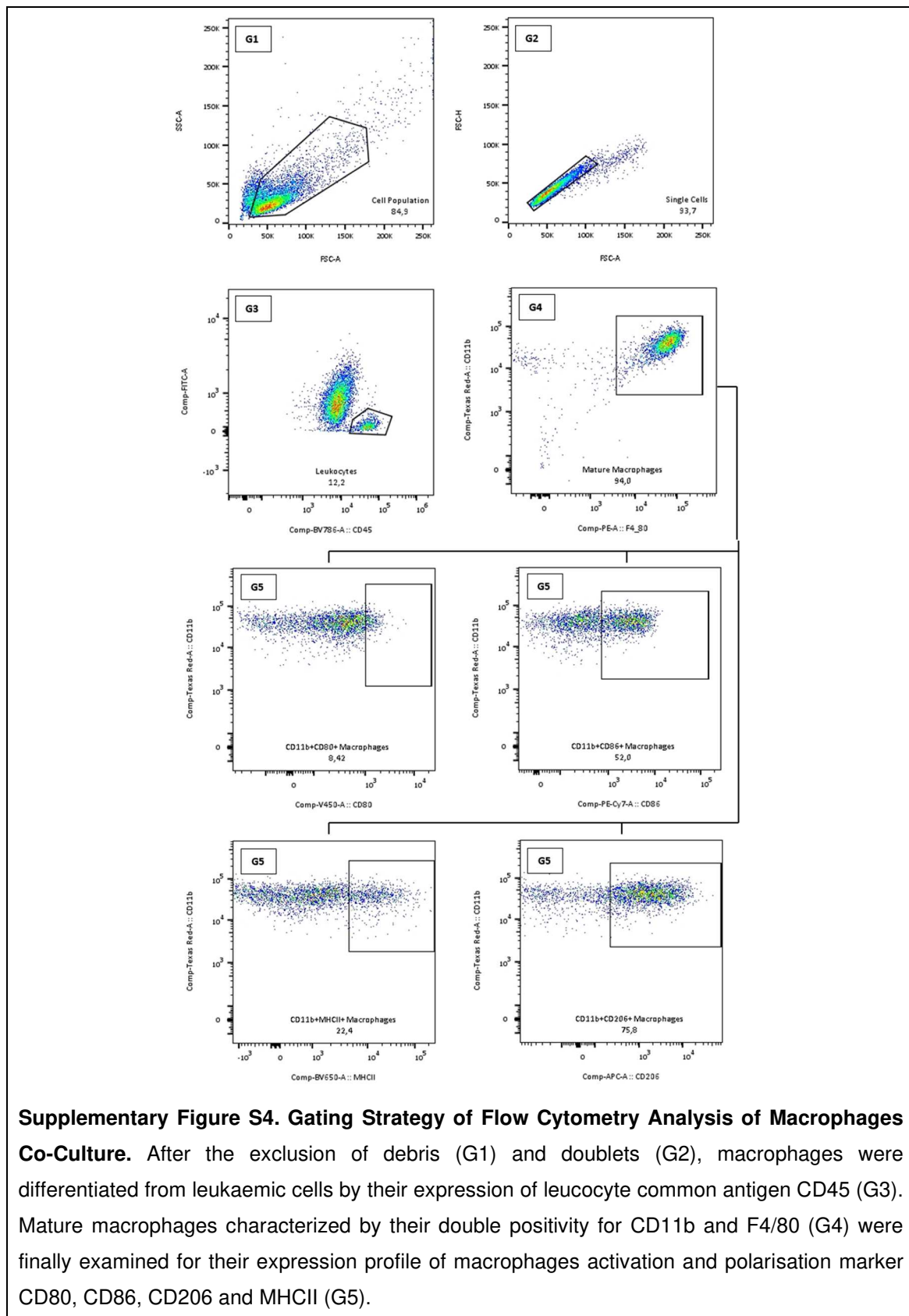
First, the whole cell population was gathered excluding debris (G1). Next, single cells were selected by doublet discrimination (G2). Then, leukaemic cells, indicated by their expression of B cell lineage marker B220 (G3), were characterised upon their Annexin V/Propidium iodide profile (G4). According to this, apoptotic cells were determined as AV⁺Pi⁻ (Q1, early apoptotic) and AV⁺Pi⁺ (Q2, late apoptotic), necrotic cells as AV⁻Pi⁺ (Q3) and viable cells as AV⁻Pi⁻ (Q4).

8.11 Supplementary Figure S3: Gating Strategy of Flow Cytometry Analysis of Calreticulin Exposure



Supplementary Figure S3. Gating Strategy of Flow Cytometry Analysis of Calreticulin Exposure. After the exclusion of debris (G1) and doublets (G2), leukaemic cells identified as GFP+ (G3) were examined for their expression of CALR on the cell surface. In order to discriminate positive from negative cells, unstained controls were performed allowing the setup of the positive gating region (G4). Thus, a gate with a frequency of less than 1 % of unstained cells was defined as positive gating region.

8.12 Supplementary Figure S4: Gating Strategy of Flow Cytometry Analysis of Macrophages Co-Culture



8.13 Table 14: Shift in Macrophages Activation and Polarisation. Co-Culture Conditions with 10 nM Nilotinib

	CD80	CD86	CD206	MHCII
L1-1 (juxtacrine)	- 5.5 %	- 0.7 %	- 3.9 %	+ 1.2 %
L1-1 (paracrine)	+ 0.2 %	+ 0.6 %	+ 1.5 %	- 4.8 %
L3 (juxtacrine)	- 2.6 %	- 2.6 %	+ 3.5 %	+ 5.6 %
L3 (paracrine)	- 2.1 %	+ 0.6 %	+ 7.5 %	- 1.2 %
L1-1 (average)	- 2.7 %	- 0.1 %	- 1.2 %	- 1.8 %
L3 (average)	- 2.4 %	- 1.0 %	+ 5.5 %	+ 2.2 %
Juxtacrine (average)	- 4.1 %	- 1.7 %	- 0.2 %	+ 3.4 %
Paracrine (average)	- 1.0 %	+ 0.6 %	+ 4.5 %	- 3.0 %
Total (average)	- 2.5 %	- 0.5 %	+ 2.2 %	+ 0.2 %

Shift in macrophages activation and polarisation in the co-culture conditions with 10 nM Nilotinib pre-treated leukaemic cells compared to the corresponding co-culture conditions with untreated leukaemic cells.

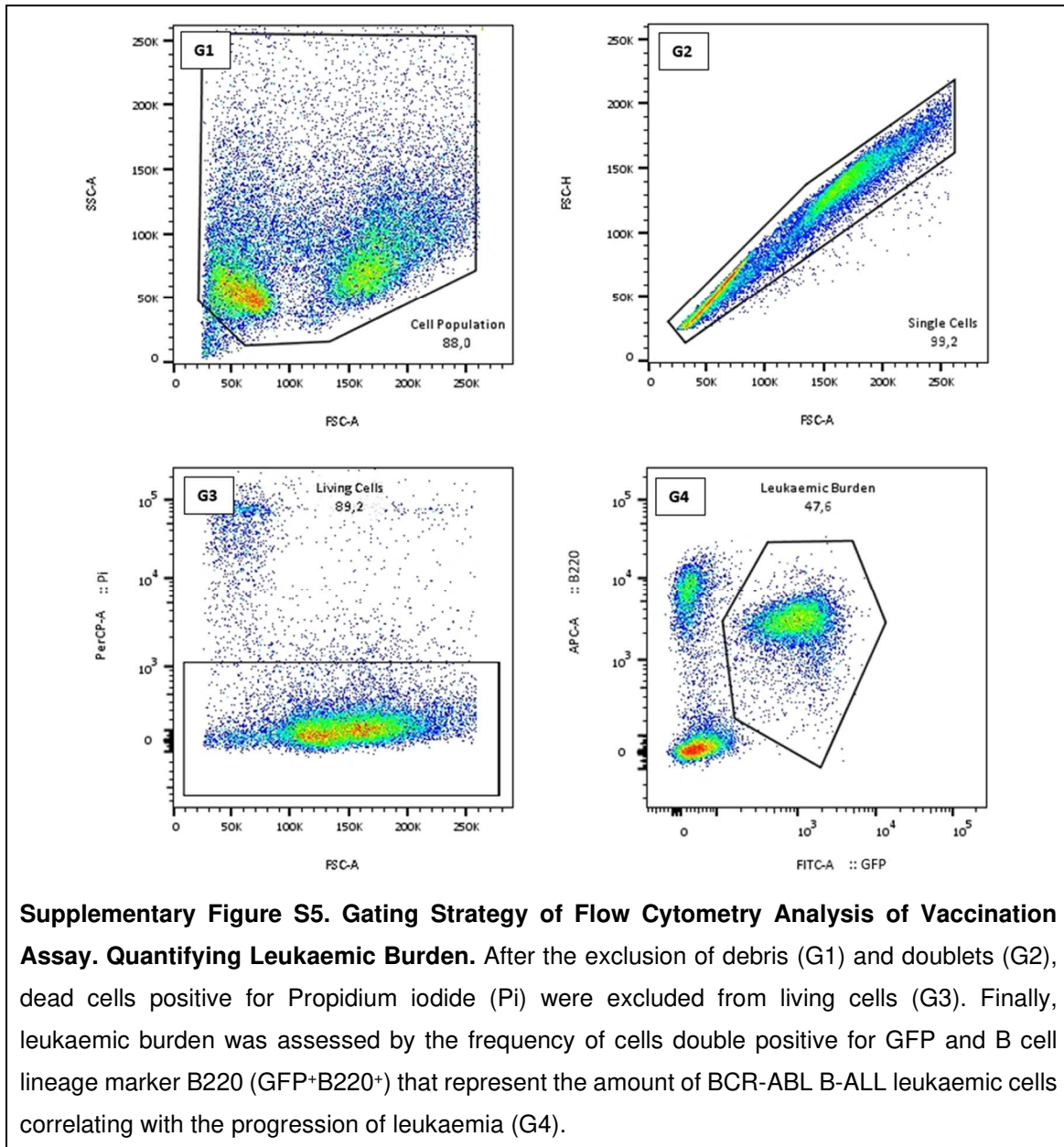
8.14 Table 15: Shift in Macrophages Activation and Polarisation. Co-Culture Conditions with 50 nM Nilotinib

	CD80	CD86	CD206	MHCII
L1-1 (juxtacrine)	- 10.0 %	+ 2.0 %	- 5.4 %	+ 1.1 %
L1-1 (paracrine)	- 1.5 %	+ 2.2 %	+ 2.5 %	- 2.7 %
L3 (juxtacrine)	+ 4.8 %	- 1.3 %	+ 3.9 %	+ 7.9 %
L3 (paracrine)	+ 1.7 %	- 20.1 %	+ 4.8 %	- 0.6 %
L1-1 (average)	- 5.8 %	+ 2.1 %	- 1.5 %	- 0.8 %
L3 (average)	+ 3.3 %	- 10.7 %	+ 4.4 %	+ 3.7 %
Juxtacrine (average)	- 2.6 %	+ 0.4 %	- 0.8 %	+ 4.5 %
Paracrine (average)	+ 0.1 %	- 9.0 %	+ 3.7 %	- 1.7 %
Total (average)	- 1.3 %	- 4.3 %	+ 1.5 %	+ 1.4 %
Shift in macrophages activation and polarisation in the co-culture conditions with 50 nM Nilotinib pre-treated leukaemic cells compared to the corresponding co-culture conditions with untreated leukaemic cells.				

8.15 Table 16: Shift in Macrophages Activation and Polarisation. Co-Culture Conditions with 1 μ M Mitoxantrone

	CD80	CD86	CD206	MHCII
L1-1 (juxtacrine)	+ 4.5 %	+ 25.4 %	+ 17.4 %	- 5.0 %
L1-1 (paracrine)	+ 6.6 %	+ 26.1 %	+ 25.5 %	- 12.9 %
L3 (juxtacrine)	+ 2.1 %	+ 22.5 %	+ 21.6 %	- 7.1 %
L3 (paracrine)	+ 4.4 %	+ 31.9 %	+ 31.9 %	- 11.0 %
L1-1 (average)	+ 5.6 %	+ 25.8 %	+ 21.5 %	- 9.0 %
L3 (average)	+ 3.3 %	+ 27.2 %	+ 26.8 %	- 9.1 %
Juxtacrine (average)	+ 3.3 %	+ 24.0%	+ 19.5 %	- 6.1 %
Paracrine (average)	+ 5.5 %	+ 29.0 %	+ 28.7 %	- 12.0 %
Total (average)	+ 4.4 %	+ 26.5 %	+ 24.1 %	- 9.0 %
Shift in macrophages activation and polarisation in the co-culture conditions with 1 μ M Mitoxantrone pre-treated leukaemic cells compared to the corresponding co-culture conditions with untreated leukaemic cells.				

8.16 Supplementary Figure S5: Gating Strategy of Flow Cytometry Analysis of Vaccination Assay. Quantifying Leukaemic Burden



9 Publication

9.1 Publication 2019

Tirado-Gonzalez I, Nevmerzhitskaya A, Descot A, Devona Soetopo, Ewelina Czlonka, Maresa Weitmann, Carolin Wachtel, Julia Slotta-Huspenina, Christine Tran-Quang, Katharina Götze, Emily Alberto, Carla Vanina Rothlin, Jacques Ghysdael and Hind Medyouf. Abstract A092: TAM receptors targeting unleashes antileukemic immunity and enables checkpoint blockade leading to eradication of leukemic cells. In: Tackling the Tumor Microenvironment: Beyond T-cells: American Association for Cancer Research; 022019:A092-A092.

10 Curriculum Vitae

CURRICULUM VITAE

CAROLIN WACHTEL

Bockenheimer Anlage 38 | 60322 Frankfurt am Main
18.06.1992 | Heppenheim an der Bergstraße
carolin.wachtel@gmx.de | +49 176 84389788



Ausbildung

- 10/2012 - 12/2019** **Studium der Humanmedizin**
Goethe Universität Frankfurt am Main
- Approbation als Ärztin (Gesamtnote sehr gut, 1,5)
- 10/2011 - 03/2012** **Studium der Biowissenschaften**
Ruprecht-Karls Universität Heidelberg
- 2002 - 2011** **Allgemeine Hochschulreife**
Liebfrauenschule Bensheim, Privates katholisches Gymnasium für Mädchen
- Abitur (Leistungsfächer Latein und Biologie, Gesamtnote 1,0)

Promotion

- seit 08/2017** **Experimentelle Doktorarbeit**
Georg Speyer Haus, Institut für Tumorbologie und Experimentelle Therapie Frankfurt
- Titel: Exploration of Nilotinib enhancing the anti-leukaemic Effects of Gas6 Deletion in Ph⁺ B-ALL by inducing Immunogenic Cell Death
 - Translationale Forschung im Bereich Hämatonkologie und Immunologie
 - Doktorvater Herr Prof. Dr. Florian Greten, Betreuerin Frau Dr. Hind Medyouf

Publikation

- 02/2019** **TAM receptors targeting unleashes antileukemic immunity and enables checkpoint blockade leading to eradication of leukemic cells**
Irene Tirado-Gonzalez, Aleksandra Nevmerzhitskaya, Arnaud Descot, Devona Soetopo, Ewelina Czlonka, Maresa Weitmann, Carolin Wachtel, Julia Slotta-Huspenina, Christine Tran-Quang, Katharina Götze, Emily Alberto, Carla Vanina Rothlin, Jacques Ghysdael and Hind Medyouf
International Cancer Immunotherapy Conference: Translating Science into Survival
September 30 - October 3, 2018; New York, NY
DOI: 10.1158/2326-6074.CRICIMTEATIAACR18-A092, Published February 2019

Praktische Erfahrungen

- seit 03/2020 **Assistenzärztin**
Klinik für Plastische und Ästhetische Chirurgie, Wiederherstellungs- und Handchirurgie von Prof. Dr. Dr. Ulrich Rieger Agaplesion Markus Krankenhaus Frankfurt am Main
- 11/2018 - 10/2019 **Praktisches Jahr**
Agaplesion Markus Krankenhaus Frankfurt am Main und Kantonsspital Luzern
Wahltertial Plastische und Ästhetische Chirurgie, Wiederherstellungs- und Handchirurgie
- Klinik für Plastische und Ästhetische Chirurgie, Wiederherstellungs- und Handchirurgie, Prof. Dr. Dr. Ulrich Rieger, Frankfurt am Main
- Pflichttertial Chirurgie
- Klinik für Allgemein- und Viszeralchirurgie, Prof. Dr. Christoph Heidenhain, Klinik für Orthopädie und Unfallchirurgie, Prof. Dr. Stefan Rehart und Klinik für Thoraxchirurgie, Prof. Dr. Joachim Schirren, Frankfurt am Main
- Pflichttertial Innere Medizin
- Medizinische Klinik, Prof. Dr. Christoph Henzen, Kantonsspital Luzern in der Schweiz
- 08/2017 - 11/2018 **Forschungsjahr**
Georg Speyer Haus, Institut für Tumorbologie und Experimentelle Therapie Frankfurt
- Wissenschaftliche Mitarbeiterin in der Arbeitsgruppe von Fr. Dr. Medyouf mit inhaltlichem Schwerpunkt Tumormikroumgebung, Tumormikroimmunologie und Tumormikroimmunflucht bei der Pathogenese maligner Veränderungen des hämatopoetischen Systems
- 06/2013 - 10/2017 **Studentische Angestellte**
Facharztpraxis chirurgie-maintaunus Bad Soden
- Ärztliche Assistenz in der Sprechstunde sowie beim ambulanten und stationären Operieren in den Bereichen Allgemeinchirurgie, Orthopädie und Unfallchirurgie, Septische Chirurgie sowie Plastische und Ästhetische Chirurgie, Wiederherstellungs- und Handchirurgie
- 06/2015 - 04/2017 **Famulatur**
Agaplesion Markus Krankenhaus Frankfurt am Main
- Stationäre Famulatur in der Klinik für Plastische und Ästhetische Medizin, Wiederherstellungs- und Handchirurgie, Prof. Dr. Dr. Ulrich Rieger
- Facharztpraxis chirurgie-maintaunus Bad Soden**
- Ambulante Famulatur im Fachbereich Allgemeinchirurgie, Orthopädie und Unfallchirurgie, Septische Chirurgie sowie Plastische und Ästhetische Chirurgie, Wiederherstellungs- und Handchirurgie, Wolfgang Hirschberger, Dr. med. Christian Riediger, Dr. med. Götz Enderle und Dr. med. Janine Hondyk
- Universitätsklinikum Frankfurt am Main**
- Stationäre Famulatur in der Medizinischen Klinik III für Kardiologie, Angiologie und Nephrologie, Prof. Dr. Andreas M. Zeiher und Prof. Dr. Helmut Geiger
- Praxis Guido Pschera Lorsch**
- Hausarztfamulatur im Fachbereich Allgemeinmedizin, Diabetologie, Ernährungs- und Sportmedizin, Chirotherapie und Naturheilverfahren, Guido Pschera

Weiterbildung

- 09/2018 **Frankfurt Cancer Conference, Turning molecular information into cancer therapies**
Universitätscampus Westend, Frankfurt am Main
- 03/2018 **Hospitation Septorhinoplastik**
Berkei Aesthetic Surgery, Dr.med. Julia Berkei, Frankfurt am Main

Auszeichnungen

2017/2018 **Deutschlandstipendium der Goethe Universität Frankfurt**
• Fördererpatenschaft durch das biomedizinisch-pharmazeutische
Forschungsunternehmen Biotest AG Dreieich

2013/2014 **Deutschlandstipendium der Goethe Universität Frankfurt**

Engagement

2015 - 2018 **Ehrenamt bei AWO Frankfurt**
Projekt Herzlich Ankommen für unbegleitete minderjährige Flüchtlinge

04/2012 **Ehrenamt an der Liebfrauenschule Bensheim**
Betreuung der Studienreise nach Poole in Südengland

2009 - 2011 **Kurssprecherin an der Liebfrauenschule Bensheim**

Sprachen und Interessen

Sprachen

- Deutsch: Muttersprache
- Englisch: fließend in Schrift und Sprache
- Spanisch: fortgeschrittene Kenntnisse
- Französisch: Grundkenntnisse

Interessen

- Klavier, Tanzen, Tennis, Yoga, Kraft- und Ausdauersport
- Literatur, Musik, Kultur, Politik, Reisen

Referenzen

Prof. Dr. Dr. med. habil. Ulrich Rieger

Chefarzt der Klinik für Plastische und Ästhetische Chirurgie, Wiederherstellungs- und Handchirurgie
Agaplesion Markus Krankenhaus, Wilhelm-Epstein-Straße 4, 60431 Frankfurt am Main
Internet: www.rieger-plastische-chirurgie.de
E-Mail: ulrich.rieger@fdk.info
Telefon: 069 9533-2544 / 4777

Wolfgang Hirschberger

Facharzt für Chirurgie, Spezielle Unfallchirurgie, Fachgebundene Röntgendiagnostik, Notfallmedizin, Durchgangsarzt
und Leitender Notarzt
Facharztpraxis chirurgie-maintaunus, Professor-Much-Straße 2, 65812 Bad Soden
Internet: www.chirurgie-maintaunus.de
E-Mail: info@chirurgie-maintaunus.de
Telefon: 06196 651610

Dr. Hind Medyouf

Leiterin der Forschungsgruppe AG Medyouf
Georg-Speyer-Haus, Paul-Ehrlich-Straße 42-44, 60596 Frankfurt am Main
Internet: www.georg-speyer-haus.de
E-Mail: Medyouf@gsh.uni-frankfurt.de
Telefon: 069 63395-540

11 Acknowledgement

At this point I would like to express my special thanks to the following persons who enabled and supported the realisation of this doctorate.

To an extraordinary degree I want to thank my supervisor Dr. Hind Medyouf for the allocation of my topic and for the intensive time of supervision, which included both content and personal support as well as scientific exchange and constructive criticism to improve my accomplishments. Next to that, I thank her not only for providing material and resources but also for the opportunity to participate in conferences and scientific symposia. Notably, my thanks go to her for the realisation of my personal concern, that is the possibility of scientific experimental research work, which Dr. Hind Medyouf gave me with confidence.

Furthermore, I would like to thank Prof. Dr. Florian Greten for taking over the responsibility of being my doctoral adviser and for his support supplied by access to the institute's facilities and laboratories.

Moreover, a great thanks is entitled to my colleagues in the Medyouf group, Irene Tirado-Gonzalez, Aleksandra Nevmerzhitskaya, Arnaud Descot, Ewelina Czlonka, Maresa Weitmann, Alexander Schäffer and Devona Soetopo, for their friendly welcome to the team, for introducing me to the practical execution of my experiments, their advice and suggestions, and, last but not least, for answering all my curious questions.

Also, I want to say thank you to all employees of the Georg Speyer Haus for creating a warm and positive working atmosphere and for their support in various ways. In particular, I would like to thank Petra Denise for her contribution in preparing and staining the histological samples.

A special thanks goes to the Deutschlandstipendium of the Johann Wolfgang Goethe-Universität Frankfurt am Main for the financial support and especially to my personal sponsors, the company Biotest AG in Dreieich.

Besides, I sincerely express my gratitude to my family and friends for both their encouragement and companionship during my studies and doctorate. And in outstanding appreciation to my dear parents, Ute and Ralf Wachtel, who have made my life possible so far and to whom I dedicate this work.

12 Schriftliche Erklärung

Ich erkläre ehrenwörtlich, dass ich die dem Fachbereich Medizin der Johann Wolfgang Goethe-Universität Frankfurt am Main zur Promotionsprüfung eingereichte Dissertation mit dem Titel

Exploration of Nilotinib enhancing the anti-leukaemic Effects of Gas6 Deletion in Ph+ B-ALL by inducing Immunogenic Cell Death

am Georg-Speyer-Haus, Institut für Tumorbologie und Experimentelle Therapie, unter Betreuung und Anleitung von Prof. Dr. Florian Greten mit Unterstützung durch Dr. Hind Medyouf ohne sonstige Hilfe selbst durchgeführt und bei der Abfassung der Arbeit keine anderen als die in der Dissertation angeführten Hilfsmittel benutzt habe. Darüber hinaus versichere ich, nicht die Hilfe einer kommerziellen Promotionsvermittlung in Anspruch genommen zu haben.

Ich habe bisher an keiner in- oder ausländischen Universität ein Gesuch um Zulassung zur Promotion eingereicht. Die vorliegende Arbeit wurde bisher nicht als Dissertation eingereicht.

(Ort, Datum)

(Unterschrift)